University of Alberta

Interhemispheric Axon Pathway Development in Mice with Agenesis of the Corpus Callosum

by

Daniel Joseph Livy

A thesis submitted to the Faculty of Graduate Studies and Research in partial fulfillment of the requirements for the degree of Doctor of Philosophy.

Department of Biological Sciences

Edmonton, Alberta

Fall, 1996

National Library
of Canada

Acquisitions and
Bibliographic Services Branch

395 Wellington Street
Ottawa, Ontario
K1A 0N4

Bibliothèque nationale
du Canada

Direction des acquisitions et
des services bibliographiques

395, rue Wellington
Ottawa (Ontario)
K1A 0N4

Your file *Votre référence*

Our file *Notre référence*

The author has granted an irrevocable non-exclusive licence allowing the National Library of Canada to reproduce, loan, distribute or sell copies of his/her thesis by any means and in any form or format, making this thesis available to interested persons.

L'auteur a accordé une licence irrévocable et non exclusive permettant à la Bibliothèque nationale du Canada de reproduire, prêter, distribuer ou vendre des copies de sa thèse de quelque manière et sous quelque forme que ce soit pour mettre des exemplaires de cette thèse à la disposition des personnes intéressées.

The author retains ownership of the copyright in his/her thesis. Neither the thesis nor substantial extracts from it may be printed or otherwise reproduced without his/her permission.

L'auteur conserve la propriété du droit d'auteur qui protège sa thèse. Ni la thèse ni des extraits substantiels de celle-ci ne doivent être imprimés ou autrement reproduits sans son autorisation.

ISBN 0-612-18068-9

Canada

University of Alberta

Library Release Form

Name of Author: Daniel Joseph Livy

Title of Thesis: Interhemispheric Axon Pathway Development in Mice with Agenesis of the Corpus Callosum.

Degree: Doctor of Philosophy

Year this Degree Granted: 1996

Permission is hereby granted to the University of Alberta Library to reproduce single copies of this thesis and to lend or sell such copies for private, scholarly, or scientific research purposes only.

The author reserves all other publication and other rights in association with the copyright in the thesis, and except as hereinbefore provided, neither the thesis nor any substantial portion thereof may be printed or otherwise reproduced in any material form whatever without the author's prior written permission.

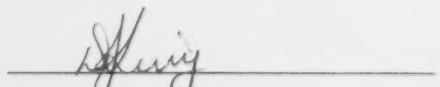

#35, 5605-50 Ave.
Yellowknife, NT
Canada X1A 1E8

August 23, 1996

University of Alberta

Faculty of Graduate Studies and Research

The undersigned certify that they have read, and recommend to the Faculty of Graduate Studies and Research for acceptance, a thesis entitled Interhemispheric Axon Pathway Development in Mice with Agenesis of the Corpus Callosum submitted by Daniel Joseph Livy in partial fulfillment of the requirements of the degree of Doctor of Philosophy.

Dr. S. Malhotra (Supervisor)

Dr. W. Gallin

Dr. A. Ahmed

Dr. D. Wahlsten

Dr. T. Shnitka

Dr. A. Elberger (External)

August 23, 1996
Date

DEDICATION

For my grandparents.

Their importance to my life cannot be expressed in words. If not for them, I would have travelled a far different path. Both passed away during the course of this research. This thesis is dedicated to their memory.

Joseph E. Poore

&

Frances R. E. Poore

Those who are remembered, never truly die.

I shall not forget.

ABSTRACT

Hereditary agenesis of the corpus callosum (CC) in mice was used as a model to study the guidance of commissural axons traversing the interhemispheric region, and the plasticity which is inherent when these normal guidance mechanisms are disrupted. Callosal agenesis results in the partial or complete absence of the CC at midplane, but may also produce structural defects in the hippocampal commissure (HC), an interhemispheric pathway that may provide structural support for early callosal axons crossing midline. A precise description of the timing and route travelled by hippocampal axons traversing the telencephalic midline in normal mice indicated that early HC axons travel over the dorsal septum and along the pia membrane lining the longitudinal fissure. About one day later, early callosal axons fasciculate along and between existing hippocampal axons atop the HC, the first time that such a relationship has been clearly established. In acallosal mice, HC formation was delayed by the continued presence of a deep cleft extending down into the septal region; this delay was correlated with the severity of the strain's CC defect expression. These results show the importance of the HC for successful CC formation and suggest that callosal agenesis may arise as a consequence of a developmental defect which affects the formation of the hippocampal commissure.

Callosal absence produces relatively few behavioural deficits. The anterior commissure (AC) has been suggested to provide an extracallosal route for the transfer of interhemispheric information in subjects with the congenital defect. Electron microscopy was used to compare AC size, axon number, and axon diameter between normal and

acallosal mice. Midsagittal AC areas did not differ, but the number of unmyelinated axons in acallosal mice was greater; this difference in axon number was accompanied by a decrease in the mean diameter of these axons which likely enabled higher numbers of axons to pass through the AC without increasing the midsagittal area. The higher number of axons present in the AC of acallosal mice suggests an increase in the efficiency and usage of this interhemispheric pathway to provide some measure of functional compensation for the loss of the corpus callosum.

ACKNOWLEDGEMENTS

This research was supported in part by financial assistance provided by the Department of Zoology, University of Alberta, a Province of Alberta Graduate Scholarship, and a Postgraduate Scholarship provided by the Natural Sciences and Engineering Research Council of Canada.

I would like to thank Dr. Doug Wahlsten who acted as co-supervisor during my program tenure. I have known Doug for many years, and during this time he has graciously served as both mentor and friend. Doug provided laboratory facilities and equipment, plus all of the mice used in this study. He also provided a wealth of advice, guidance and support. It has been my privilege to know and work with him.

Dr. Sudarshan Malhotra acted as supervisor during my program tenure. I am grateful to him for providing me with laboratory facilities and equipment, including the electron and confocal microscopes. His advice and guidance have been greatly appreciated.

Dr. Warren Gallin was the third member on my supervisory committee. He provided valuable criticisms and suggestions during the preparation of this manuscript and throughout the tenure of my program.

I would like to thank Dr. Andrea Elberger for agreeing to act as external examiner in my thesis defense, and for providing many thoughtful and useful suggestions for the improvement of this manuscript.

Violet Sparks and Rakesh Bhatnagar have provided excellent technical assistance over the years, for which I am very appreciative. I am grateful to Dr. Hiroki Ozaki for

instructing me in the use of lipophilic dyes. I would like to thank all of my fellow students for their suggestions and support, and extend special mention and thanks to Melike Schalomon for her assistance in axon counting. I should also like to thank Delaine Glass and David Sereda for providing a much needed pair of hands when mine were non-functional.

I have been fortunate to have some wonderful friends who have gone out of their way to help and support me, and I thank them all. Special thanks must be extended to Ron and Flora Player, Blaine, Wendy and Kyle McDonald, and Aaron Elniski. Their generosity will always be remembered.

Finally, I would like to thank my best friend, who is also my wife, Kara. It takes a special person to endure the ups and downs ever-present in the life of a research scientist, and she is such a person. Her support for me has never wavered. She has displayed patience and tolerance far beyond the norm, and has proved an inexhaustible source of strength and encouragement. She has been both companion and colleague, and I am very grateful and fortunate to have had her with me through this journey.

Table of Contents

General Introduction....1

Experiment 1

- Introduction....19
- Methods....21
- Results....30
- Discussion....54

Experiment 2

- Introduction....62
- Methods....63
- Results....66
- Discussion....67

Experiment 3

- Introduction....68
- Methods....71
- Results....75
- Discussion....96

Experiment 4

- Introduction....101
- Methods....103
- Results....104
- Discussion....105

Experiment 5

- Introduction....109
- Methods....112
- Results....119
- Discussion....139

Summary and Conclusions....144

References....154

Appendix A....184

List of Tables

1.1 Number of Litters and Embryos Collected from Each Mouse Strain....24

1.2 Frequency of Callosal Absence and Defect in Relation to the Time of Initial Crossing by Hippocampal Axons....50

3.1. Number and Body Weight Range of Embryos in Sagittal Series Brains....74

5.1 Anterior Commissure Morphometric Data....120

5.2 Mean and Standard Deviation of Areas and Axon Numbers in the Total Anterior Commissure....125

5.3 Mean and Standard Deviation of Areas and Axon Numbers in the Anterior Part of the Anterior Commissure....127

5.4 Mean and Standard Deviation of Areas and Axon Numbers in the Posterior Part of the Anterior Commissure....128

5.5 Mean and Standard Deviation of Combined, Myelinated, and Unmyelinated Axon Density in the Total Anterior Commissure....130

5.6 Mean and Standard Deviation of Combined, Myelinated, and Unmyelinated Axon Density in the Anterior Part of the Anterior Commissure....131

5.7 Mean and Standard Deviation of Combined, Myelinated, and Unmyelinated Axon Density in the Posterior Part of the Anterior Commissure....132

5.8 Mean and Standard Deviation of Axon Diameters....134

List of Figures

1.1 Relationship of Embryo Body Weight and Gestational Age....26

1.2 Dye Crystal Placement....29

1.3 Development of the Hippocampal Commissure in Mouse Embryos....35

1.4 Early Fornix Presence in the Medial Septal Region....37

1.5 Growth of the Hippocampal Commissure in Normal Hybrid Mice....41

1.6 Parasagittal Approach to Midline by Callosal Axons....44

1.7 Extension of the Interhemispheric Fissure into the Medial Septal Region....47

1.8 Comparison Among Strains of Their HC Axon Crossing Times....49

1.9 Growth Cones of Hippocampal Axons at the Telencephalic Midline....53

3.1. Sagittal View of Third Ventricle Neuroepithelium....78

3.2. Change in Number of Third Ventricle Mitotic Figures in the Midplane Region During Growth....80

3.3. Change in Density of Mitotic Figures in the Midplane Region During Growth....82

3.4. Third Ventricle Cells at the Septal Midline....85

3.5. Subventricular Cells from the Lateral Ventricle....88

3.6. Subventricular Cells and the Corpus Callosum....90

3.7. Continued Midline Notch Presence in Older Embryos....92

3.8. Anomalous Gap Presence in Acallosal Embryos....95

5.1. Midsagittal Morphology of the Mouse Anterior Commissure....117

5.2. Ultrastructure of the Mouse Anterior Commissure....122

5.3. Myelinated AC Axon Diameters....136

5.4. Unmyelinated AC Axon Diameters....138

List of Abbreviations

AAC - anterior part of the anterior commissure

AC - anterior commissure

C - cerebral cortex

CC - corpus callosum

F - columns of the fornix

HC - hippocampal commissure

LCF - longitudinal cerebral fissure

LV - lateral ventricle

M - midline

PAC - posterior part of the anterior commissure

PSFO - primordium of the subfornical organ

S - septal region

VT - velum transversum

GENERAL INTRODUCTION

The study of abnormal nervous systems can provide a better understanding of the processes involved in the development and functioning of the normal nervous system. One important developmental issue that has been addressed by such study is the precision of growth by axon pathways that connect the two hemispheres of the brain. Commissural axons travel long distances from their origin sites in one hemisphere, cross midline at a specific time and location in concordance with their environmental surroundings, and then continue their travel through the opposite hemisphere to their target locations. Developmental delays or structural omissions in these pathways may arise due to inherent defects within the axons or their cell bodies, or from defects in the environmental milieux upon which the axons depend for physiological and structural support and guidance.

Agenesis of the corpus callosum (CC) is one example of a neurological defect in axon pathway formation, resulting in the partial or complete absence of callosal axons bridging the midline region between the two cerebral hemispheres of the brain. The corpus callosum is of particular interest because it is the largest tract of projection fibres connecting the cerebral hemispheres of the brain (Aicardi, Chevrie, and Baraton, 1987), containing approximately 200 million axons in humans (Tomasch, 1954; Aboitiz, Scheibel, Fisher, and Zaidel, 1992). The absence of this pathway therefore produces a profound change in the structural architecture seen in the brain. The CC is present in all mammals except monotremes and marsupials (Granger, Masterton, and Glendenning, 1985). Most of the

connections through the CC provide communication between homotopic areas of the cerebral neocortex, although many heterotopic connections are also present (Ivy and Killackey, 1981; Segraves and Rosenquist, 1982a,b; Lomber, Payne, and Rosenquist, 1992).

Callosal anomalies that are similar to those seen in callosal agenesis have been produced by surgical lesion (Lent, 1984), irradiation (Lent and Schmidt, 1986), biochemical alteration (Gravel and Hawkes, 1990; Gravel, Sasseville and Hawkes, 1990), and by the use of genetic manipulation (Müller, Cristina, Li, Wolfer, Lipp, Rüüke, Brandner, Aguzzi, and Weissmann, 1994; Qui, Anderson, Meneses, Pedersen, and Rubenstein, 1995; Stumpo, Bock, Tuttle, and Blackshear, 1995). Although useful, each of these techniques involves some form of invasive manipulation that also produces anomalies secondary to the interruption of the axon pathway by destroying surrounding tissues and/or effecting systemic responses.

In contrast to these manipulative techniques, incomplete penetrance allows the observation of callosal defects that vary in their severity without the necessity of experimental intervention and the concomitant trauma that often results (see Lipp, Schwegler, Crusio, Wolfer, Leisinger-Trigona, Heimrich, and Driscoll, 1989). Penetrance refers to the proportion of animals having a particular genotype that also display a particular phenotype (Wahlsten, 1982a). Inbred strains of mice are bred brother by sister for at least 20 generations to be considered isogenic, and at least 60 generations to ensure homozygosity at every genetic locus (Green, 1981); each animal within an inbred strain should therefore have an identical genotype. If all animals with a common genotype show the phenotype in question, the penetrance is considered to be complete or 100%, but if only a fraction of the animals show the phenotype, the penetrance is considered incomplete. For example, I/LnJ

mice never develop a CC, demonstrating complete penetrance of the defect. In contrast, about 50% of BALB/c mice and 70% of 129 mice show a complete or partial absence of callosal fibres. Incomplete penetrance of a genetic mutation therefore results in the manifestation of normal and abnormal development and functions in animals with identical genetic backgrounds.

The study of callosal agenesis in humans is confronted with several problems. Although some behavioural deficits have been found, the effects are often quite subtle and sophisticated testing is required for their detection (Lassonde, Sauerwein, Chicone, and Geoffrey, 1991; Sauerwein, Nolin, and Lassonde, 1994). The human corpus callosum forms prenatally, beginning at about the twelfth week of gestation (Rakic and Yakovlev, 1968). Callosal agenesis is often identified in association with other neurological anomalies, making it difficult to apportion symptoms to specific defects (Wisniewski and Jeret, 1994). Gupta and Lilford (1995) found only seventy cases of human fetal callosal agenesis reported in the English literature. They reviewed the developmental outcomes of these fetuses and found that callosal agenesis was originally diagnosed in association with other anomalies in 56% of these cases, of which only 13% (2 cases) were reported to be developing normally. In contrast, 85% of the fetuses with apparent isolated agenesis were reported to be developing normally, while the remaining 15% displayed some level of deficit. The ontogenetic determination of this defect in humans is rendered virtually impossible due to the ethics involved with research in human fetal development.

In contrast, the mouse provides an excellent model for the study of callosal agenesis. Callosum formation also occurs prenatally in mice, increasing the validity of comparison to

humans since the developmental morphology of mammals is more similar at earlier stages of ontogeny. Callosal agenesis in some strains of mice does not appear to be associated with other neurological defects, permitting a direct analysis of the development of the callosal defect. As well, the genetic backgrounds in most strains of mice are well established and several strains that display callosal agenesis have been identified. This allows comparisons among different genetic strains to determine how their developmental processes affecting callosum formation differ.

Callosal agenesis in the mouse was first reported by King and Keeler (1932). The initial research into the defect concentrated on its mode of inheritance and Keeler (1933) indicated that the defect followed Mendelian single-locus inheritance. This view was later challenged by King (1936), but the unfortunate extinction of the strain prevented any further investigation. A similar callosal defect was rediscovered in BALB/cJ and 129/J mice by Wimer (Wahlsten, 1974a) which precipitated new investigations into the mode of inheritance of the defect as well as investigations into its pathology.

All commissures develop prenatally in the mouse brain following a distinct order of appearance according to their morphological age (Wahlsten, 1981). The use of chronological age as an indicator of morphological development is ineffective because of the variability in developmental rates both between and within strains. Wahlsten and Wainwright (1977) produced a morphological time scale of development in F_2 hybrid mice that was used to detect differences in the morphological development of prenatal inbred mice and to adjust for these differences. The development of F_2 hybrids was found to be about 0.5 days ahead of C57BL/6J mice (a normal inbred strain), which were in turn about 0.5 days ahead of

BALB/c, A/J and DBA inbred strains (Wahlsten and Wainwright, 1977). These differences among strains indicate the importance of equating the level of morphological development when comparing between strains to ensure that delays observed in the formation of certain brain structures are not the result of a more general delay in overall body growth, and hence delayed brain growth.

These developmental differences among strains continue to exist postnatally. A developmental time scale produced by Wahlsten (1974b) demonstrated similar differences in development of the brain and behaviours of mice at 32 days gestational age. Development in inbred strains lagged behind that in F_2 hybrids by 1-3 days, and differences of up to 1 day were found between different inbred strains (Wahlsten, 1975; Wainwright, 1980).

The interhemispheric axon pathways that form in the mouse brain reach midline in the following order: posterior commissure, optic chiasm, stria terminalis, habenular commissure, anterior commissure, hippocampal commissure, and finally the corpus callosum (Wahlsten, 1981). The last three of these are by far the largest commissural pathways and are of the most interest to this study. All three pathways cross midline through the medial septal region. During early brain development, bilateral evaginations in the telencephalon produce the two telencephalic vesicles which are surrounded by the meninges and are separated at midline by the interhemispheric fissure. Cells migrate from the third ventricle rostrally and the lateral ventricles medially to form the septal region immediately ventral to the fissure. As the septal region expands, the interhemispheric fissure fuses; the medial walls of the fissure contact, interrupting the meninges, which rejoin dorsal to the contact area to reform the floor of the fissure (Glas, 1975). The remaining cells of the meninges are then

phagocytized by macrophages. In this way, the fissure is moved both rostrally and dorsally by the migrating septal cells.

The first of the three large commissures to form in the septal area is the anterior commissure (AC) at about 14 days after conception (E14) in normal mice (Glas, 1975; Wahlsten, 1981; Silver, Lorenz, Wahlsten, and Coughlin, 1982). The AC consists of two distinct fibre tracts. The anterior tract (AAC) originates in the anterior piriform cortex, the olfactory tubercles and the anterior olfactory nucleus (Jouandet and Hartenstein, 1983; Lent and Guimarães, 1991) and migrates to the lateral edge of the septal region. The posterior tract (PAC) originates in the posterior piriform cortex, perirhinal cortex, and the lateral nucleus of the amygdala (Jouandet and Hartenstein, 1983; Lent and Guimarães, 1991) and migrates to meet the AAC. These two tracts combine to form two distinct halves of one commissure as they pass through the septal region; axons within these tracts maintain their topographic organization (Pires-Neto, Lent, and Hartmann, 1994). Smaller satellite bundles frequently split off from this main bundle of axons (Wahlsten, 1974a). Some of these satellite bundles rejoin the main bundle, some travel along beside the main bundle, and others have been observed to travel very unique routes to terminate in areas very different from their originally intended target sites (Cassells and Wahlsten, 1989).

One of the most prominent causes of the formation of satellite bundles is collisions with the columns of the fornix. The fornix columns contain axons connecting the hippocampus with the mamillary bodies and septal nuclei (Swanson and Cowan, 1979; Swanson, Köhler and Björklund, 1987). These axon bundles remain ipsilateral through the medial septal region, lying just lateral to midline. Axons of the fornix columns and the

ipsilateral AC arrive at the same location at about the same time, providing an excellent opportunity for collisions to occur between the two axon tracts (Wahlsten, 1981). These collisions may vary greatly in severity and appear to be more common in some strains of mice than in others. BALB/c mice appear to be particularly susceptible to such collisions, however there is no correlation between the severity of collision in the AC and the severity of the callosal defect (Livy and Wahlsten, 1991).

Axons of the hippocampal commissure (HC) have been reported to cross midline dorsal to the AC at about E15 (Wahlsten, 1981). Hippocampal research has concentrated on the structure and development of the hippocampal formation, and the routing of axons in the adult hippocampal commissure; relatively little is known about the prenatal development of the HC. The adult hippocampal commissure is typically considered to be comprised of two parts, the ventral HC, which lies at the caudal edge of the septum just rostral to the subfornical organ, and the dorsal HC, which lies immediately ventral to the rostral part of the splenium and caudal part of the body of the CC (Blackstad, 1956; Demeter, Rosene, and van Hoesen, 1985; LaMantia and Rakic, 1990a; Wahlsten and Bulman-Fleming, 1994). In rodents, these two structures are continuous, forming one large hippocampal commissure; in primates, these two structures are distinct and separated by the hippocampal decussation, a projection of axons arising from the hippocampal formation and crossing midline obliquely to the contralateral septal region (Demeter *et al*, 1985).

The dorsal HC in the adult rat carries axons from the entorhinal cortex, presubiculum, and possibly the rhinal fissure (Shipley, 1975; Swanson and Cowan, 1977; Swanson, Wyss, and Cowan, 1978; Wyss, Swanson, and Cowan, 1980). The ventral HC in the adult rat

contains homotopic projections from the CA3 region and the pyramidal cells from the hilar region of the dentate gyrus in the hippocampal formation, as well as heterotopic connections from the CA3 region to the CA1 region (Gottlieb and Cowan, 1973; Laurberg, 1979; Wyss *et al*, 1980; Voneida, Vardaris, Fish, and Reiheld, 1981; van Groen and Wyss, 1988). Homotopic projections have also been found connecting the CA1 regions (Voneida *et al*, 1981; van Groen and Wyss, 1988). Other projections include heterotopic connections from the CA1 region to the subiculum and entorhinal cortex (Voneida *et al*, 1981; some evidence exists for a return connection from entorhinal cortex to the CA1 region - see Witter, Griffioen, Jorritsma-Byham, and Krijnen, 1988), and from the medial entorhinal area to the dentate gyrus and from the lateral entorhinal area to the inner dentate gyrus area (Wyss, 1981). Axons from more septal regions in the hippocampal formation were found in the more caudal areas of the HC, while those axons from the more temporal areas were found in the more rostral area (Wyss *et al*, 1980). Similarly, fibres arising from areas near the ependyma of the lateral ventricles cross in more dorsal regions of the HC, while those arising along the pial border cross through the ventral region. In the neonatal rat, homotopic connections were present between the CA1, CA3, and dentate regions, however heterotopic connections between these areas were not found (Buchhalter, Fieles, and Dichter, 1990).

The HC system in primates is greatly reduced relative to that seen in the rat (LaMantia and Rakic, 1990a), suggesting that the HC in primates may be non-functional (Wilson, Isokawa, Babb, and Crandall, 1990; Wilson, Isokawa, Babb, Crandall, Levesque, and Engel, 1991). This reduction is most evident in the ventral HC due to a paucity of commissural connections between the main bodies of the hippocampi, however the dorsal

HC appears proportionately similar to rodents, with connections mainly between the parahippocampal gyri (Amaral, Insausti, and Cowan, 1984; Demeter *et al*, 1985; Demeter, Rosene, and van Hoesen, 1990). In humans, Gloor, Salanova, Olivier, and Quesney (1993) have questioned the presence of a ventral HC but have found evidence of a hippocampal decussation and of a functional dorsal HC.

Callosal axons cross midline immediately dorsal to the HC very close to E16 in normal hybrid mice (Ozaki and Wahlsten, 1992). Silver *et al* (1982) suggested that CC axons cross midline using the "sling", a layer of subventricular cells that form a bridge between the lateral ventricles just anterior to the HC. Cells covering the surface of the sling have been identified as primitive astrocytes and radial glial cells (Hankin and Silver, 1986). Sling cells remain along the ventral surface of the rostral CC until about E18 at which time some of the cells begin to degenerate, while others remain as astrocytes and oligodendroglial cells (Hankin and Silver, 1988).

The sling is only about 200μm long and callosal axons rostral to the sling are prevented from entering the septal region by another layer of subependymal cells called the "corticoseptal barricade" (Hankin and Silver, 1986). Caudal to the sling, callosal axons cross along the dorsal surface of the hippocampal commissure (Silver *et al*, 1982).

A similar sling structure has been identified in the cat (Silver, Smith, Miller and Levitt, 1985) and rat (Katz, Lasek, and Silver, 1983) but not in the rhesus monkey (LaMantia and Rakic, 1990a). Valentino and Jones (1982) were not able to identify this structure in the rat; a bed of glial cells were noticed, but were not organized in any pattern and were not thought to contribute to CC axon migration. Instead, they suggested that the first callosal

axons may exclusively use the dorsal surface of the HC as a guide.

In fact, Wahlsten (1987a) found that callosal axons in abnormal BALB/c mice were able to exclusively use the dorsal surface of the HC to cross the midplane. In mice from acallosal strains the structural integrity of the sling was often damaged at midline due to the presence of a fluid-filled gap, or bulge, at the base of the longitudinal fissure, usually resulting in abnormal CC morphology. The use of the HC by these CC axons usually occurred relatively late in development and the resulting callosum was often abnormal in size and shape, and appeared sitting directly on top of the HC. A similar use of the HC by callosal axons in normal mice could not be determined. The Wahlsten (1987a) methodology employed an eosin stain which does not differentiate between individual axons; the early callosal axon bundle in normal mice occupies a position dorsal and rostral to the HC making it impossible to determine the location of crossing by the early callosal axons.

Tract-tracing using non-selective stains such as eosin (Silver *et al*, 1982) and toluidine blue (Zaki, 1985) limits pathway descriptions to gross structure. The binding of silver stain to neurofilament protein (Gambetti, Autilio-Gambetti, and Papasozomenos, 1981) permits greater specificity in the staining of axons (Glas, 1975; Edwards, Schneider, and Caviness, 1986) but is relatively insensitive. Neurofilament antibody has greater sensitivity for neurofilament protein within axons but still does not provide complete staining of individual axonal structure and does not allow differentiation between axons from differing origin sites (Edwards, Crandall, Wood, Tanaka, and Yamamoto, 1989; Silver, Edwards, and Levitt, 1993).

Horseradish peroxidase (HRP) is an *in vivo* tracer that uses active axonal transport

to label axons and axon tracts (Innocenti and Clarke, 1984; Olavarria and van Sluyters, 1985; Lent, Hedin-Periera, Menezes, and Jhaveri, 1990); however, HRP labelling is inconsistent, especially in neonates, and often produces a reaction product that can obscure details of morphology (Dehay, Kennedy, and Bullier, 1988; Norris and Kalil, 1990) and the requirement of living tissue makes its use inconvenient, especially for prenatal investigation. In contrast, fluorescent lipophilic tracers can be used with fixed tissue, provide precise labelling of individual axons, and permit the differentiation of axons from different origins by the use of dyes with different emission spectra. Their passive transport within the lipid bilayer of membranes makes them particularly suited for prenatal research (Elberger, 1993).

Using fluorescent lipophilic dyes, Ozaki and Wahlsten (1992) found that callosal axons arrive at midline along a rostral-caudal gradient. Axons from all regions of the cortex originated at about 0.4g in normal hybrid B6D2F_2 mouse embryos, but those axons originating from the frontal cortex grew faster and crossed midline first, followed by axons from the parietal, then temporal, and finally the occipital cortex. Axons arising from more lateral areas crossed ventral to axons from more medial cortical regions.

After the callosal axons cross midplane, the callosum undergoes a period of rapid growth until about 6 days after birth at which time it is within the adult range of size (Wahlsten, 1984). Myelination of the axons begins at about 11 days after birth, followed by a period of rapid myelin content increase between 14 and 90 days of age, and then a more gradual increase to about 240 days of age (Sturrock, 1980). Myelinated axons account for approximately 18% of all axons in the callosum at 90 days of age and about 28% at 240 days of age, with the diameter of these axons being about double that of the unmyelinated axons

(Sturrock, 1980).

Myelination in the cat CC occurs along a rostral-caudal gradient; axons in the genu of the CC begin myelination between P13 and P15 and reach the adult complement by the fourth month whereas those from the splenium begin between P17 and P21 and do not reach the adult complement until after the fourth month (Looney and Elberger, 1986). Transection of the cat CC prior to the third week of age reduces both visual acuity and binocular representation within cortical neurons (Elberger, 1982; Elberger, 1984; Elberger and Smith, 1985). Myelination of axons denotes their physiological maturation but this is obviously not a requirement for the effect of the callosum on visual system development, but may instead be a product of the pattern of connections established by callosal axons (Elberger, 1988).

The increase in the diameter of axons during myelination would suggest a corresponding increase in the size of the callosum. In the mouse, the actual increase in callosum size is relatively small (Wahlsten, 1984), suggesting that some axons are eliminated during the myelination process. Axon elimination has been demonstrated in the CC of the Rhesus monkey (LaMantia and Rakic, 1990a; LaMantia and Rakic, 1990b), the CC of the cat (Koppel and Innocenti, 1983; Berbel and Innocenti, 1988), and in the optic nerve of the cat (Williams, Bastiani, Lia, and Chalupa, 1986) and rat (Crespo, O'Leary, and Cowan, 1985). Axon elimination has been described in certain areas of the rat CC soon after birth (Ivy and Killackey, 1981), but the overall number of axons remains fairly stable at 12 million until day 60 (Gravel *et al*, 1990). This may indicate that the number of axons being eliminated is matched by the production of a similar number of new axons and axon collaterals. The initial exuberance of axon numbers may arise from the production of an

excess of axon collaterals, which are then removed to sculpt the adult pattern of connections (O'Leary, 1992; Simon and O'Leary, 1992); a similar regression of dendritic branches from callosal neurons produces the adult-like pattern of dendrite morphology in rat neocortex (Koester and O'Leary, 1992). Despite the elimination of large numbers of axons from the callosal tract, the size of the callosum may still increase over time which is likely due to the growth and myelination of the remaining axons, and the differentiation of glial cells (LaMantia and Rakic, 1990b).

Considering the large fluctuations which occur in axon numbers during this early period of development, it is not surprising that environmental variations have an impact on the eventual size of the CC. A complex rearing environment leads to an increase in callosum size in rats (Juraska and Meyer, 1985; Juraska and Kopcik, 1988) but early handling has no effect on callosum size in BALB/c mice (Bulman-Fleming, Wainwright, and Collins, 1992). Wahlsten (1982b) found that callosal defects were more prevalent in mice bred by commercial suppliers than in his own lab. This was due in part to differences in breeding protocols; callosal anomalies were found to be more prevalent in mice that were *in utero* while their mother was still nursing a previous litter (Wahlsten, 1982c). A similar protocol has produced callosal defects associated with a flat-face appearance in ddN mice (Ozaki, Murakami, Toyoshima, and Shimada, 1984).

Maternal environment contributes to the overall environmental variability. Brain weights are higher in offspring from F_1 hybrid mothers compared to inbred BALB/c mothers; among inbreds, BALB/c maternal environments often result in higher brain weights (Wahlsten, 1983). Low protein diets fed to BALB/c mothers increased the incidence of

offspring born with reduced CC size (Wainwright and Stefanescu, 1983), but this may have been due to a general retardation in fetal growth rate (Wainwright and Gagnon, 1984). Similar effects were found in inbred BALB/c pups that had been removed from their mothers for 24 hours shortly after birth (Wahlsten, Blom, Stefanescu, Conover and Cake, 1987). However, no differences in the incidence of callosal agenesis were found between inbred BALB/c pups from an F_1 maternal environment and those from an inbred BALB/c environment (Bulman-Fleming and Wahlsten, 1988). Prenatal exposure to alcohol inhibits the development of both the corpus callosum and the anterior commissure, but the callosal effect is due to an overall inhibition of fetal development (Cassells, Wainwright, and Blom, 1987).

The mouse is a polytocous animal; litter size has a large inverse effect on brain weight but does not affect the incidence of callosal defect (Wahlsten and Bulman-Fleming, 1987; Bulman-Fleming and Wahlsten, 1988). This inverse effect of litter size is much more profound on the body weight of the pups after birth (Wainwright, Pelkman and Wahlsten, 1989). The microenvironments present within the uterus affect the development of some pups differently. Those embryos at either end of the uterine horn are usually larger (McLaren, and Michie, 1960; Healy, McLaren and Michie, 1960; Bulman-Fleming and Wahlsten, 1991), particularly those at the ovarian end (McLaren, 1965; Kalter, 1975). Thyroxine-treated A/WySn mouse embryos with cleft lip displayed decreased mortality when implanted at the ovarian end relative to those embryos implanted elsewhere in the uterus (Juriloff and Harris, 1985). The right uterine horn tends to produce a higher ovulation rate, number of copora lutea, and fetal and placental weights (McLaren, 1963; Barr, Jensch,

and Brent, 1970; Wiebold and Becker, 1987), however little evidence is available to suggest that these environmental differences within the uterus contribute to the alteration of callosum size in any consistent manner (Bulman-Fleming and Wahlsten, 1991).

Conflicting reports have been produced regarding the effect of sex on callosum growth. Early handling of rats increases callosum size in males, but decreases callosum size in females (Berrebi, Fitch, Ralphe, Denenberg, Friedrich, and Denenberg, 1988). Testosterone has been postulated as being a causal factor in increased callosum size (Fitch, Berrebi, and Denenberg, 1987), and male rats have been found to have larger callosa, even after controlling for their larger body (and therefore brain) size (Berrebi *et al*, 1988). However, this view was challenged by other reports citing increased callosal size in females (DeLacoste-Utamsing and Holloway, 1982; Allen, Gorski, Shin, Barakat, and Hines, 1987 [from Berrebi *et al*, 1988]), while others indicate that no gender differences exist (Juraska and Meyer, 1985; Kertesz, Polk, Howell, and Black, 1987; Juraska and Kopcik, 1988). The gender issue has proven rather contentious, however a recent meta-analysis of all gender-related studies has shown that indeed no real differences can be found between the sexes in humans (Bishop and Wahlsten, 1996).

The effects of these variations have complicated the search for the mode of inheritance of the CC defect. The callosal defect seen in BALB mice is similar to the defect described by King and Keeler (Wahlsten, 1989a). The defect is clearly autosomal recessive (Wahlsten, 1974a; Wahlsten, 1982b,d; Lipp and Waanders, 1990), and polygenic (Wahlsten, 1982d; Wahlsten and Smith, 1989). The defect displays true incomplete penetrance when there is no genetic segregation (Wahlsten, 1989b). Evidence to support a two-locus mode

of inheritance was provided by Wahlsten and Smith (1989) and Lipp and Waanders (1990). Livy and Wahlsten (1991) described a model that demonstrated the involvement of two loci in strains with incomplete penetrance (BALB and 129), and the involvement of a third loci in the I/LnJ strain that shows complete penetrance of the defect.

The polygenic nature and incomplete penetrance associated with the callosal defect may indicate the disruption of more than one developmental process during the formation of the corpus callosum. In some mice with callosal agenesis, defects have been seen in the size and shape of the hippocampal commissure, suggesting difficulties in the guidance of HC axons across the telencephalic midline. While these defects are not as severe or frequent as those seen during CC development, in mice with severe defects in HC structure the corpus callosum does not form (Livy and Wahlsten, 1991). Clearly, there is some developmental anomaly occurring at the telencephalic midline that affects CC development but which also occurs early enough to affect hippocampal commissure development. In minor defects, both the HC and CC can recover to form normal structures. Moderately severe defects may affect HC development and sling formation, but the HC may still be able to provide a substrate for late crossing callosal axons; HC morphology is normal in these animals but the resulting CC is often abnormal in size and shape. Very severe defects affect midline structures to such an extent that the HC is not able to recover. This in turn affects any future developments within the area.

The cause of callosal agenesis remains uncertain, however the defect that is responsible occurs early enough to have an impact on HC development. Little research has been devoted to the study of hippocampal commissure formation yet a precise description

of HC development is required to fully understand the relationship between the formation of the HC and callosal agenesis. The research described herein consists of five different parts as indicated below:

Experiment 1. *Retarded Formation of the Hippocampal Commissure in Acallosal Mouse Embryos.* A detailed description is provided of the timing and the route travelled by hippocampal axons as they cross the telencephalic midline during early HC formation in a normal mouse strain and in four acallosal mouse strains. In normal mice, this description is extended into the time of early callosal axon crossing in order to determine the relationship between callosal and hippocampal axons during early CC formation.

Experiment 2. *Axon-Substrate Interaction at the Ultrastructural Level.* A continuation of Experiment 1, electron microscopy was used to observe contact between the early hippocampal and callosal axons and their guiding substrates during midline crossing in a normal mouse strain.

Experiment 3. *Formation of the Medial Septal Region.* Commissural axons cross through the medial septal region. Retarded development in this area may result in the absence of the cells which are necessary to guide the hippocampal axons across midline. A mitotic index was created to show the proliferation of cells that migrate to form the septal region, to determine if there are differences in the timing or amount of cell proliferation between normal and acallosal mice.

Experiment 4. *Identification of Guiding Substrates at the Telencephalic Midline.* If commissural axons are not able to cross midline, it is possible that some specific guiding substrate is missing. In this study, several antibodies were used to discover the presence of possible cellular substrates that may be responsible for the guidance of hippocampal axons across the telencephalic midline in normal mice.

Experiment 5. *Commissural Plasticity in Mice with Callosal Agenesis.* If callosal axons are not able to cross midline, the brain loses its largest source of interhemispheric communication, so why is there relatively little behavioural deficit seen in these animals? It has been suggested that the anterior commissure may be used to maintain this communicative ability; however, the increase in volume and diversity of information carried would imply a modification of AC structure to allow this increased function. Using electron microscopy, a comparison was made between normal and acallosal mice to examine differences in AC size, axon number and axon diameter to determine whether AC structure is physically altered to allow for such an increase in interhemispheric communication.

EXPERIMENT 1[1]

INTRODUCTION

An accurate description of the route travelled by commissural axons is important for understanding the structural defects that arise during commissure formation. The mouse forebrain provides an excellent model for studying the traverse of the telencephalic midline by developing commissural axons. Inherent defects in the structure of the ventral hippocampal commissure (HC) and corpus callosum (CC) have been described in several strains of mice (Livy and Wahlsten, 1991; Ozaki and Wahlsten, 1992; Wahlsten and Bulman-Fleming, 1994), but the route taken by axons travelling through the hippocampal commissure has received little attention. These axons can first cross midline by passing through the medial septum, over the top of the medial septum at the base of the longitudinal fissure, and have also been suggested to travel extracerebrally through the pia membrane lining the base of the longitudinal fissure (Glas, 1975). Axons of the corpus callosum cross midline between the HC and the pia membrane at about E16 in normal hybrid mice (Wahlsten, 1981; Ozaki and Wahlsten, 1992), which is about one day after the hippocampal axons cross (Glas, 1975; Wahlsten, 1981). Despite intensive study, the precise route travelled by callosal axons remains elusive. This is due in part to the difficulty in

---

[1]A version of this chapter has been accepted for publication: "Livy DJ, and Wahlsten D (1996). Retarded formation of the hippocampal commissure in embryos from mouse strains lacking a corpus callosum. *Hippocampus*."

differentiating between callosal and hippocampal axons at the time of crossing. In some cases the two structures have been considered as one due to the indistinct border between CC and HC (Glas, 1975; Wahlsten and Smith, 1989). Silver *et al* (1982) suggested that CC axons cross midline using the "sling", a layer of subventricular cells that forms a bridge between the lateral ventricles just anterior to the HC, but it is not yet clear whether these cells guide the first callosal axons to cross midline. The close apposition between CC and HC axons has led to the suggestion that the HC plays a role in guiding early CC axons across midplane in rodents (Valentino and Jones, 1982). HC formation is retarded in some mice with callosal agenesis, suggesting a causal relationship between HC formation and CC agenesis (Wahlsten, 1987a; Livy and Wahlsten, 1991).

Non-selective staining methods do not conclusively reveal axon routing. Staining axons with silver and/or hematoxylin/eosin (Glas, 1975; Silver *et al*, 1982; Wahlsten, 1987a), or neurofilament antibody (Silver *et al*, 1993), does not distinguish between axons of differing origins, nor does this indicate axonal position relative to cellular structure. Lipophilic dyes (Honig and Hume, 1989) diffuse within the membrane of the axons, providing a precise labelling of axon position, allowing the route travelled by the axons to be seen. The use of two dyes with different spectral properties permits differential labelling between sides of the brain or different structures within the brain. The fine labelling provided by lipophilic dyes permits a detailed view of growth cone morphology (Godement, Vanselo, Thanos, and Bonhoeffer, 1987; Ghosh and Shatz, 1992) and the change in complexity of hippocampal axon growth cones as they approach and cross midline. A similar description of growth cone morphology in developing callosal axons has revealed a

decrease in structural complexity soon after the growth cones cross the midline region (Ozaki and Wahlsten, 1992).

In this experiment, the formation of the hippocampal commissure in normal hybrid mice is examined to provide a more precise description of the timing and location of first crossing of the HC axons and to show the relationship between the HC and CC during early development. This description is then used as a baseline for comparison with HC development in strains of acallosal mice. It will be shown that early HC axons cross midline in close association with the pia membrane and that early callosal axons cross midline while contacting existing hippocampal axons. In the acallosal strains, hippocampal axons are unable to cross due to the presence of a cleft extending deep between the hemispheres.

METHODS

Animals

Normal development was described using the F_2 offspring (B6D2F_2) from hybrid B6D2F_1/J parents (C57BL/6J females x DBA/2J males) obtained from the Jackson Laboratories, Bar Harbor, Maine, at 7-8 weeks of age, then raised and bred at the University of Alberta. Acallosal development was described in two inbred strains, BALB/cWah1 (BALB), bred and maintained at the University of Alberta, and 129/J (129), obtained from the Jackson Laboratories, Bar Harbor, Maine, at 7-8 weeks of age, then raised and bred at the University of Alberta. Although the expression of CC deficiency is high in these two

strains, the incidence of total CC absence is relatively low. The F_1 offspring from a BALB x 129 ($C129F_1$) cross show no CC defect, which supports a two-locus recessive model of inheritance (Livy and Wahlsten, 1991). Among the F_2 offspring from crossing two $C129F_1$ mice, there is about a 25% incidence of total CC absence (Wahlsten and Schalomon, 1994, plus unpublished data). Recombinant inbred strains are now being formed from pairs of 129 x BALB F_2 mice (Wahlsten and Sparks, 1995), and in one of the RI lines (#1) every adult animal in recent litters has had complete absence of the CC and greatly reduced HC, as is often seen in the strain I/LnJ (Lipp and Waanders, 1990; Livy and Wahlsten, 1991). This study used both the $C129F_2$ offspring and one line (RI-1) of recombinant inbred animals at the sixth generation of full-sib mating.

All mice were housed in 29 x 18 x 13 cm opaque plastic mouse cages with Aspen-Chip bedding (Northeastern Products Corp., Warrensburg, New York) with a few sheets of tissue added. Pregnant females were provided with a Nestlet for improved nest building and free access to food (non-autoclaved Wayne Rodent Blox 8604) and tap water. Room temperature was maintained at approximately 23°C with a 12/12 hour light cycle (lights on at 6 am).

Embryo Collection

One male and one to three females between 80 and 150 days old were placed together in a cage for 4 hours or overnight, after which the females were checked for vaginal plugs. Plugged females were weighed and housed individually for the duration of gestation.

Conception (0.0 days) was considered to be the midpoint between plug detection and the previous plug check. B6D2F_2 embryos were extracted between gestational days 14 and 16.5 (E14-E16.5) to obtain body weights ranging between 0.250g and 0.700g to encompass initial midline crossing by both hippocampal and callosal axons. As proposed by Kaufman (1992), all mice studied prenatally are referred to as embryos even though some have completed organogenesis and might be considered by some to be fetuses. Development is generally slower in inbred strains than in healthy hybrids (Wahlsten and Wainwright, 1977; Wahlsten, 1987a), and therefore to observe early midline crossing by hippocampal axons in acallosal strains, embryos were removed between E15 and E17 to obtain body weights ranging between 0.300g and 0.600g. The number of litters and embryos collected from each of the strains and providing usable data is shown in Table 1.1.

For extraction of the embryos, pregnant females were euthanized with sodium pentobarbital (120 mg/kg IP) and their uteri removed and rinsed in a solution of 0.9% saline in ice. The uteri were cut open and each embryo was separated from its placenta by cauterizing the umbilical artery. Embryos were then rinsed in ice-cold 0.9% saline, carefully blotted to remove excess fluid, and weighed to the nearest mg (see Fig. 1.1). Immediately after weighing, each embryo was perfused intracardially with 3-5mL of 10mM phosphate-buffered saline (pH 7.6) followed by 10-15mL of 4% paraformaldehyde in 0.1M phosphate buffer (pH 7.6) using a peristaltic perfusion pump, stereomicroscope, and micropipettes. After removing the scalp, the embryo head was placed in fresh fixative overnight. The following day the occipital bone was removed and the head was placed in fresh fixative and stored until the dye crystals were inserted.

Table 1.1: Number of Litters and Embryos Collected from Each Mouse Strain.

STRAIN	NUMBER OF LITTERS	NUMBER OF EMBRYOS
$B6D2F_2$	22	149
$C129F_2$	10	77
BALB/cWah1	7	30
129/J	7	33
RI-1	6	40

Fig. 1.1. Relationship of Embryo Body Weight and Gestational Age. Body weight versus gestational age from day of conception in 22 litters of B6D2F_2/J embryos, 10 litters of C129F_2 embryos, and 7 litters of BALB and 129 embryos. Shown are the linear relationships of litter mean body weight to gestational age of the litter which accounts for approximately 73% of the variance in body weight in B6D2F_2 embryos, 74% in C129F_2 embryos, 86% in BALB embryos, and 90% in the 129 embryos. The addition of a quadratic term did not significantly improve the fit of any line (with $p=0.10$ in a litter means analysis - Abbey and Howard, 1973).

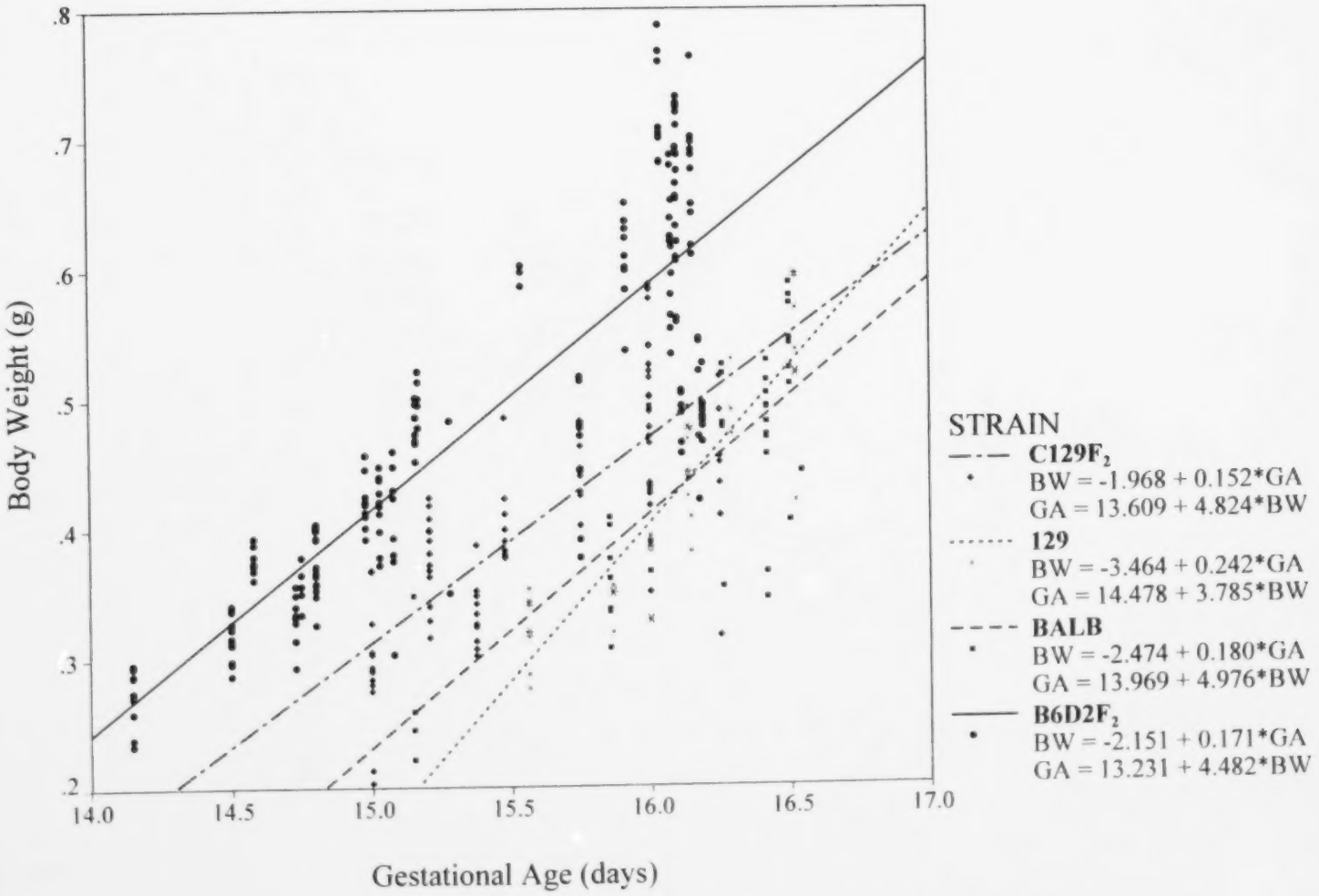
Body Weight (g)
.8
.7
.6
.5
.4
.3
.2
14.0
14.5
15.0
15.5
16.0
16.5
17.0
Gestational Age (days)
STRAIN
C129F2
BW = -1.968 + 0.152*GA
GA = 13.609 + 4.824*BW
129
BW = -3.464 + 0.242*GA
GA = 14.478 + 3.785*BW
BALB
BW = -2.474 + 0.180*GA
GA = 13.969 + 4.976*BW
B6D2F2
BW = -2.151 + 0.171*GA
GA = 13.231 + 4.482*BW

Dye Insertion

Labelling of axonal membranes was achieved using crystals of the fluorescent carbocyanine dye DiI (1,1'-dioctadecyl-3,3,3',3'-tetramethylindocarbocyanine perchlorate) and the aminostyryl probe DiA (4-(4-dihexadecylaminostryryl)-N-methylpyridinium iodide) (Molecular Probes, Oregon). The brain was extracted from the skull and the caudal parts of the occipital and entorhinal cortices were removed to expose the hippocampal fimbria. A crystal of either DiI or DiA, between 30 and 50μm in diameter, was placed in the area of the hippocampal fimbria using the tip of a fine dissecting pin. Most brains were double-labelled; either the right and left fimbria were labelled with contrasting dyes, or both fimbria were labelled with one dye and the frontal cortex (if applicable) was labelled with the contrasting dye (see Fig. 1.2). After insertion of dye crystals, the brains were placed in fresh fixative and stored in the dark at room temperature for at least 4 weeks, although some brains were stored up to two years with no apparent loss of labelling quality. Some brains were stored at 37°C to increase the rate of dye diffusion (Senft, 1990).

Sectioning and Photography

Sections were cut using a microslicer (DSK - DTK 1500E) and a sapphire knife (Pelco). Preliminary results indicated that tissue at these young ages suffered extensive damage due to shear stress during cutting, particularly at ages where midline fusion was limited and only one or two axons were crossing midplane. Gelatin infiltration was found

Fig. 1.2. Dye Crystal Placement. Typical placement of dye crystals (*) within the frontal cortex (a) and in the hippocampal fimbria (b). Several crystals were inserted in different spots in the frontal cortex to maximize the number of callosal fibres labelled. The dashed line in (a) is the approximate location of the cut made to expose the fimbria. Using a stereomicroscope, the brain was placed on its frontal pole and supported at each temporal pole using a pair of fine Graefe forceps. A thin vibratome blade was used to make the cut through the hippocampus, using the forceps as a guide for the cut. Only one cut was made through the brain to prevent excess damage.

a

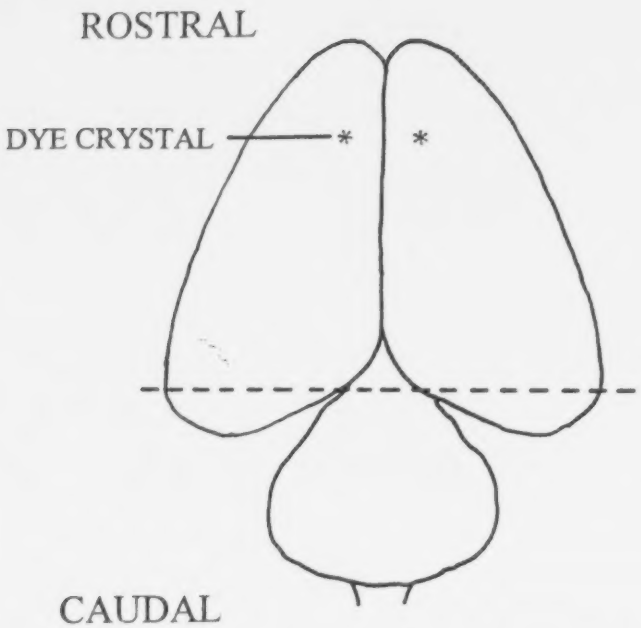
ROSTRAL
DYE CRYSTAL
CAUDAL

b

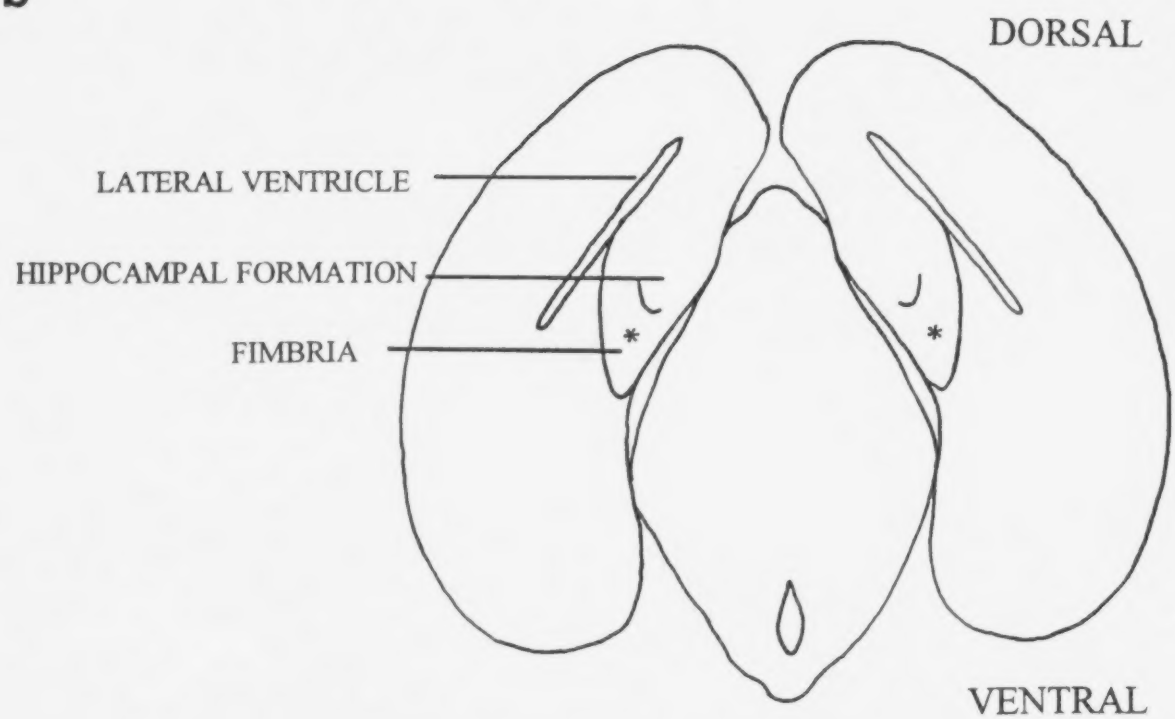
DORSAL
LATERAL VENTRICLE
HIPPOCAMPAL FORMATION
FIMBRIA
VENTRAL

to provide the necessary structural support. The brains were first rinsed in 0.1M phosphate buffer for 2 hours at 37°C. They were then infiltrated with 2% gelatin at 37°C for 6 hours, and then with 5% gelatin at 37°C for 12-24 hours, after which the gelatin was fixed using 4% paraformaldehyde for 48 hours at 4°C. The brain was removed from the fixative and glued caudal surface down to the microslicer stage using a cyanoacrylate glue. Coronal sections cut at 30-60μm were submerged in a 1:1 mixture of 8% paraformaldehyde in 0.2M phosphate buffer (pH 10.0) and glycerin at 4°C overnight and then mounted on glass slides using the same solution and coverslipped. To provide staining of cell nuclei, 0.02% bis-benzimide was added to the overnight solution of certain sections (Senft, 1990).

Most sections were immediately viewed and photographed with a Leitz epifluorescence microscope equipped with a rhodamine filter for DiI (N2) and a band-pass filter for DiA (L3). In some cases a fluorescein filter set was used (I2/3) to view DiA. Best results for photography were obtained using Kodak P800/1600 Ektachrome film at 1600 ASA, primarily due to the low intensity of the DiA viewed using the L3 filter. Sections not immediately photographed were stored at 4°C until viewing was possible (usually within 48 hours). Certain brains were viewed using a Leitz Confocal Laser Scanning Microscope (provided by the Dept. of Anatomy, U. of Alberta) and a Molecular Dynamics CLSM, to provide a more enhanced view of axon movement and location.

RESULTS

In all brains, clear and complete growth cones could be observed, indicating complete

anterograde transmission of the dyes. In older embryos retrograde labelling also provided information about commissural axon origins, although this labelling was often more difficult to observe due to contralateral labelling. No evidence of transcellular labelling was found. Gelatin infiltration did not appear to interfere with the observation of either dye, nor did it appear to facilitate further diffusion of either dye. The bis-benzimide gave a clear view of the pia membrane and other cells that were present in the midline region. In most animals, all of the axons within the hippocampal commissure appeared to be labelled, although there were some older embryos in which the dye did not include all HC fibres.

Body Weight vs. Chronological Age

Chronological age is a poor indicator of mouse embryo development (Wahlsten and Wainwright, 1977). A more accurate assessment of developmental stage in the brain is provided by the body weight of the embryo (Ozaki and Wahlsten, 1992; Wahlsten and Bulman-Fleming, 1994). Although brain weight would be the most accurate measure of developmental stage within the brain, removal of the brain from the skull increases the risk of tissue damage, particularly at the delicate telencephalic midline where there may only be a few axons or cells conjoining the two hemispheres.

Fig. 1.1 shows the approximately linear relationship between body weight and chronological age of gestation between E14.5 and E16.5 in B6D2F$_2$ embryos, which is similar to previous results (Ozaki and Wahlsten, 1992; Wahlsten and Bulman-Fleming, 1994). No significant difference was found in development rate between the B6D2F$_2$,

$C129F_2$, and BALB embryos, although the $C129F_2$ embryos appeared to lag about half a day and the BALB embryos lagged about 1 day behind the $B6D2F_2$ embryos. The 129 embryos demonstrated a higher rate of development than all other strains but also displayed a more pronounced lag of about 1.5 days in their development.

HC Development in $B6D2F_2$ Embryos

The descriptions of axonal movement and growth that follow were based on the observations of all embryos within four time periods: prior to midplane crossing by HC axons, initial midplane crossing by HC axons, general growth of the HC, and the early midplane crossing by callosal axons. Specific observations were sometimes limited to only a few embryos, but were inferred to be accurate for all embryos if the observations fit within the general pattern of observations seen in embryos that were less and more mature.

The columns of fornix were present in the septal midline region of the youngest embryo at 0.259g (Fig. 1.3a). From the dye insertion site, the hippocampal axons moved rostrally and medially through the brain and then turned sharply ventromedially towards midline, just rostral to the lamina terminalis which is defined here as the most anterior border of the third ventricle. Upon reaching the midline area, the fornix columns turned ventrally towards the anterior commissure. The columns of the fornix were initially far apart, largely due to the presence of the longitudinal cerebral fissure which extended deep between the hemispheres with its floor located just above the anterior commissure (Fig. 1.3b). As growth continued, fusion of the telencephalic vesicles progressed dorsally and rostrally, and the

fornix columns rapidly thickened and moved closer to midplane. Axons appeared to grow along the dorsal surface of existing fornix fibres toward midplane with extensive branching apparent. These axons were identified by their large and complex growth cones (see Fig. 1.4). Axons migrating within the fornix column could not be differentiated due to the fluorescence of the surrounding fibres.

As the columns of the fornix made their ventromedial turn, some axons emerged and moved towards midline, even in the youngest embryo (see Fig. 1.3a). These axons moved through the cells forming the medial border of the septal area and contacted the pia membrane lining the longitudinal fissure. In younger embryos, contact at the pia did not appear to be directed to any particular location along the depth of the fissure. Shortly before the first midplane crossing of the HC axons, most of the contact with the pia was very close to, but not necessarily directly at, the bottom of the fissure. After contacting the pia, many of the growth cones turned ventrally and migrated along the pia (Fig. 1.4). No growth cones were seen to turn dorsally. Axons emerging from the fornix fibres were seen all along the length of the ventromedial progression of the fornix column (Fig. 1.4). With increasing maturity, newly arriving axons continued to travel along the dorsomedial surface of existing fibres, providing increased contact between these fibres and the pia membrane. However, these axons were prevented from crossing by the continued presence of the pia-lined cleft at midline (Fig. 1.3b). Prior to the first crossing, these axons turned away from midline and reentered the fornix column, becoming indistinguishable from the surrounding fornix fibres.

As development proceeded, the floor of the longitudinal fissure continued to move dorsally as the midline fused. The first HC axons to cross midline remained in contact with

Fig. 1.3. Development of the Hippocampal Commissure in Mouse Embryos. (a) Well-formed columns of fornix can be seen in the midline region about 800μm from the frontal pole at 0.259g body weight in normal B6D2F$_2$ embryos. One DiA-labelled axon can be seen extending out of the column towards midline. This particular axon has contacted the pia membrane lining the longitudinal fissure (arrows). *(b)* The cleft formed by the longitudinal fissure (shown by arrows) extends deep between the hemispheres and prevents hippocampal axons from crossing midline early in development as shown in this 0.345g BALB embryo. *(c)* A complex growth cone contacting the pia membrane in a 0.490g BALB embryo. The lower process from this cone (arrow) is extending ventrally to cross midline. Other growth cones may make contact farther up the fissure, but they typically proceed in a similar way. *(d)* A typical early axon crossing shown here in a 0.595g 129 embryo, but which appears similar in all other strains. Note that the small bundle of crossing axons is at the immediate base of the longitudinal fissure (arrow). *(e)* DiI-labelled axon (indicated with arrows) extending across midline and continuing up the dorsomedial surface of the contralateral fornix in a 0.413g B6D2F$_2$ embryo. Although some axons were present in the middle of the fornix column, newly arriving and migrating axons were only seen on the dorsal surfaces of existing axons. *(f)* The bridge-like structure formed by the crossing HC fibres is shown in this 0.410g B6D2F$_2$ embryo. Some of the dye has diffused into the surrounding tissue, which in this section provides a descriptive view of the entire midline region including the future floor of the longitudinal fissure (solid arrows), and the cleft extending deep between the hemispheres to the point of fusion (open arrow). *(g)* Midsagittal section of the 0.620g B6D2F$_2$ embryo shown in Fig. 1.6. Several early DiA-labelled (green) callosal axons (arrows) which have just crossed the midplane can be seen sitting directly on top of the HC (red). *(h)* Confocal view of a midsagittal section during early callosal axon crossing in 0.692g B6D2F$_2$ embryo. Note that callosal axons appear as a bundle just rostral to the HC, but that individual callosal axons (arrows) have already extended across midline along hippocampal axons at the dorsal edge of the HC. (Scale: a - f, 50μm; g - h, 20μm)

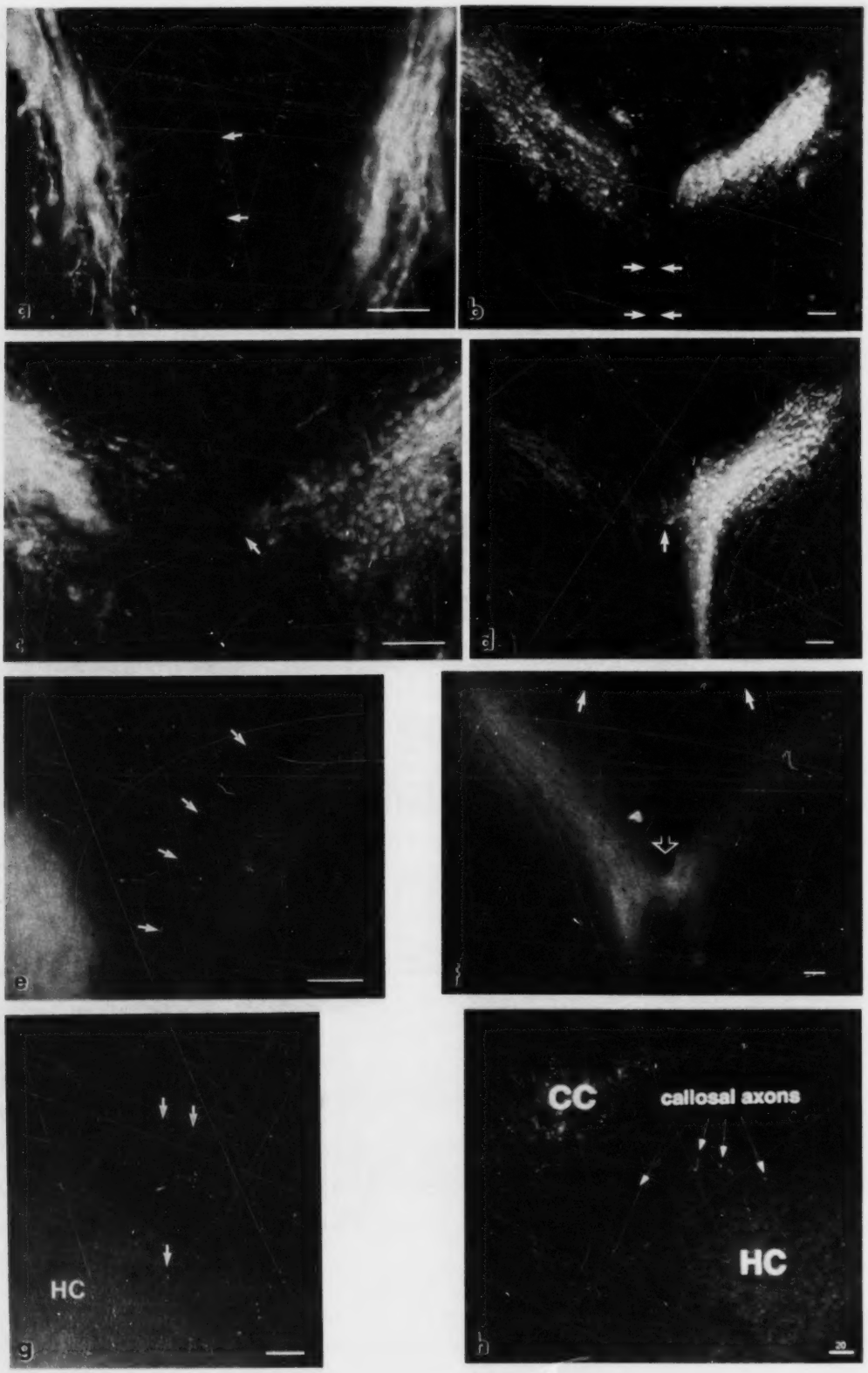
a
b
c
d
e
f
g
HC
h
CC
callosal axons
HC

Fig. 1.4. Early Fornix Presence in the Medial Septal Region. As development proceeds, the columns of fornix (F) move closer together in the septal region (S) and an increasing number of axons extend from the columns to contact the pia. In this 0.275g B6D2F_2 embryo the growth cone of one of these axons (arrow) has just contacted the pia and has started to migrate ventrally along the pia. Note the complexity in many of the growth cones seen. (Scale: 50μm)

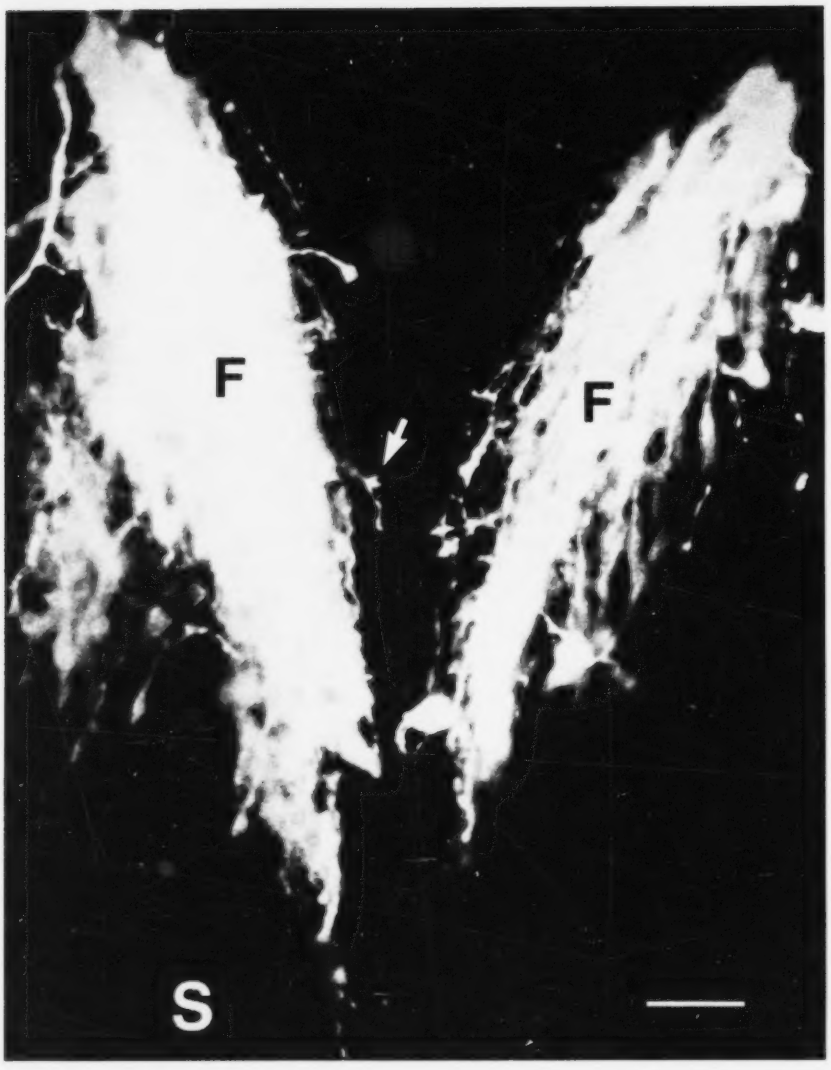
F
F
S

the pia membrane and followed the contour of the fissure floor (Fig. 1.3c). The first few axons did not appear to precede a large bundle of axons-in-waiting. Instead, an increasing number of fibres gradually emerged from the fornix column to cross. Later crossing axons were dorsal to those crossing previously but still followed along the fissure floor. The first two or three axons to cross did not necessarily associate with each other. Some axons were separated by as much as 60μm along the rostrocaudal axis and 40μm along the dorsoventral axis. However, a small cylindrical bundle of axons was very quick to form at the very base of the fissure (Fig. 1.3d) and subsequent axons were seen to fasciculate along these existing axons.

The initial crossing of midline was made earlier by axons from the right hemisphere in 6 of 8 brains labelled and viewed appropriately, whereas one brain showed a similar development between sides and one clearly had initial crossing from the left side. The earliest HC axon crossing was seen in the brain of a 0.328g embryo which was surprisingly well formed and was the only one to appear in this manner. In most embryos of this age, axons had not yet crossed or were just about to cross. Most of the early crossings occurred between 0.340g and 0.360g body weight, but several larger embryos were found with no crossing. The largest embryo with no crossing was 0.391g; the fornix columns were well formed but an unusually deep fissure continued to separate the hemispheres.

New axons approaching midline were seen along the dorsal surface of the ipsilateral fornix and then across midline on top of existing HC fibres. They continued up the dorsomedial surface of the contralateral fornix and fimbria up to their target areas in the hippocampal formation (Fig. 1.3e). Soon after initial crossing, individual axons were still

apparent; however by 0.400g a larger bridge-like structure spanned midline (Fig. 1.3f). Continued growth dorsally and rostrally resulted in a bridge that was roughly cylindrical in shape at midline with a dorsal-ventral height of about 200μm at 0.620g body weight. Fig. 1.5 shows the rate of dorsal growth of the HC during this time of gestation. The initial formation of the HC bridge occurred at the bottom of the longitudinal cerebral fissure and by 0.600g the gradual accumulation of axons in the HC eventually reached or surpassed the dorsal limit of the primordium of the subfornical organ just caudal to the HC (Wahlsten and Bulman-Fleming, 1994). Fusion of the hemispheres in the regions ventral and posterior to the HC appeared to be complete, but the zone directly anterior to the HC was initially filled by a loose plexus of fibres that later became the cavum septi pellucidum (Hankin, Schneider, and Silver, 1988).

The visibility of individual HC fibres crossing midline was limited to those on the dorsal surface. These axons did not tightly fasciculate along other fibres but rather formed a loose association. By about 0.450g, some axons had travelled far enough into the contralateral hemisphere to be labelled by the dye inserted into the fimbria. In cases where the dye was transported retrogradely, cell bodies that were labelled appeared primarily in the CA3 region of the hippocampus (Swanson and Cowan, 1977).

Interaction Between HC and CC Fibres

Callosal axons were seen crossing midline in association with hippocampal axons as early as 0.485g, but these callosal axons originated from the cingulate cortex and not the

Fig. 1.5. Growth of the Hippocampal Commissure in Normal Hybrid Mice. Growth of the HC in B6D2F$_2$ embryos occurs in a fairly linear manner from the time of early crossing to about 0.7g body weight. Thickness reaches about 200μm by about 0.6g body weight.

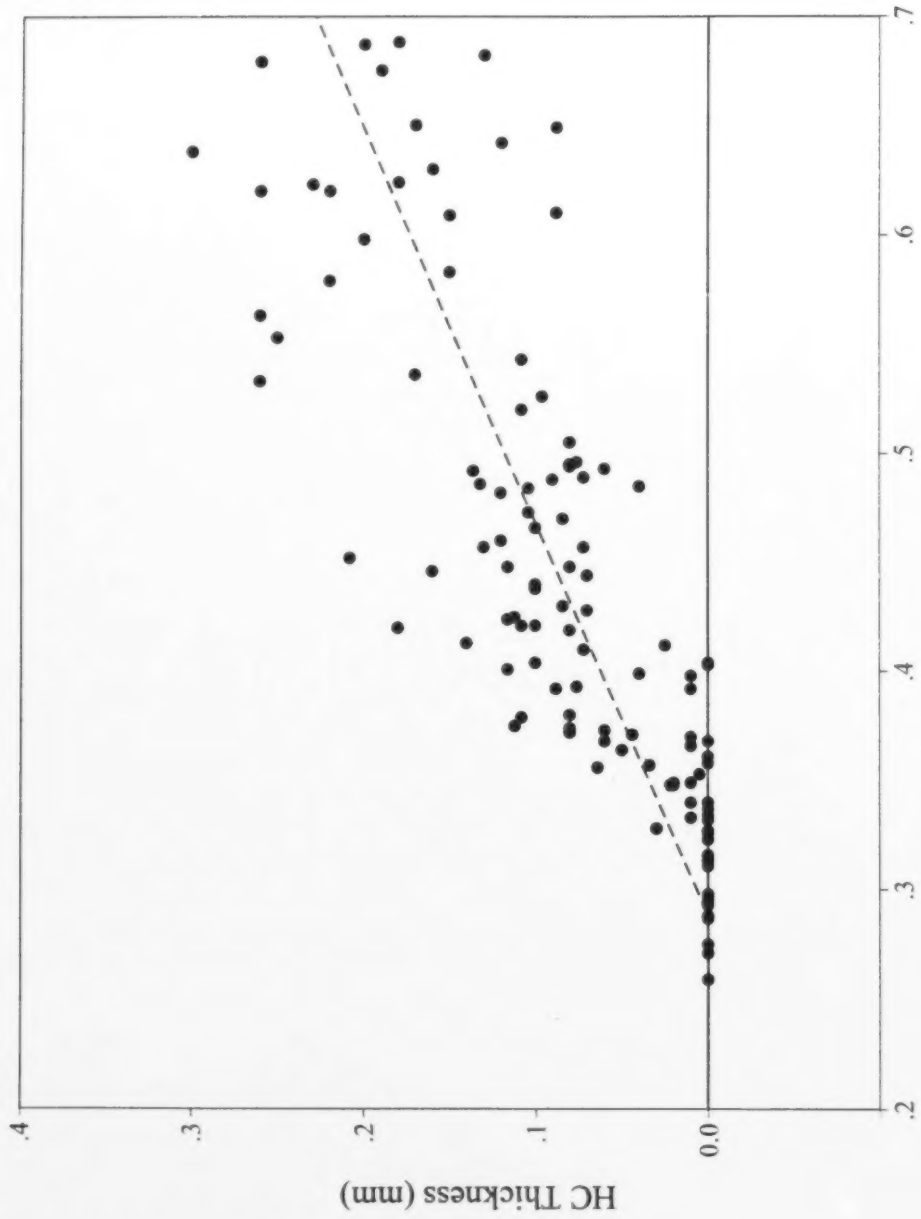
HC Thickness (mm)
.4
.3
.2
.1
0.0
.2
.3
.4
.5
.6
.7
Body Weight (g)

frontal cortex. Axons have previously been shown to emerge from the cingulate cortex and cross midline this early in the development of rats (Koester and O'Leary, 1994). The first definitive crossing of CC frontal cortex fibres occurred in an embryo of 0.620g. Fig. 1.6 is a parasagittal view of this brain in which all of the labelled callosal fibres are emerging from the cortex and growing directly towards the HC. Fig. 1.3g is a midsagittal view from this same embryo. A few callosal axons can be seen directly on top of the HC while a few other fibres appear at the rostral edge. Confocal reconstruction showed that these axons reached midway through the adjacent section, after which there was a gap of about 30μm before axons from the contralateral hemisphere could be seen. This is the first time the early crossing of callosal fibres has been seen with such clarity and precision. The callosal axons did not follow a continuous straight path, but rather appeared to weave between, and fasciculate along, the loose association of hippocampal axons at the dorsal HC edge.

Fig. 1.3h is a confocal image of the midsagittal plane from a 0.692g embryo which shows several callosal axons intermixed among the hippocampal axons at the dorsal edge of the HC. Callosal fibres rapidly form a small bundle on top of the HC and by 0.700g the CC appeared relatively large, just dorsal and rostral to the HC in most brains. A layer of cell bodies was seen immediately ventral to the callosal fibres in the area rostral to the HC, but cell body presence was almost non-existent at the interface between the HC and CC. These cells were likely the sling cells described by Silver *et al* (1993). Cell bodies were seen as a wedge-shaped mass along the medial edge of the lateral ventricle at the level of the floor of the longitudinal fissure as early as 0.586g, but no cell bodies were seen to span the hemispheres in a bridge-like structure until 0.682g, when they were located rostral to the HC

Fig. 1.6. Parasagittal Approach to Midline by Callosal Axons. Parasagittal section of a 0.620g B6D2F_2 embryo showing the callosal axons (CC) extending down from the frontal cortex directly in line with the top of the hippocampal commissure (HC). At the midsagittal plane, the callosal axons were seen crossing directly on top of the HC in association with hippocampal axons (see Fig. 1.3g). (Scale: 50μm)

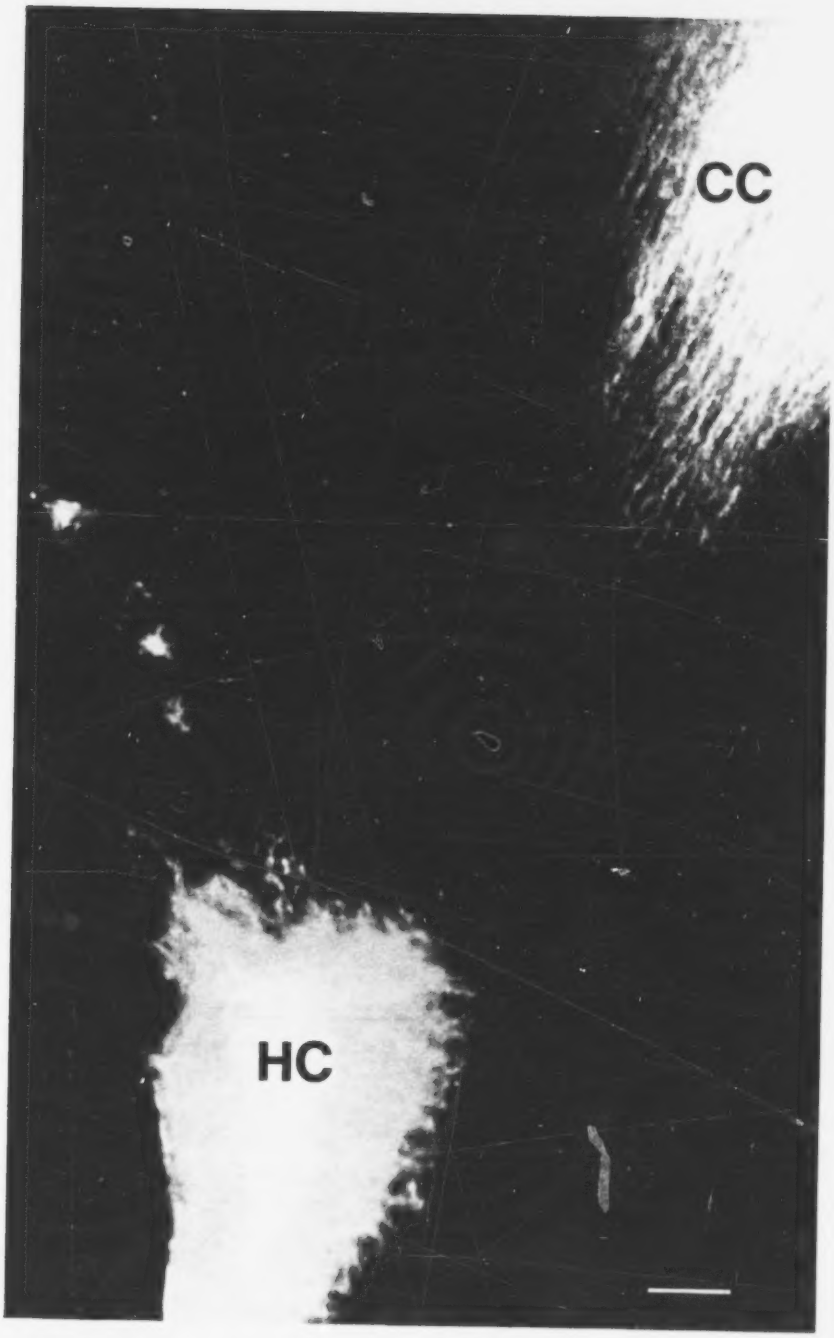
CC
HC

and ventral to a well-formed CC.

HC Development in Acallosal Mice

The pattern of development in the acallosal strains was remarkably similar to that in the B6D2F_2 embryos up until the time of first crossing. Fornix columns were present early and axons emerged from the columns to extend to midline, but the cleft formed by the longitudinal fissure remained deep, long past the time of first crossing in B6D2F_2 mice (Fig. 1.7). As indicated in Fig. 1.8, HC axons first crossed midline at about 0.470g in BALB embryos and at about 0.520g in 129 embryos. The time of first crossing for the C129F_2 embryos was at 0.440g, earlier than either of the parent strains, but in the RI-1 embryos it was necessary to extend the body weight range of collected embryos in order to see any evidence of hippocampal axon crossing, which eventually occurred much later than any of the other strains at about 0.750g. Despite the obvious delay in crossing, the first HC axons in RI-1 embryos crossed midline at the ventral tip of the longitudinal fissure and appeared to remain in contact with the pia membrane as they crossed, similar to the B6D2F_2 embryos. In the RI-1 embryos, callosal axons were seen in the midline region after about 0.600g and had begun to form Probst bundles in the larger embryos. The differences in crossing times between the acallosal strains is correlated with their adult expression of the CC defect (see Table 1.2)

Fig. 1.7. Extension of the Interhemispheric Fissure into the Medial Septal Region. Coronal section of a 0.503g BALB embryo stained with bis-benzimide. The non-stained areas show the location of hippocampal axons (HC) which are definitely in the correct location for crossing. These axons are not able to cross due to the small cleft (arrows) which can be seen still extending down directly in the middle of the septal region (S) where crossing would have occurred. (Scale: 50μm)

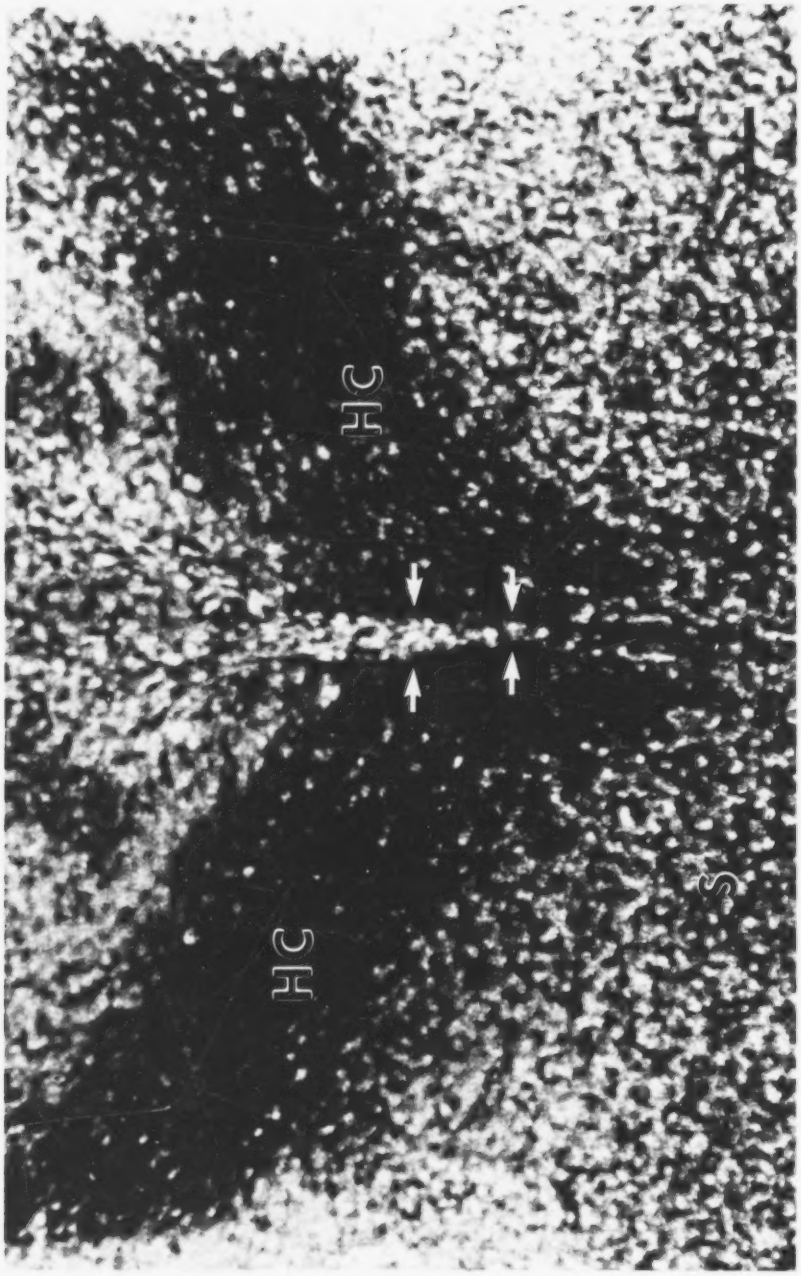
HC
HC
HC
S

Fig. 1.8. Comparison Among Strains of Their HC Axon Crossing Times. Crossing of the telencephalic midline by hippocampal axons in all strains. Inverted triangles (▼) indicate embryos in which crossing has not yet occurred, while those pointing up (▲) indicate crossing has occurred. Arrows indicate the approximate median weight of first crossing for each strain, which occurs at about 0.350g in B6D2F_2 embryos, at about 0.470g in BALBs, 0.520g in 129s, 0.440g in C129F_2 embryos, and approximately 0.750g in RI-1 embryos. Crossing appears to be increasingly delayed in strains with a higher frequency of CC defect.

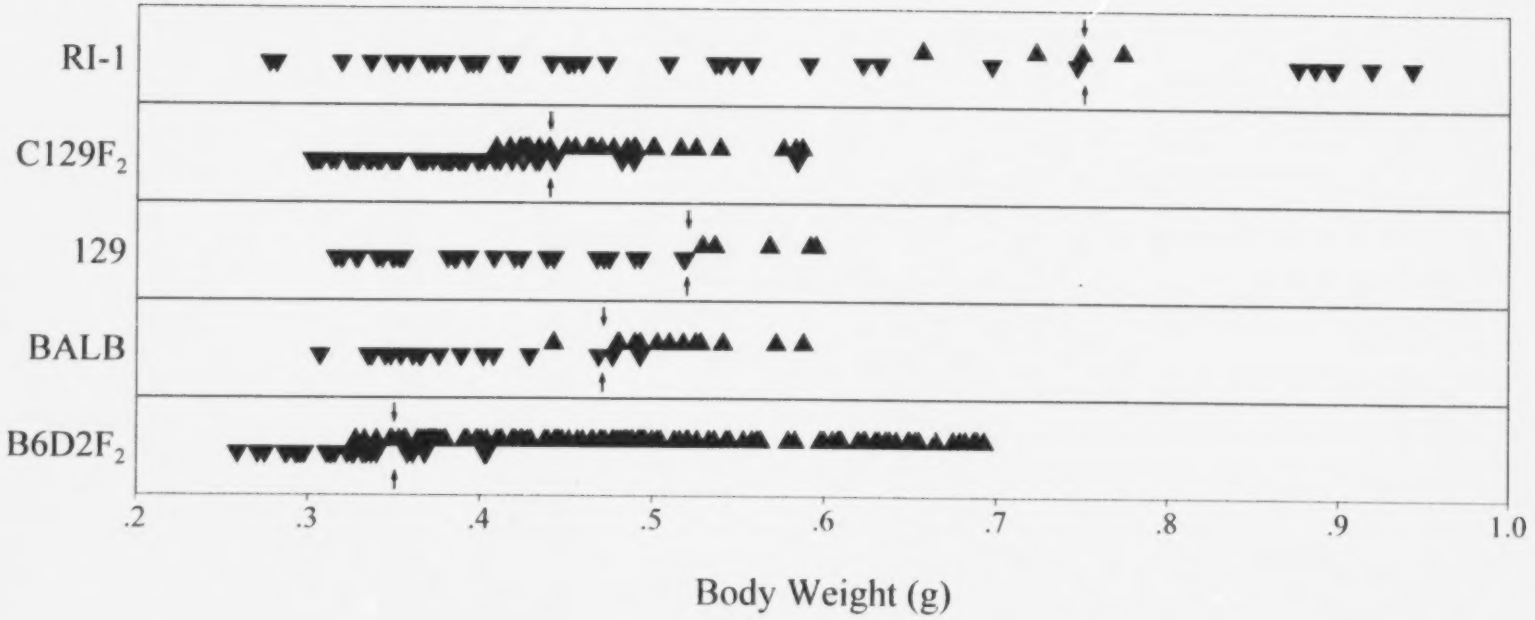
RI-1
C129F2
129
BALB
B6D2F2
.2
.3
.4
.5
.6
.7
.8
.9
1.0
Body Weight (g)

Table 1.2: Frequency of Callosal Absence and Defect in Relation to the Time of Initial Crossing by Hippocampal Axons.

STRAIN	% CC ABSENCES	% CC DEFECT	INITIAL HC CROSSING (g)
B6D2F$_2$	0[ce]	0[ce]	0.350
C129F$_2$	24[dg]	33[dg]	0.440
BALB/cWah1	20[c]	55[ac]	0.470
129/J	16.67[f]	70[b]	0.520
RI-1	100[dg]	100[dg]	0.750

[a]Livy and Wahlsten (1991)
[b]Wahlsten (1982)
[c]Wahlsten (1987)
[d]Wahlsten and Schalomon (1994)
[e]Wahlsten and Smith (1989)
[f]Ward, Tremblay, and Lassonde (1987)
[g]unpublished observations

Growth Cone Structure

Growth cone size and complexity changed during the growth of the hippocampal axons through the midline region in mice from the $B6D2F_2$ and acallosal strains. Prior to the first crossing, almost all growth cones emerging from or along the dorsomedial surface of the fornix columns were large and complex with extensive branching, particularly in those axons closest to the base of the longitudinal fissure (see Fig. 1.3b). Growth cones that had contacted and were migrating ventrally along the pia remained larger but no longer displayed the same degree of extensive branching (see Fig. 1.4). An abrupt change in structure was usually noted in axons that had just crossed midline. A complex structure was maintained right up to midline, from which a single fibre emerged and continued up into the contralateral hemisphere (Fig. 1.9a). Growth cones of those axons that had crossed midline were all smaller with a very simple, flat morphology. Early after the initial crossing, individual growth cones could still be seen as axons approached and crossed midline. However, once the commissure had formed into a small bundle, only those axons immediately on the dorsal surface could be seen. Of these, most growth cones were small and simple in structure.

The variability in the sizes and shapes of growth cones prior to midline crossing is shown in Fig. 1.9b and is contrasted with growth cones of axons after crossing midline. This structural variability has also been found in the first callosal axons to approach midline (Ozaki and Wahlsten, 1993). Growth cones continually change their shape during axonal growth (Godement, Wang, and Mason, 1994; Halloran and Kalil, 1994) and the variability seen must result at least partly from the snapshot view of growth cone structure at the time

Fig. 1.9. Growth Cones of Hippocampal Axons at the Telencephalic Midline. (a) Diagram of an axon which has just crossed midline. The complex growth cone can be seen along the medial edge of the fornix column (F) contacting the base of the longitudinal cerebral fissure (LCF) right at midplane (long dashed line), from which a single simple process has emerged. *(b)* A brief representation of growth cones from axons prior to midplane (M) crossing, and after, in which the change to a much simpler morphology after crossing is evident. (Scale: 50μm)

a
LCF
F
b
M

of fixation.

DISCUSSION

The results clearly indicate that the first hippocampal axons to cross midline travel over the dorsal septum and along the pia membrane lining the longitudinal fissure. These axons appear to remain in contact with the pia membrane as they cross but no axons penetrate the membrane. These axons do not appear to precede a larger "main bundle" of axons as is seen in callosal axon outgrowth (Ozaki and Wahlsten, 1992); instead axon emergence is continual and gradual from the fornix columns. Earlier axons emerging from the fornix columns migrate toward midline but are unable to cross due to the presence of a deep cleft formed by the longitudinal fissure.

Dorsal fusion of the fissure eventually enabled midline crossing by the hippocampal axons at about 0.350g or E14.8 in B6D2F_2 embryos. Axons arriving earlier migrated ventrally along the pia to the approximate location of crossing and then re-entered the fornix columns. This is in contrast to callosal axons that will wait a few hours for midline development to support their crossing (Ozaki and Wahlsten, 1993). Delayed development results in callosal axons forming a large Probst bundle (Probst, 1901) from which axons will either cross midline if development allows (Ozaki and Wahlsten, 1993), or will emerge to make ipsilateral connections (Ozaki and Shimada, 1988). Axons within Probst bundles formed by surgical transection of the midline region during the time of callosal development retain their electrical function, and in the neonate they are able to emerge from the bundle

and cross midline after the insertion of a nitrocellulose bridge (Lefkowitz, Durand, Smith, and Silver, 1991). Hippocampal axons that failed to pass through the HC in the most severely affected acallosal embryos appeared to rejoin the columns of the fornix rather than form a local whorl, although their eventual fates are unknown.

The results also provide clear support for the use of the HC by early callosal axons to cross midline. These CC axons fasciculated along and between the hippocampal axons at the dorsal edge of the HC. This is the first time that CC axons have been clearly seen to directly associate with hippocampal axons during their traverse of midline this early in the development of a normal mouse. Wahlsten (1987a) has observed CC axons crossing on the dorsal surface of the HC in an acallosal mouse strain, but this was much later in development and the resulting CC was often abnormal in size and shape. The role of these early callosal axons remains unclear. Although they may provide structural support for subsequent callosal axons during midline crossing, early dye-labelled "main bundles" of callosal axons were usually seen at the dorsal-rostral edge of the HC. A more comprehensive distribution of cortical dye placements would demonstrate whether a main bundle of callosal axons was also present immediately dorsal to the HC. The early callosal axons may act as pioneers for the main bundles, establishing the existence of an intact substrate for crossing and perhaps effecting a signal change for main bundle crossing.

The earliest callosal axons to interact with the HC axons originated from the cingulate cortex. Koester and O'Leary (1994) reported an early emergence of callosal axons from the ventromedial cingulate cortex in the rat and have suggested that these axons may act as pioneers, defined as the first axons to cross midline, for the corpus callosum.

Although these cingulate axons may be the first callosal axons to cross midline, their use as a structural support by callosal axons from the cerebral cortex is questionable. Fasciculation along the cingulate axons would obviate the need for sling cells guiding the cortical callosal axons to midline, however callosal axons have been shown to orient toward midline after contacting the lateral wedge of sling cells (Wahlsten, 1987a). Also, axons that use an existing axon pathway for directional guidance often display a simplified growth cone morphology (Dodd and Jessell, 1988; Harrelson and Goodman, 1988), yet growth cone morphology is complex in early cortical callosal axons first approaching midline and then less complex after crossing (Ozaki and Wahlsten, 1992).

Growth cone complexity is thought to be related to environmental assessment occurring within the cone (Bovolenta and Mason, 1987; Norris and Kalil, 1991; Tessier-Lavigne and Placzek, 1991); however it may also be a characteristic of neuronal origin (Nordlander, 1987). Callosal axons continue to display some degree of complexity during their growth through the contralateral hemisphere until they migrate up into their cortical target sites (Norris and Kalil, 1990; Halloran and Kalil, 1994). Growth cone complexity was also demonstrated by the hippocampal axons approaching midline, although less so in those migrating along the pia, and for a short distance into the contralateral hemisphere as these axons made critical decisions about direction of travel. Once crossing was complete, growth cone complexity appeared to markedly decrease, corresponding to the appearance of axons fasciculating along existing axons.

The cell bodies that formed a wedge towards midline from the longitudinal fissure are likely the sling cells purported to provide support for early crossing callosal axons.

These cells did not span midline until well after early callosal axon crossing and then only in a position rostral to the HC. Their presence lateral to midline at the time of callosal axon crossing may provide a barrier to prevent callosal axon entry into the septal region (Hankin and Silver, 1986) and may guide the CC fibres in the direction of midplane (Wahlsten, 1987a). A similar sling structure has been identified in the cat (Silver, *et al*, 1985) and rat (Katz, *et al*, 1983). Cells covering the surface of the sling have been identified as primitive astrocytes and radial glial cells (Hankin and Silver, 1986). Silver *et al* (1993) identified primitive astroglial and radial glial cells at midline prior to the arrival of callosal fibres but no cell bridge was seen until later in development when callosal axons had already crossed.

The sling has been thought to be critical for successful callosal formation because damage to the sling occurring naturally (Wahlsten, 1987a) or by experimental intervention (Silver and Ogawa, 1983; Schmidt and Lent, 1987) results in the absence of callosum formation; however, such damage also extends to other structures, including the HC, which may have a direct impact on callosal axon crossing. Although damage to these structures may result in Probst bundle formation rostral and dorsal to the HC (Silver *et al*, 1982), this does not necessarily indicate the site of first crossing by callosal axons, as suggested by the variability in Probst bundle positioning described by Ozaki and Wahlsten (1993). Hankin and Silver (1988) have indicated that the sling cells form a floor along the ventral surface of the rostral CC, dorsal to the cavum septi pellucida, which axons do not penetrate. Such a floor for callosal axons would also constitute a ceiling for HC fibres, yet the movement of the hippocampal axons crossing on the dorsal surface of the HC did not appear to be influenced by any overlying structure and, in fact, callosal axons have been shown

intermingling and fasciculating along with hippocampal axons during midline crossing.

During CC formation in the cat, axons from the visual cortex form a transient projection through the sling into the ipsilateral fornix, suggesting that these axons were able to pass through the sling cells or were present prior to sling cell arrival (McConnell, Ghosh, and Shatz, 1994). This may also explain the interaction between hippocampal and callosal axons; they may interact before the sling cells bridge the hemispheres, or the axons may be able to penetrate through any sling cells or processes that may be present. Both the HC and sling may be essential for successful formation of the intact CC. The polygenic involvement and incomplete penetrance associated with the CC defect in several of the acallosal mouse strains (Wahlsten, 1982d) suggests that more than one structure may be involved in guiding the callosal axons across midline. However, the intimacy expressed between these HC and CC fibres very early in CC development indicates the particular importance of normal HC development for normal CC development.

This importance is clearly demonstrated in the acallosal strains. HC development in these strains was delayed by the continued presence of the longitudinal fissure extending deep between the hemispheres. The eventual time of initial crossing by the HC axons was later in strains with a more severe incidence of adult CC defect. Initial crossing occurred at about 0.470g or E16.25 in BALB embryos and about 0.520g or E16.5 in 129 embryos. Because most adults of these strains have a normal HC structure (Livy and Wahlsten, 1991), it is likely that HC development continues normally once the axons do cross midline (Wahlsten, 1987a). However in the strains I/LnJ and RI-1 with 100% total CC absence, adult HC structure is often abnormal (Livy and Wahlsten, 1991). Initial crossing by hippocampal

axons may be too late to permit the normal growth of the HC. In the RI-1 embryos, first crossing was estimated as about 0.750g or E17.5, but there were several older embryos that had not displayed crossing. HC absence in adult mice has never been reported, and therefore it can be presumed that the HC axons do eventually cross in all animals. This suggests there is a large window of competence for these axons to cross midline. Callosal axons in RI-1 mice arrive at midline prior to first crossing by the HC axons and must wait for these axons to cross and then for the HC to grow to the proper position to support callosal axon crossing. The callosal axons eventually grow back into the ipsilateral hemisphere to form Probst bundles before this can occur (Ozaki, Murakami, Toyoshima, and Shimada, 1987; Wahlsten, 1987a; Ozaki and Shimada, 1988). Therefore, the crossing of the interhemispheric fissure by callosal axons appears to be directly affected by the time of initial crossing by the hippocampal axons.

The substrate used by commissural axons crossing midline is often specific for that event. Commissural axons display an affinity for specific glial cells in the grasshopper (Bastiani and Goodman, 1986) and in Drosophila (Jacobs and Goodman, 1989). In the mammalian forebrain, neurons and radial glia have been identified at the site of the prospective optic chiasm and are thought to be required for the successful formation of the chiasm by retinal ganglion cell axons (Marcus and Mason, 1995; Marcus, Blazeski, Godement, and Mason, 1995; Sretavan, Puré, Siegel, and Reichardt, 1995). Axons of the anterior commissure cross midline through the medial septum dorsal to the preoptic recess using a tunnel-shaped formation of glial cell processes (Silver *et al*, 1982). In vertebrates, floor plate cells have been identified in the ventral midline of the spinal cord and brainstem

which release a diffusible chemoattractant that orients spinal commissural axon growth in vitro (Tessier-Lavigne, Placzek, Lumsden, Dodd, and Jessell, 1988; Placzek, Tessier-Lavigne, Jessell, and Dodd, 1990), and may provide a physical substrate for these axons to cross midline (Bovolenta and Dodd, 1990; Kuwada, Bernhardt, and Chitnis, 1990; Yaginuma, Homma, Kunzi, and Oppenheim, 1991). The lack of these cells disrupts the normal pattern of axon crossing (Bovolenta and Dodd, 1991). It is possible that similar events occur during hippocampal axon crossing; early axons that emerge from the fornix columns and grow toward midline may be orienting in response to a chemoattractant. Such chemical signals may emanate from the pial cells lining the longitudinal fissure, which would explain the early axon emergence toward the pia from the fornix column; however, the greater growth cone complexity and extensive branching seen in axons approaching the area immediately ventral to the fissure suggests that chemical signals are released from the area of hemispheric fusion, perhaps due to the degradation of the trapped pia membrane. Once these axons contact the pia membrane they grow along the pia across midline. In some embryos, axons reached the midline but did not cross despite the lack of an obvious obstruction. This may indicate the necessity of a second event for completion of the crossing event which is likely to be specific for the substrate that provides physical guidance to the crossing axons. The proximity between axon and pia suggests that the pia provides this contact guidance, although it is known that later in development the pia does not act as a substrate for callosal axons, even when their usual midline substrate is missing in BALB mice (Wahlsten, 1987a).

Differential staining with lipophilic dyes has demonstrated the interaction between

callosal axons and hippocampal axons when early callosal axons cross midline. Although bis-benzimide labelling did not show any cells at midline, this does not preclude the presence of cell processes which could also aid the growth of axons across midline. Combining carbocyanine dye labelling with immunohistochemical techniques (Elberger and Honig, 1990) should enable the observation of axon interaction with specific substrate antigens. Similarly, the use of photo-oxidized DiI with regular and/or immuno-electron microscopy (von Bartheld, Cunningham, and Rubel, 1990) should provide a very detailed view of hippocampal axons as they first cross midline to determine if they remain in contact with the pia or whether there is another substrate present. Increased precision in dye labelling should determine whether later axons also travel within the columns of fornix and the HC as well as on their dorsal surface. It should also permit the identification of developing projection patterns of the hippocampal axons. In adult rat HC, axons from more septal regions in the hippocampal formation are found in the more caudal areas of the HC, while those axons from the more temporal areas are found in the more rostral area; fibres arising from areas near the ependyma of the lateral ventricles cross in more dorsal regions of the HC, while those arising along the pial border cross through the ventral region (Wyss *et al*, 1980). Of particular interest is whether any particular axon can indeed cross within the commissure or whether only certain axons from particular origins cross the midline first.

EXPERIMENT 2

INTRODUCTION

The results of Experiment 1 suggest that the first hippocampal axons cross the telencephalic midline in close apposition to the pia membrane lining the longitudinal fissure and that the first callosal axons cross midline by fasciculating along existing hippocampal axons at the dorsal surface of the hippocampal commissure. Observation at the ultrastructural level is necessary to verify whether direct contact does indeed appear between these structures, or whether a third substrate is mediating that contact. Electron microscopy was used in conjunction with two specific preparation techniques to observe this contact. Fixation using tannic acid provides an excellent view of the apposition between membranes (Hayat, 1981) and was used to observe the apposition of hippocampal axons with the pia membrane. The differentiation of CC and HC axons is necessary to observe any interaction that may occur between them. Axons were labelled with DiI and/or DiA and the dyes were photooxidized using diaminobenzidine to produce a reaction product discernable at the electron microscopic level (Sandell and Masland, 1988; Bhide and Frost, 1991).

METHODS

EM Preparation for Hippocampal Axon - Pia Membrane Apposition

Two B6D2F_2 embryos from one litter at gestational age E15.1 with body weights 0.387g and 0.444g were perfused intracardially with 3-5mL of 10mM phosphate-buffered saline (pH 7.6) followed by 10-15mL of fixative consisting of 1% paraformaldehyde, 4% glutaraldehyde, and 0.01% tannic acid in 0.1M phosphate buffer (pH 7.3) followed by 40-50mL of 4% glutaraldehyde in 0.1M phosphate buffer. The brains were then extracted and one was blocked parasagitally (0.387g embryo), whereas the other was blocked coronally (0.444g embryo) by cutting off the caudal half of the brain through the thalamus. Each brain was rinsed in 0.1M phosphate buffer (2x30min), postfixed in 2% OsO_4 in 0.1M phosphate buffer for 4 hours, and then rinsed again in 0.1M phosphate buffer (2x15min). The brains were dehydrated through an ethanol series (1x15min 50%; 1x15min 70%; 2x15min 90%; 2x15min 95%; 2x20min 100%) and then rinsed in propylene oxide (2x20min). They were then infiltrated with a graded series of Epon 810 starting with a 1:2 mixture of Epon and propylene oxide and gradually increasing the concentration to pure Epon in which the brains were left for 48 hours. The brains were then placed cut side down onto a coverslip over which an Epon-filled embedding mold was placed. The Epon was cured for 48 hours at 60°C, after which the embedding mold was removed, and the tissue block dipped in liquid nitrogen to remove the coverslip.

Tissue blocks were trimmed by cutting 1μm thick sections using glass knives on a

Reichert-Jung Ultracut E ultramicrotome. Several thick sections were stained every 20-30μm using Toluidine Blue O to determine position within the brain and to provide information about angle-of-cut adjustment. Upon reaching the midsagittal plane and the coronal location of HC crossing, thin sections were cut using a DuPont diamond knife in the same microtome. Sections obtained were picked up on either 2x1mm copper slot grids or 1mm copper aperture grids. Certain grids were coated with either 0.25% Formvar or 0.25% Butvar, or carbon, or a combination of Formvar or Butvar and carbon. Sections were then stained for 2 hours using 4% uranyl acetate (aq) and for 1 minute with Sato's lead citrate (aq) and then viewed using a Philips 400 TEM.

Photooxidation of Di-Labelled Axons

Two B6D2F$_2$ embryos from an E16.75 litter with body weights 0.738g and 0.791g and one P0 neonate weighing 1.265g were extracted and/or perfused as described in Experiment 1. Brains were extracted from the skulls, and the lipophilic dyes DiI and DiA were inserted into the hippocampal fimbria and frontal cortex as described in Experiment 1. Coronal sections were cut at 100μm using a vibratome and steel blade from the P0 and 0.791g embryo brains, while the 0.738g embryo brain was sectioned horizontally at 200μm. Sections were cut and stored in PBS (pH 7.6). Sections were visually inspected and selected for the proximity of callosal and hippocampal axons to midplane. Selected sections were rinsed (1x5min) in Tris buffer (pH 8.2) and then submerged in a solution of 0.1% diaminobenzidine (DAB) in Tris buffer. The sections were photooxidized with a Leitz

Laborlux epifluorescence microscope equipped with filters for viewing both DiI and DiA using a 10x objective. After bringing the Di-labelled axons into focus, the sections were left under fluorescence excitation while submerged in the DAB solution for 60 minutes. Sections were then rinsed (2x10min) in Tris buffer and briefly viewed using a Leitz Dialux microscope to ensure that the brown photooxidation reaction product was present.

Sections were then processed for observation by electron microscopy. Selected sections were rinsed (2x10min) in 0.1M phosphate buffer (pH 7.4) and then post-fixed in 2% OsO_4 for 2 hours. Sections were then rinsed (3x10min) in acetate buffer (pH 5.2), followed by en bloc staining in 2% uranyl acetate in 0.1M sodium acetate for 2 hours and rinsed again (2x15min) in acetate buffer. Sections were then dehydrated through an ethanol series (1x10min 50%; 1x10min 70%; 2x10min 90%; 2x10min 95%; 2x15min 100%) and then rinsed in propylene oxide (2x15min). They were then infiltrated using a graded series of Epon 810 in propylene oxide beginning with a 1:2 mixture and gradually increasing to pure Epon which was left on the sections for 24 hours. Sections were then placed in an embedding mold in fresh Epon which was cured for 48 hours at 60°C. After curing, the embedding mold was cut away from the tissue block and the blocks were trimmed to expose the midplane region. Thick sections (about 1μm) were cut using glass knives on a Reichert-Jung Ultracut E ultramicrotome and stained using Toluidine Blue 0 and viewed to determine whether the position of cut was through the appropriate midline region. Thin sections (about 90nm gold) were then cut using a DuPont diamond knife and collected on copper grids varying between 50 - 200 mesh. These sections were then stained for 2 hours with 4% uranyl acetate (aq) and for 1 minute with Sato's lead citrate (aq) and then viewed using a

Philips 400 TEM.

RESULTS

Early HC Formation

The results from these observations were inconclusive. Section instability prevented accurate viewing; most sections disintegrated in the electron beam. The application of various grid coatings improved section stability in some cases, but usually proved too thick to provide informative resolution. Section thickness was increased with limited success also due to both instability of preparation and decreased resolution. An additional problem was noted with insufficient osmium penetration into the tissue.

HC - CC Interactions

Photooxidation of both DiI and DiA produced a brown-pigmented reaction product visible to the unaided eye and very clear under light microscopy. Unfortunately, no difference in reaction product colour was noticed between DiI- and DiA-labelled axons, preventing their visual differentiation. Examination at the EM level maintained this finding; no apparent difference was seen between DiI- and DiA-labelled axons. In sections from the brain with single-labelling in the HC, little difference was apparent in the appearance of axons that had received photooxidation of DiI from those oxidized by OsO_4 alone. In

sections not postfixed in OsO_4, a clear difference was seen between axons that were photooxidized and those that were not, however very little cytoarchitecture was apparent in these areas, likely due to the relatively mild fixation procedure to which these areas were exposed.

DISCUSSION

Despite the lack of obvious results from these experiments, these procedures should not necessarily be discounted as irrelevant for these purposes. An increased precision in tissue sampling (see Experiment 5) would provide a greater degree of section stability. The use of a high-powered electron microscope (about 500 kEV) would also enable the resolution of detail in thicker sections or in sections supported by a thick layer of medium. The use of photooxidized Di-labelling remains suspect as a means of providing differentiation between HC and CC axons, however it may be used in combination with immunoelectron labelling to provide a detailed description of the interaction between axons and their supporting substrates (von Bartheld *et al*, 1990; Smiley and Goldman-Rakic, 1993). The reconstruction of serial sections from electron microscopy (eg: Shoukimas and Hinds, 1978; Hall and Russell, 1991; Sorra and Harris, 1993) would also enable the detailed three-dimensional description of axon growth and substrate contact as axons make their way through the midline region. Until these technical considerations can be implemented, the exact relationship between the HC axons and the pia membrane will remain uncertain.

EXPERIMENT 3

INTRODUCTION

Axon outgrowth requires the presence of structurally supportive substrates such as glial cells or other axons (Raper, Bastiani, and Goodman, 1983; Hatten, Fishell, Stitt, and Mason, 1990; Wang, Baird, Hatten, and Mason, 1994). In acallosal mice, the continued extension of the interhemispheric fissure deep in the medial septal region would disrupt the presence of any substrates that would normally serve to provide structural support for commissural axons crossing midline. In normal mice, the growth of the septal region allows the medial hemispheric surfaces to fuse and moves the fissure farther anterior. The continued fissure presence in mice from acallosal strains suggests that they have a defect in the growth of the septal region; measurement of the midsagittal thickness of this region indicated that the rate of septal growth was indeed retarded in the acallosal strains (Wahlsten and Bulman-Fleming, 1994)

A reduction in the number of cells entering the septal region could result from a decrease in the rate of cell proliferation, a decrease in the number of cells actively undergoing mitosis, or a defect in the migration of postmitotic cells to their target sites. Cell proliferation initially occurs in the neuroepithelium, or ventricular zone, which is the layer of cells immediately adjacent to the lumen of the ventricle. Sauer (1935a,b, 1936, 1937) noted that the neuroepithelium consists of columnar cells that span the neuroepithelial layer

in a perpendicular orientation relative to the lumenal surface. Nuclei of these cells demonstrate interkinetic nuclear migration (Seymour and Berry, 1975), a radially oriented movement of the nuclei between the juxtalumenal surface (mitotic zone) and the (distal) deep ventricular layer (synthetic zone). The position of the nuclei denote their mitotic phase; nuclei in the synthetic zones are labelled one hour after short pulse ^{3}H-thymidine labelling (Sidman, Miale, and Feder, 1959) indicating that the nuclei are actively synthesizing DNA material, whereas nuclei in the mitotic zone display mitotic figures. The orientation of the mitotic spindles may indicate the fate of the daughter cells; those parallel to the lumenal surface produce daughter cells that remain attached to the lumenal surface (Sauer, 1935a,b), while daughter cells produced when mitotic spindles are oriented perpendicular to the lumen may then leave the ventricular layer (Smart, 1973; Zamenhof, 1987). The specific direction of parallel orientation may influence the direction of ventricular growth (Smart, 1985; Tuckett and Morris-Kay, 1985).

The subventricular layer (Boulder Committee, 1970) first appears in the area of the ganglionic eminences at E11 in the mouse (Smart, 1976; Sturrock and Smart, 1980) and E16 in the rat (Altman and Bayer, 1990). Subventricular cells are mitotically active; Smart (1976) indicated that the subventricular layer accounted for approximately 50% of dividing cells in the E14 mouse brain. By E15, mitotic activity in the ventricular layer decreased sharply, followed by a decrease in the subventricular layer at E16. The subventricular layer assumes the role of primary germinative layer after the differentiation of the neuroepithelium just prior to birth (Altman and Bayer, 1990), and maintains this role into adulthood (Paterson, Privat, Ling, and Leblond, 1973; Smart, 1976; Sturrock, 1979; McDermott and

Lantos, 1990). In the adult, the subventricular zone produces both neurons and glia (Blakemore, 1969; Privat and Leblond, 1972; Lois and Alvarez-Buylla, 1993). The glial cells differentiate to both oligodendrocytes and astrocytes (Paterson, 1983; Levison and Goldman, 1993).

Neuroblasts migrate out from the ventricular layer attached to radial glial fibres that span the area between the ventricular layer and the pia membrane lining the surface of the brain (Rakic, 1971, 1972; Hatten, 1990). The glial fibres span the cortical strata in fascicles, initially in a straight radial orientation from the ventricle, and gradually becoming arched as the relative positions of cortex and ventricle change during growth (Misson, Edwards, Yamamoto, and Caviness, 1988; Gadisseux, Evrard, Misson, and Caviness, 1989; Gadisseux, Kadhim, van den Bosch de Aguilar, Caviness, and Evrard, 1990; Misson, Austin, Takahashi, Cepko, and Caviness, 1991). The migration of daughter cells from one proliferative cell has been suggested to occur along specific fascicles of radial glia, producing an ontogenetic column of cells in the cortex (Turner and Cepko, 1987; Rakic, 1988; Wetts and Fraser, 1988), however tangential migration has been described using retroviral (Walsh and Cepko, 1988; Austin and Cepko, 1990), chimaeric (Balaban, Teillet, and LeDouarin, 1988) and transgenic (Tan and Breen, 1993) techniques. Such migration has also been found to occur by progenitor cells within the ventricular layer (Fishell, Mason, and Hatten, 1993).

Many studies on cell birth and migration have been performed using ^{3}H-thymidine, however several recent studies (Miller and Nowakowski, 1988; Schiffer, Giordana, Cavalla, Vigliani, and Attanasio, 1993; Fike, Goffel, Chou, Wijnhoven, Bellinzona, Nakagawa, and Seilhan, 1995) have used bromodeoxyuridine (BrdU), a thymidine-analog that may be

incorporated into the DNA of dividing cells, labelling all neural progenitor cells undergoing their last mitotic division. BrdU can be detected using anti-BrdU antibodies with fluorescent tags, affording the possibility of double-labelling with antibodies to other antigens. Several litters of mice were labelled with BrdU to provide information on the birth and migration of the cells into the medial septal region. Additionally, a developmental series of brains in sagittal and coronal orientation was observed to provide more detail on the movements of cells and development of morphological structures occurring within the septal region during the time of hippocampal commissure development.

METHODS

BrdU Immunohistology

Intraperitoneal injections (50μg per gram body weight) of BrdU (Sigma) dissolved in a solution of 0.007N NaOH in 0.9% saline were given to seven pregnant B6D2F_1 female mice 24 hours prior to litter extraction. Litters of the B6D2F_2 embryos were extracted (as described in Experiment 1) between gestational days E13.75 and E16.1, producing embryos with body weights between 0.186g - 0.708g. Embryos were perfused intracardially with about 5mL of 10mM phosphate-buffered saline (PBS - pH 7.6) immediately followed by about 20mL of 70% ethanol using a peristaltic perfusion pump, stereomicroscope, and micropipettes. Two longitudinal slits were made in the dorsal skull using a diamond knife to expose the brains and the heads were then postfixed in 70% ethanol for 24 hours. Brains

were then extracted and placed in a 30% sucrose buffer overnight, and then placed in OCT embedding solution, frozen at -20°C and sectioned at 10μm using a cryostat at -20°C. Sections were mounted on slides and rehydrated, followed by immersion in 0.07N NaOH for 2 minutes and then in 0.1M PBS (pH 8.5) for 30 seconds to partially denature the DNA to single strands against which the BrdU antibody is directed (Gratzner, 1982). The presence of BrdU was detected by direct immunofluorescence using an anti-BrdU antibody conjugated to fluorescein isothiocyanate (FITC) (Becton-Dickinson) diluted 1:5 in PBS. The sections were incubated in anti-BrdU antibody for 30 min, rinsed (2x5min) using PBS (pH 7.4), and then mounted using glycerol/p-phenylenediamine (Johnson and Nogueira Aranjo, 1981). Sections were viewed using a Zeiss epifluorescence microscope equipped with an FITC filter set.

Hematoxylin-Eosin Histology

Cell proliferation and cytoarchitecture were compared and contrasted between normal hybrid B6D2F_2 embryos and embryos from the inbred strains BALB/cWah1 and 129/J (also included were embryos from the substrain 129/ReJ, which demonstrate similar callosal defects - see Livy and Wahlsten, 1991). Embryos included in this study were compiled from several previous studies that had been undertaken in the lab of Dr. D. Wahlsten, but none of which had been used for this particular purpose. These embryos were extracted (as described in Experiment 1) and immersed in Bouin-Duboscq fixative (Humason, 1972) for about 5 minutes (until the brains appeared yellow). To facilitate entry of fixative into the brain, the

scalp was removed and two longitudinal slits were made parasagitally in the skull. The embryos were then placed in 50mL fresh fixative and placed on a rotator for 48 hours. The embryos were decapitated, and the heads placed in 70% ethanol and returned to the rotator for another 48 hours with one ethanol change after 24 hours. The embryo heads were embedded in paraffin by standard procedure (Humason, 1972). The resulting paraffin blocks were trimmed and 10μm serial sections were cut from each block in either the sagittal or coronal plane. Two rows of 10 sections were set on 1% gelatin-subbed slides and allowed to dry overnight at 37°C. Sections were then stained using hematoxylin-eosin (Humason, 1972) to differentiate nuclei, which appear a dark purple, from extranuclear tissue, which appears pale pink in colour.

Embryos with brains cut in the sagittal plane were included up to 0.6g body weight and those cut in the coronal plane were included up to 0.7g. Table 3.1 shows the number and body weight range of embryos included from each strain in each cutting orientation.

For brains cut in the sagittal plane, a Leitz Dialux microscope with a drawing tube attachment was used to make tracings of the ventricular layer, velum transversum, anterior commissure (AC) and hippocampal commissure (HC), if present, of the midsagittal section, and then the third and sixth sections from either side of the midsagittal plane at a magnification of 100x. The number of mitotic figures present in the lumenal ventricular layer, deep ventricular layer, and the subventricular layer of the third ventricle were counted between the junction of the primordium of the subfornical organ (PSFO) and velum transversum (VT) dorsally to the level of the dorsal surface of the anterior commissure (AC) perpendicular to the ventricular surface ventrally in each traced section (see Fig. 3.1). The

Table 3.1: Number and Body Weight Range of Embryos in the Hemotoxylin/Eosin Stained Brains.

STRAIN	SAGITTAL SERIES		CORONAL SERIES	
	# of Embryos	Body Weights (g)	# of Embryos	Body Weights (g)
$B6D2F_2$	14	0.175 - 0.594	12	0.264 - 0.689
BALB/cWah1	16	0.308 - 0.592	11	0.270 - 0.699
129/J	8	0.262 - 0.598	7	0.259 - 0.672

area of the ventricular layer was measured using a Numonics digitizing tablet connected to a PC and the SigmaScan digitizing morphometry program.

For brains cut in the coronal plane, tracings were made of the entire cytoarchitecture of the midline region using the same apparatus as above. Approximately every third section was drawn within the range of HC/CC crossing as well as several sections rostral and caudal to this range in an attempt to establish appropriate boundaries for counting mitotic figures. Unfortunately, such boundaries were not able to be adequately established with sufficient precision, and therefore the coronal results were recorded in a descriptive manner.

Statistics

Multiple regression was used to obtain the best prediction of the number of mitotic figures during the developmental period indicated for all strains. Dummy coding for strain indicated if differences existed between strains for this relationship (an α level of 0.05 was used to indicate a significant improvement in the fit of prediction for individual strains). All statistics were performed using SPSS for Windows v6.1.

RESULTS

BrdU Immunohistochemistry

BrdU was detected as punctate staining within the nucleus of the cell. The procedure

worked well with little background staining. In those sections observed, cells were identified to have migrated well into the intermediate layer and subplate region with some cells present in the cortical plate. Unfortunately, this procedure was assessed to be cost-ineffective for this purpose and was therefore halted after the processing of too few brains to provide informative data.

Cell Proliferation in the Third Ventricle

Most mitotic figures were seen in the area of the dorsal PSFO (Fig. 3.1). Very few mitotic figures were apparent through the ventral area, however one mitotic figure was seen just dorsal to the AC in most of the sections viewed in all strains (see Fig. 3.1). All mitotic figures viewed appropriately displayed spindle orientation parallel to the ventricular surface. Within the range of body weights observed, few mitotic figures were observed in the subventricular layer and were not included in the overall mitotic numbers.

Fig. 3.2 shows the relationship between the total number of mitotic figures in the ventricular layer and body weight for each strain. Body weight accounts for approximately 93% of the variance in mitotic figure number across all strains; the addition of dummy variables for strain did not improve the goodness of fit. Mitotic activity in the ventricular layer occurs only in the juxtalumenal position and therefore the number of mitotic figures is constrained by the length of the ventricular layer. Fig. 3.3 shows the change in mitotic figure number per mm of ventricular layer length during growth. Again, no difference was found between strains, and very little difference is present between this curve and that shown

Fig. 3.1. Sagittal View of Third Ventricle Neuroepithelium. A typical sagittal section through the third ventricle neuroepithelium shown here through the midplane of a 0.317g $B6D2F_2$ embryo (rostral to the left, caudal to the right). Neuroepithelial areas and lengths were measured between the junction of the primordium of the subfornical organ (PSFO) and the velum transversum (VT) dorsally to the level of the dorsal surface of the anterior commissure (AC) perpendicular to the ventricular surface ventrally. The small arrows show the location of various nuclei in mitosis. Most of the mitotically active cells were located dorsally in the area of the PSFO, although one mitotic figure was often located just dorsal to the AC (open arrow) in most of the sections viewed. Also shown is the apparent rostral migration of post-mitotic cells (asterisk) from the third ventricle to an area just dorsal to the hippocampal commissure (HC). These cells eventually extend rostrally to the area of the HC where they lie just lateral to the longitudinal fissure (see Fig. 3.5). (Scale: 50μm)

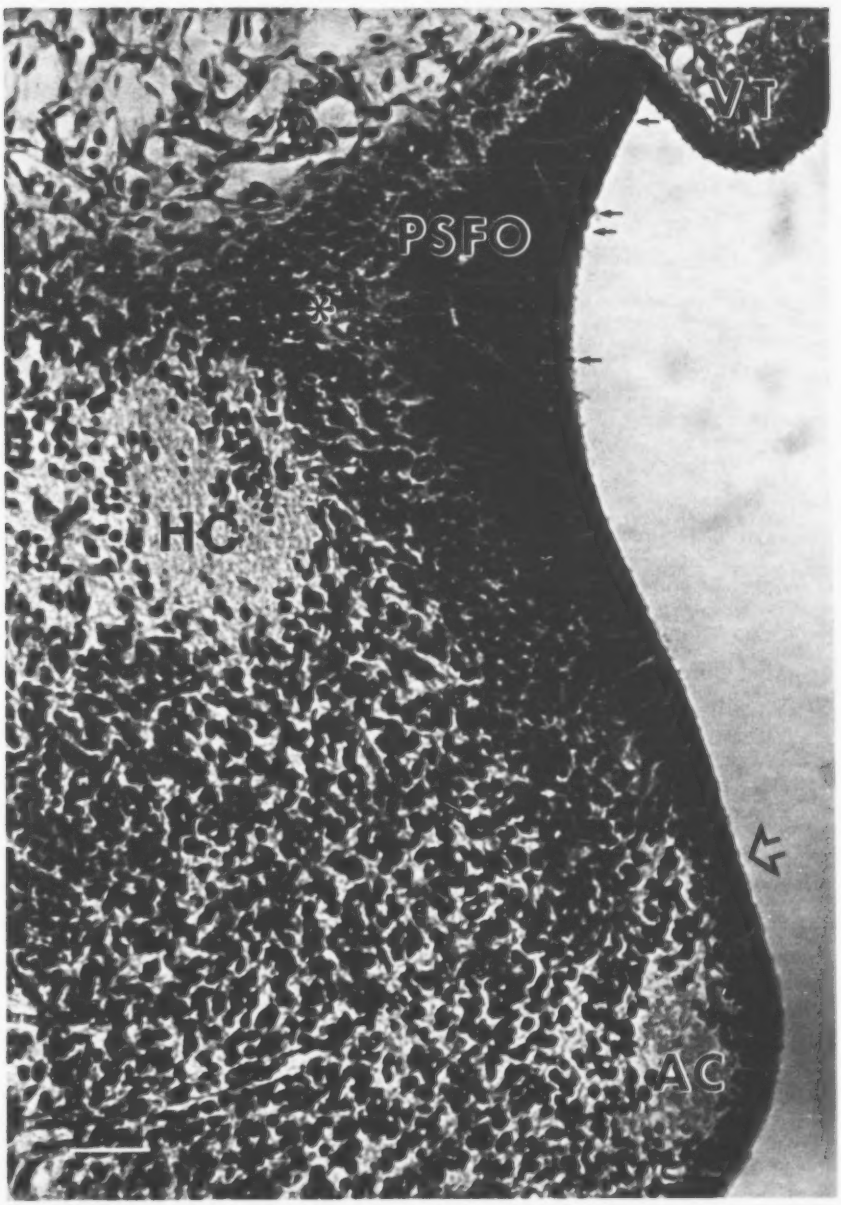
VT
PSFO
HC
AC

Fig. 3.2. Change in Number of Third Ventricle Mitotic Figures in the Midplane Region During Growth. Relationship between the total number of mitotic figures in the third ventricle and embryo body weight for each strain. This relationship configures to the biological decay curve $e^x/(1+e^x)$ as shown. The addition of dummy coding for strain indicated no differences between strains. Body weight accounted for approximately 93% of the variance in mitotic figure number across all strains.

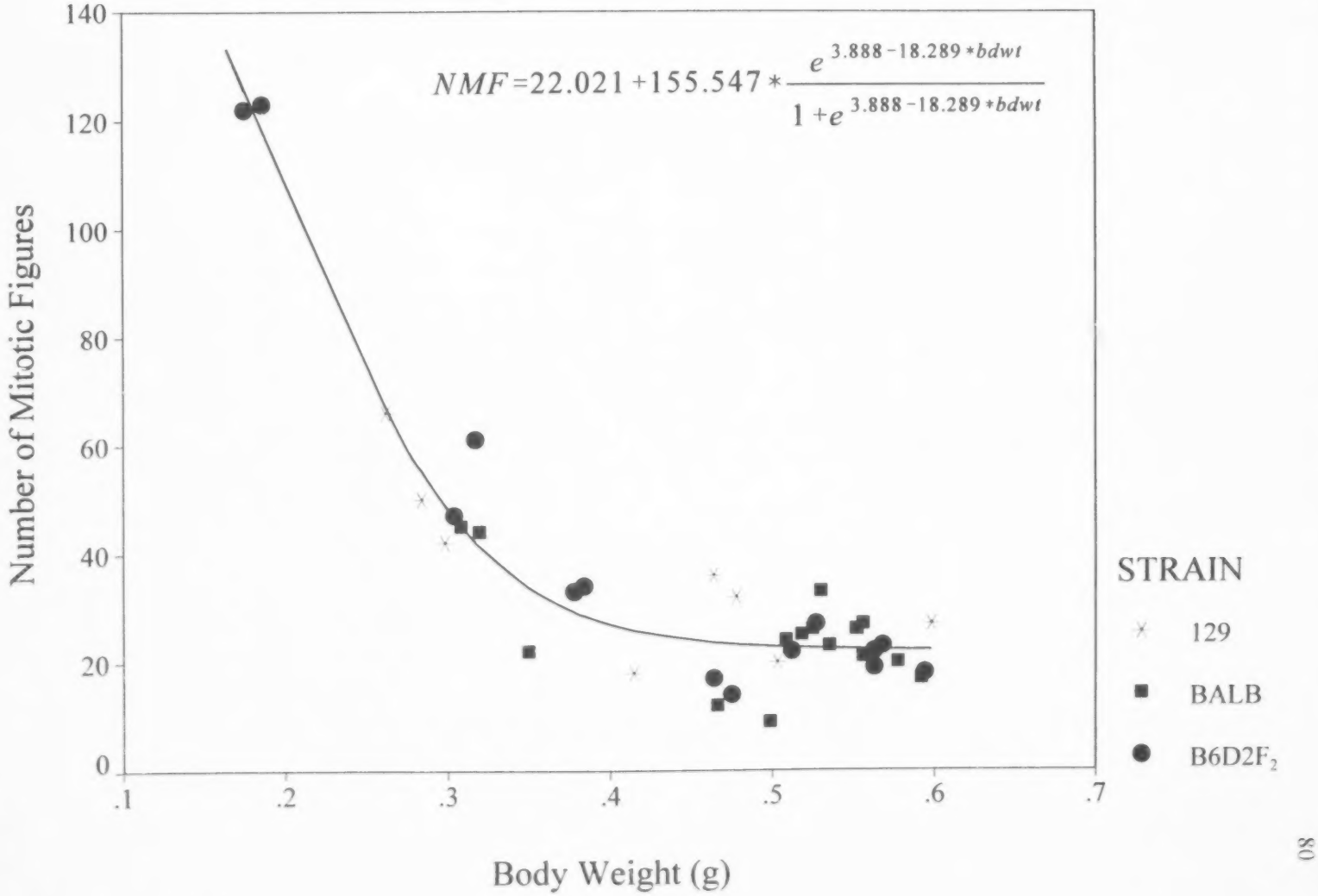
$NMF = 22.021 + 155.547 * \frac{e^{3.888 - 18.289 * bdwt}}{1 + e^{3.888 - 18.289 * bdwt}}$
Number of Mitotic Figures
140
120
100
80
60
40
20
0
.1
.2
.3
.4
.5
.6
.7
Body Weight (g)
STRAIN
129
BALB
B6D2F2

Fig. 3.3. Change in Density of Mitotic Figures in the Midplane Region During Growth. Relationship between the number of mitotic figures per mm of ventricular layer length and embryo body weight for each strain. Because mitotic figures only appear within the juxtalumenal layer of the third ventricle, the number of mitotic figures may be constrained by the length of the ventricular layer. As shown in Fig. 3.2, the relationship configures to the biological decay curve $e^x/(1+e^x)$. Dummy coding indicated no differences between strains. Mitotic figure density accounted for approximately 88% of the variance in body weight across all strains.

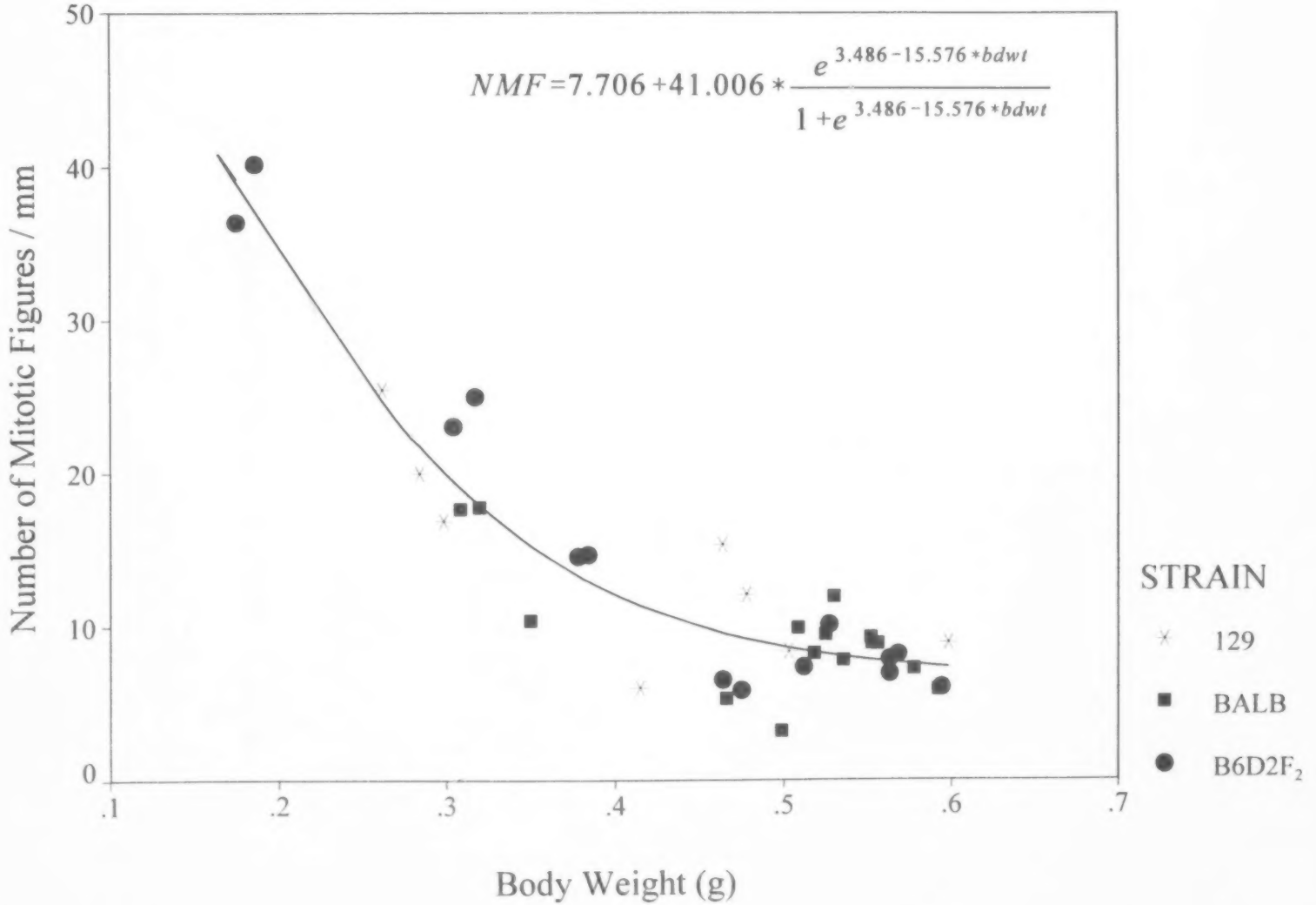
$NMF = 7.706 + 41.006 * \frac{e^{3.486 - 15.576 * bdwt}}{1 + e^{3.486 - 15.576 * bdwt}}$
Number of Mitotic Figures / mm
50
40
30
20
10
0
.1
.2
.3
.4
.5
.6
.7
Body Weight (g)
STRAIN
129
BALB
B6D2F2

in Fig. 3.2, suggesting that the number of mitotic figures is not affected by changes in ventricular length within each strain.

Coronal Cytoarchitecture

A comparison between strains of cell proliferation in the coronal plane was not possible due to an inability to provide sufficient control over the relative location and position within the brain for comparison purposes. Qualitative observation of these coronal sections indicated no apparent difference between the strains in location or number of mitotic figures. This was supported by the lack of difference when comparing the cytoarchitecture of the septal and cortical areas between the strains. Mitotic figures were seen along the entire medial aspect of the lateral ventricle with a concentration of figures at the medial ventricular flexure near the cortico-septal boundary. The only apparent structural difference was the continued presence of the cleft at midline in the acallosal strains which appeared to block the normal passage of HC axons across midline as suggested in Experiment #1.

HC axons traversing midline appeared to associate with the pia membrane, but also with a small population of darkly-staining cells present at the junction between the ventromedial cingulate cortex and the pia membrane (Fig. 3.4). These cells could be differentiated at about 0.3g and were very prominent by 0.4g. They appeared to be continuous caudally with the third ventricle as shown in Fig. 3.1. In brains with a deep cleft at midline, these cells were present as a layer lateral to the fissure. Hippocampal axons approached and appeared to contact these cells but also passed through this cell layer to

Fig. 3.4. Third Ventricle Cells at the Septal Midline. A coronal view of a 0.264g B6D2F_2 embryo showing the location of two small populations of cells (arrows) just lateral to the longitudinal fissure near the septal midline. These cells appeared continuous with cells emanating from the third ventricle (see Fig. 3.1). Some hippocampal axons contacted these cells during their approach to midline but it is unclear whether these cells provide guidance information to HC axons. (Scale: 50μm)

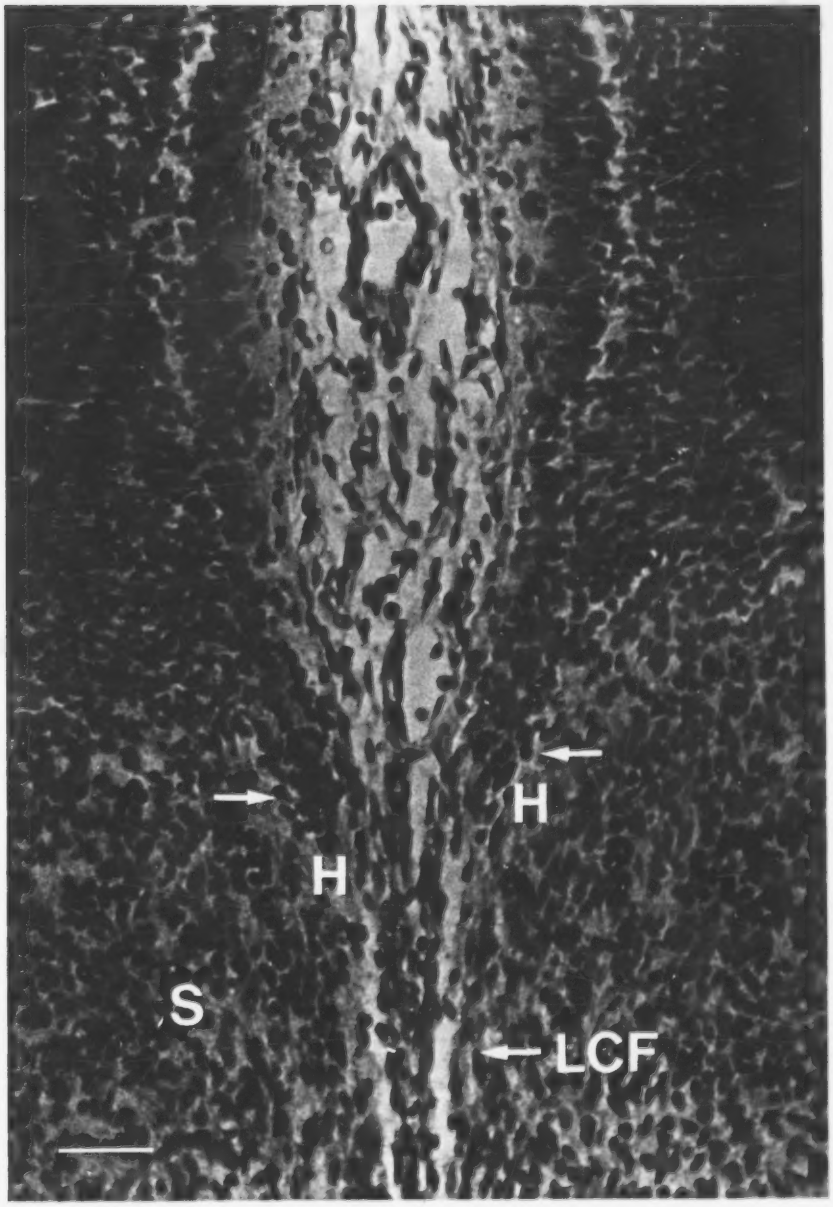
H
H
S
LCF

contact the pia. These cells did not span the midline area as a bridge although in older animals they appeared continuous with cells migrating medially from the lateral ventricles.

HC axons contacted the cells migrating to midline from the subventricular zone in the area of the medial flexure of the lateral ventricle. These cells were likely the sling cells described by Silver *et al* (1982). They were abundant in the area rostral to the HC, forming a clear demarcation between the cortical and septal areas (Fig. 3.5a). Caudally, these cells were much more diffuse, forming a loose accumulation of cells apparent among the axons of the HC (see Fig. 3.5b). In the $B6D2F_2$ mice, these cells were first seen to span the midline region at 0.643g but this was again more as a loose accumulation of cells. A more definite wedge of cells appearing as a solid substrate was not seen until 0.689g in $B6D2F_2$ mice (see Fig. 3.6), well after the time of first crossing by callosal axons.

As described in Experiment 1, a deep cleft extended down into the septal region in the younger $B6D2F_2$ embryos. This cleft was similar to the sulcus medianus telencephali medii (SMTM) described in humans by Rakic and Yakovlev (1968). With increasing age, the cleft appeared farther rostral and dorsal due to hemispheric fusion and growth of the septal region. It was interesting to note the apparent continued presence of a small, pia-filled groove or notch at the bottom of the interhemispheric fissure at midline in $B6D2F_2$ mice after midline traverse by the hippocampal axons (Fig. 3.7). This notch did not appear to impede the crossing of either the hippocampal or callosal axons and in some cases the very bottom of the notch was not apparent due to the volume of axons in the area. The notch was not a unique structure but rather appeared as a gradual and continual extension of the deeper cleft appearing in the more rostral regions. In the area near the very caudal part of the HC, the

Fig. 3.5. Subventricular Cells from the Lateral Ventricle. Coronal section of a 0.567g $B6D2F_2$ embryo showing subventricular cells emanating from the medial flexure of the lateral ventricle. *(a)* Rostral view - cells from the lateral ventricles form a clear demarcation (arrows) between the septal region (S) and the cortical region (C). These cells may create the cortico-septal barricade described by Hankin and Silver (1986) who proposed that the barricade prevented axonal movement between these regions in rostral brain areas. *(b)* Caudal view - subventricular cells can be seen extending from the lateral ventricle towards midline (arrows) but are much more diffuse and form neither a clear demarcation between septal (S) and cortical (C) regions, nor a solid mass which may be used as a bridge by axons approaching midline. (Scale: 50μm)

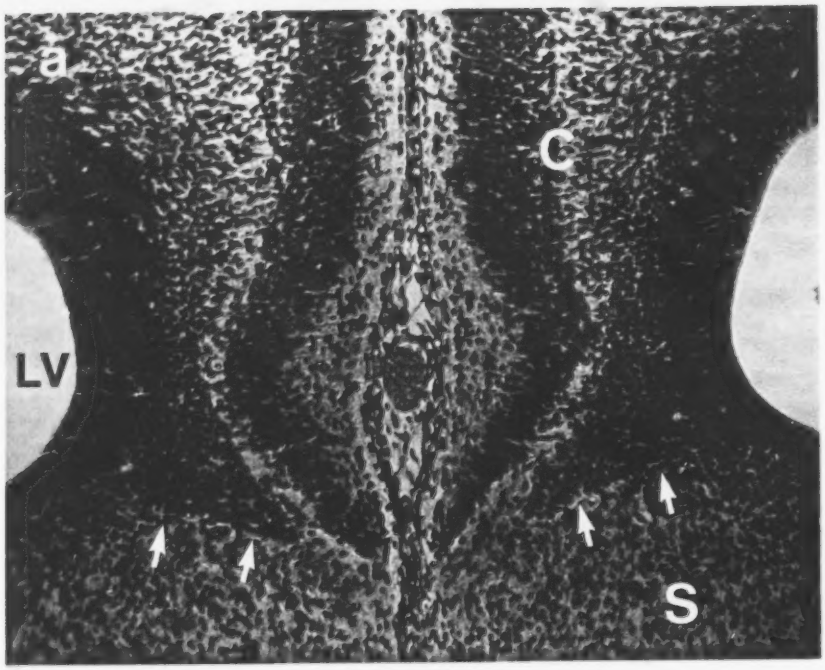
a
C
LV
S

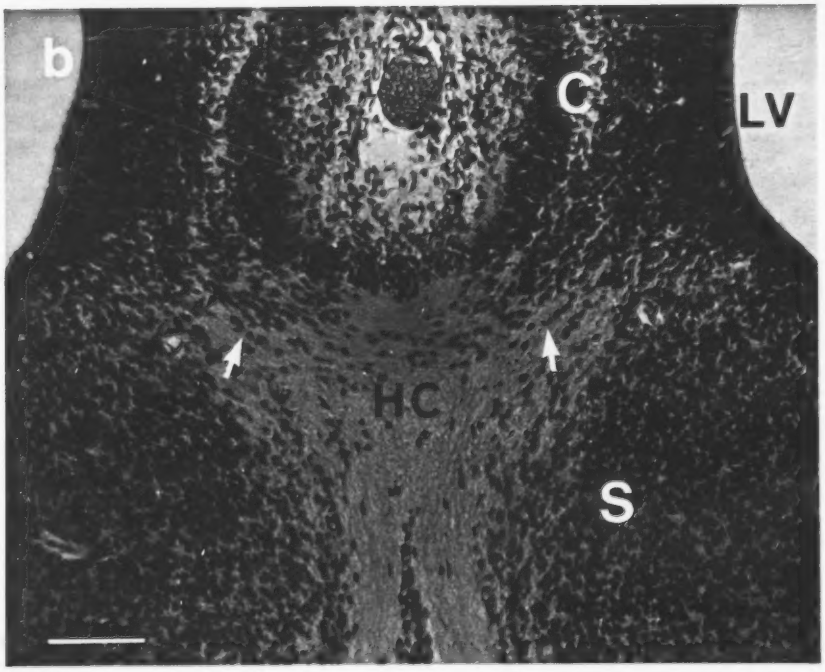
b
C
LV
HC
S

Fig. 3.6. Subventricular Cells and the Corpus Callosum. Coronal view of a 0.689g B6D2F$_2$ embryo showing the thick wedge of subventricular cells (arrows) from the lateral ventricles (LV) extending towards midline. These cells can be seen under a well-formed corpus callosum (CC) and may be responsible for initially guiding these axons toward midline. This was the first age at which these cells were seen to span midline in a cohesive "bridge-like" manner. (Scale: 50μm)

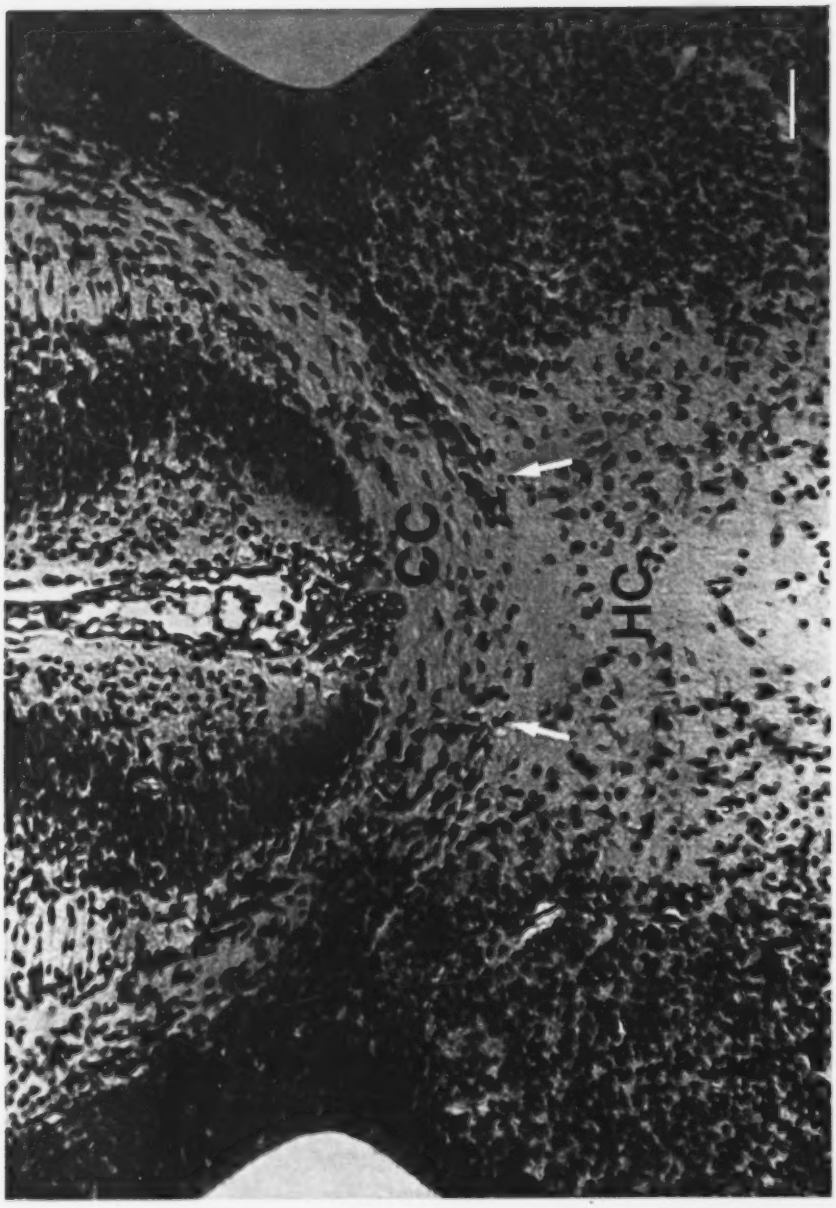
CC
HC

Fig. 3.7. Continued Midline Notch Presence in Older Embryos. Coronal section of a 0.611g $B6D2F_2$ embryo showing the presence of a small notch (arrows) at the midline. This notch was continuous with the cleft extending into the septal region seen farther rostrally. Similar to the cleft, the notch is lined with the pia membrane. Although this notch structure was present in older embryos (see Fig. 3.6), it did not appear to interfere with midline traverse by either hippocampal or callosal axons. Size of the notch decreased with both age and caudal positioning within the brain. (Scale: 50μm)

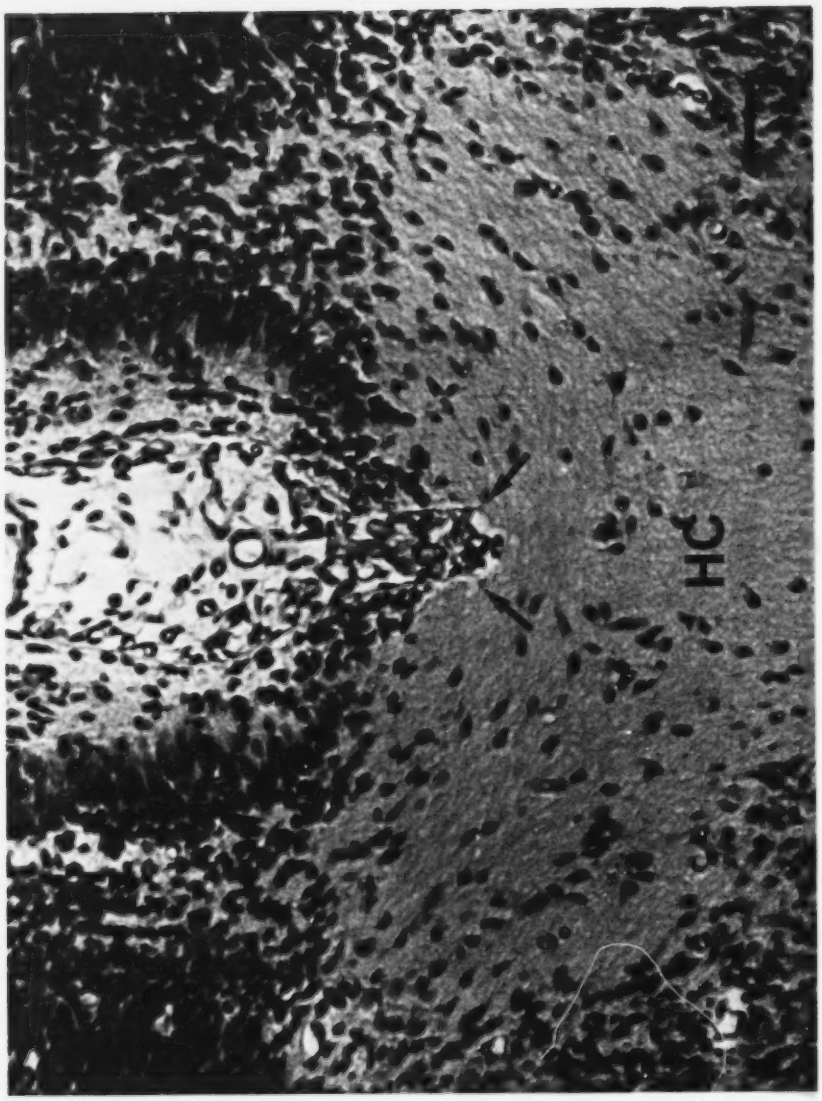
O
HC

notch was not as apparent and in older brains the fissure floor in this area appeared relatively "flat".

The acallosal strains demonstrated a similar cytoarchitecture to that of the B6D2F_2 mice. The only apparent difference was the continued presence of the cleft extending deep within the septal region which resulted in the ventral deflection of hippocampal axons upon their arrival at midline. In each of the BALB embryos, the pia membrane was observed within the cleft, similar to the B6D2F_2 embryos, but a narrow gap was also apparent between the pia and the adjacent septal cells. In most BALBs this gap was present along the entire length of the cleft with a more pronounced bulge apparent bilaterally, just ventral and lateral to the area of the fissure floor. A similar gap, or bulge, was previously described by Wahlsten (1987a) and was suggested to disrupt the substrate that guides callosal axons across midline. The size of the bulge increased caudally within the brain, usually appearing largest in the area of hippocampal axon arrival at midline. In older BALBs, the bulge occupied much of the midline region ventral to the midline notch (see Fig. 3.8). Caudally in these animals, the HC was still present but was interrupted in spots by this gap. Blood filled the gap unilaterally in the 0.592g BALB embryo (see Fig. 3.8), but was the only embryo in which blood was observed.

The gap was present in all BALB brains observed but only in the largest 129 brain (0.672g). In the rostral part of this 129 brain, the gap was small and located at the base of the pia membrane within the cleft; moving caudally within this brain, the cleft moved dorsally and the gap maintained its ventral position, gradually increasing in size. The consistency in structure of these gaps would suggest that they do not result from artifact. In

Fig. 3.8. Anomalous Gap Presence in Acallosal Embryos. In some of the acallosal embryos, a gap in the tissue was apparent immediately ventrolateral to the floor of the longitudinal fissure and the cleft in the septal region. *Top:* Coronal view of a 0.672g 129 embryo showing the gap (arrows) at midline. Gap size increased rostral to caudal within the septal region but in older brains hippocampal axons were still observed crossing midline. *Bottom:* Coronal view of a 0.592g BALB embryo showing a blood-filled gap (arrows) lateral to midline and rostral to the main bulk of HC axons crossing midline. (Scale: 50μm)

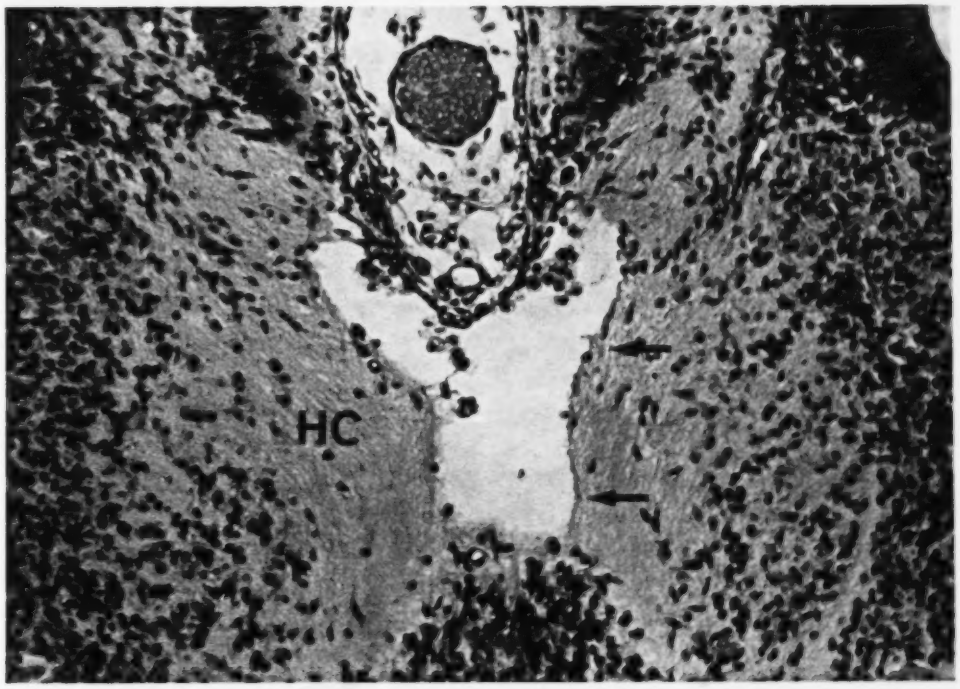
HC

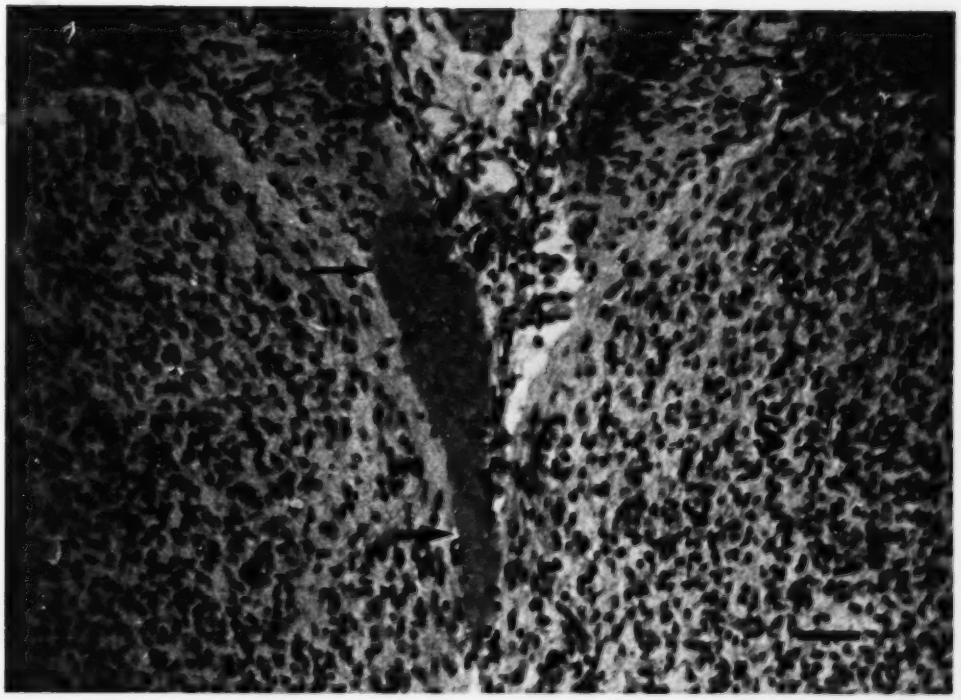

some embryos it appeared as though the pia membrane had simply become detached from the surrounding tissue, maintaining a few remnant connections, however in most brains the gap appeared to be filled with fluid. No other anomalies could be seen in the immediate vicinity of the bulge areas that could account for the formation of such a structure.

DISCUSSION

The results indicate that the number of mitotic figures in the rostral aspect of the third ventricle does not differ between the normal and acallosal mouse strains. Qualitative observations suggest a similar finding for the medial aspect of the lateral ventricles, however an accurate count will have to be made to substantiate this observation. The lack of difference between strains indicates that the difference in septal growth between normal and acallosal mice reported by Wahlsten and Bulman-Fleming (1994) is not due to a difference in the number of proliferating cells. Therefore, the differences apparent between strains in their septal development may be due to a lower rate of mitotic cycling in the acallosal strains, or perhaps a difference in the rate or direction of migration of the differentiated cells. Smart (1984) reported a slower rate of migration of cells to the medial cortical plate than to the isocortical plate, which was proposed to reflect a different developmental strategy for the evolutionarily "newer" isocortical area. The septal region is an even older phylogenetic area and may also demonstrate a slower rate of migration. This is supported by the paucity of mitotic figures observed in the subventricular layer near the midline region which may indicate a general delay in septal region development relative to other areas of the brain.

Therefore, a very subtle change in the acallosal strains may result in relatively large differences in the timing of development in the midline region.

Recent evidence has indicated that cell fates are determined prior to leaving the neuroepithelial layer (McConnell and Kaznowski, 1991; McConnell, 1992), and callosal axons have been seen to emerge from cortical neurons during their migration to the cortical plate (Auladell, Martinez, Alcantara, Supèr, and Soriano, 1995). Therefore, anomalies in cell migration may not only depend on the physical migratory process, but also on the presumed fate of the cell. The cytoarchitecture observed in the present study appeared similar in all strains and similar to that reported in hybrid mice by Crandall and Caviness (1984). This suggests that cell proliferation and migration to the cortical plate does not differ between strains, but further observation will be required to determine the validity of this statement for cells in the septal region.

Wahlsten (1987a) determined that the thickness of the medial cortex from the medial flexure of the lateral ventricle to the longitudinal fissure remained relatively unchanged between E16 and E18 (0.38g - 0.76g) in BALB brains. Although cortical measurements were not made in the present study, differences in cortical thickness were not apparent when comparing within the acallosal strains or between the normals and acallosals; however it must be noted that an accurate measurement of this area will have to be repeated after coronal positioning can be determined with greater precision.

The movement of HC axons toward midline appeared to follow the general pattern established in Experiment 1. HC axons were initially unable to cross midline due to the presence of the longitudinal fissure extending ventrally in the septal region. During their

growth to midline, these axons often contacted a layer of cells lateral to the pia membrane that appeared contiguous with the third ventricle. Silver *et al* (1993) identified two columns of RC1-positive (primitive astroglial) cells extending rostrally from the lamina terminalis to appear at midline in a zipper-like fashion in conjunction with midline fusion between the hemispheres. They indicated that these cells spanned the midline region and were later joined by the subventricular cells from the lateral ventricles to form the midline "sling" structure. In the present study, the rostrally projecting cells were not observed to span the midline region but instead appeared to remain lateral to the pia membrane lining the longitudinal fissure. These cells were contacted by axons traversing the hemispheres, but their presence in these cases was always dorsal to the axons and did not appear to form a ventral bridge as suggested by Silver *et al* (1993). Similarly, both hippocampal and callosal axons contacted the postulated sling cells from the lateral ventricles during their growth toward midline, however these cells did not appear to form a bridge-like structure until after the time of crossing by callosal axons. As indicated in Experiment 1, these sling cells did form a dense wedge lateral to midline and may be responsible for directing callosal axons toward midline. It is unclear whether the cells emanating rostrally from the third ventricle play any role in the guidance of axons toward midline, however it is possible that they may provide an intermediate signal during axonal approach to midline.

The cause of the gap formation in some of the acallosal mice is uncertain. Wahlsten (1987a) suggested that the formation of this gap may be due to differences in growth rates between the medial cortex and the adjacent septal areas while midline fusion is delayed. Differential growth within the brain has been suggested to affect the vasculature within the

brain (van Overbeeke, Hillen, and Vermeij-Keers, 1994) and to produce the brain's flexures (Goodrum and Jacobson, 1981; Pikalow, Flynn, and Searls, 1994). If the migration of septal cells into the midline region is compromised in these strains, it is certainly plausible to consider that this would create tensions between different cell layers which would lead to a degradation of tissue integrity. This stress existing within the tissue could be further augmented by dynamic tensions produced by the movement of large cell volumes; Silver *et al* (1982) have suggested that the influx of subventricular cells into the septal region may generate tension that causes the medial surfaces of the lateral ventricles to draw in and form the medial flexure.

The continued presence of a midline cleft extending into the septal region in the acallosal mice is indicative of the extended time period required for the fusion of the hemispheres. It is assumed that midline fusion results from the ingrowth of cells to this region, the forced apposition of the midline membranes, and the subsequent degradation of these membranes, resulting in "one" continuous structure. However, it is possible that cell presence in the midline region is normal and that the process of "fusion" conjoining the two hemispheres may somehow be deficient. In a study of midline defects within the bodies of human infants, Martínez-Frías (1995) reported that fusion (closure) defects were the most frequently observed midline anomaly. Optiz and Gilbert (1982) have proposed that the midline region in chordates is a primary developmental field and that although polygenic buffering systems are generally adequate in protecting developing systems, their effectiveness is compromised during midline development, resulting in a high proportion of midline developmental anomalies. Optiz (1993) further extended this theory to

blastogenesis, proposing the entire embryo as a primary developmental field, again with compromised midline buffering, resulting in very severe, usually lethal, defects, as well as the occurrence of monozygotic twinning. A decreased buffering capacity within the acallosal strains may play a role in the delayed fusion of the telencephalic midline. Such a theory may be applicable when considering the decrease in incidence of callosal agenesis in hybrid offspring from acallosal inbred parents (Wahlsten, Sparks, and Bishop, 1996).

EXPERIMENT 4

INTRODUCTION

The growth of axons within the developing brain is guided by specific cues in their environment. These cues have been identified to assume two forms, substrate-bound molecules which provide guidance through physical contact (see Dodd and Jessell, 1988; Hynes and Lander, 1992) and chemotropic factors, released by distant target sites, which establish diffusible gradients and provide directional guidance to axons (see Tessier-Lavigne and Placzek, 1991; Tessier-Lavigne, 1992; Tessier-Lavigne, 1994). Contact guidance cues may provide both permissive (Rauvala and Pihlaskari, 1987; Matsunaga, Hatta, Nagafuchi, and Takeichi, 1988; Mendez-Otero, Schlosshauer, Barnstable, and Constantine-Paton, 1988) and repulsive (Fawcett, Rokos, and Bakst, 1989; Stahl, Mueller, von Boxberg, Cox, and Bonhoeffer, 1990; Raper and Kapfhammer, 1990) information, respectively encouraging or inhibiting axonal extension into these areas. Experimental evidence has also indicated the presence of chemoattractive (Heffner, Lumsden, and O'Leary, 1990; Placzek *et al*, 1990; Zheng, Felder, Connor, and Poo, 1994) as well as chemorepulsive factors (Fitzgerald, Kwiat, Middleton, and Pini, 1993; Pini, 1993).

Laminin is one of the major extracellular matrix (ECM) glycoproteins providing permissive contact guidance for developing axons (Liesi, Dahl, and Vaheri, 1984; Hammarback, Palm, Furcht, and Letourneau, 1985; Hall, Neugebauer, and Reichardt, 1987).

It has been identified on the surface of glial cells (Liesi, Dahl, and Vaheri, 1983; Faivre-Bauman, Puymirat, Loudes, Barret, and Tixier-Vidal, 1984); glial cells are thought to provide structural support for the extension and outgrowth of axons in part due to their expression of several different guidance molecules on their cell surface (Neugebauer, Tomaselli, Lilien, and Reichardt, 1988; Smith, Rutishauser, Silver, and Miller, 1990). Laminin has also been identified on glial cells which are associated with axonal pathways in the developing brain including the fornix and corpus callosum (Liesi and Silver, 1988).

In this experiment, immunohistochemical techniques were used to investigate the presence of glial cells and the ECM protein laminin during the time of growth by hippocampal axons across the telencephalic midline. Vimentin and glial fibrillary acidic protein (GFAP) are both intermediate filaments known to be expressed by glial cells (Lazarides, 1980). Vimentin is the major cytoskeletal protein found in immature glial cells (Dahl, Rueger, Bignami, Weber, and Osborn, 1981) and its expression has been described as early as E12 in rat brain (Bignami, Raju, and Dahl, 1982). In contrast, the expression of GFAP is not found until about E18 (Bignami and Dahl, 1974; Raju, Bignami and Dahl, 1981; Valentino, Jones, and Kane, 1983), reflecting the differentiation of glial cells into oligodendrocytes and astrocytes and the resultant onset of myelination (Dahl, 1981). Due to the variability in midline development already shown in several mouse strains, the investigation of both vimentin and GFAP expression in the developing midline of mouse brain remains valid and potentially very useful. Glial cells have also been identified by the presence of J1-31 (Predy, Singh, Bhatnagar, Singh, and Malhotra, 1987), a protein unique from both vimentin and GFAP; the expression of this protein increases dramatically in

reactive astrocytes which are proximal to a site of injury or disease process in the CNS (Eng, 1988; Malhotra, Svensson, Aldskoguis, Bhatnagar, Das, and Shnitka, 1992). While no external force has been suggested to affect the course of midline development, the midline region does experience some level of internally generated trauma due to the fusion of the hemispheres and degradation of glial and pial membrane cells at the midpoint between the hemispheres. Such activity may produce a response similar to that seen in cases of externally applied trauma.

METHODS

Four B6D2F_2 embryos from one litter at gestational age E15.3 with body weights 0.436g, 0.441g, 0.471g, and 0.507g, were obtained as described in Experiment 1. Each embryo was perfused intracardially with 3-5mL of 10mM phosphate-buffered saline (pH 7.6) followed by 10-15mL of 8% paraformaldehyde in 0.1M phosphate buffer (pH 7.6) using a peristaltic perfusion pump, stereomicroscope, and micropipettes. After gelatin infiltration (described in Experiment 1), brains were cut coronally at 20-30μm using a microslicer (DSK - DTK 1500E) and a sapphire knife (Pelco). Sections were stored in 0.1M phosphate buffer (pH 7.6) and viewed to determine those sections in which the HC was crossing midline. Adjacent sections were then mounted on slides subbed with 1% gelatin.

Indirect immunofluorescence staining was performed using MAb mouse anti-human J1-31 ascites fluid (1:500 dilution), rabbit anti-cow GFAP (Dakopatts; 1:1000 dilution), rabbit anti-mouse laminin (Sigma; 1:1000 dilution), and MAb mouse anti-human vimentin

ascites fluid (Sigma; 1:300 dilution). Control sections were incubated with normal mouse and rabbit serum (Sigma) as appropriate diluted 1:500 and 1:1000 respectively. Sections were rinsed in PBS (3x5min) followed by incubation with 30% goat serum for 30 minutes, and then an additional rinse in PBS (1x5min). Each section was double-labelled using primary antibodies to J1-31 and GFAP, or laminin and vimentin. After incubation with primary antibody overnight, sections were washed in PBS (3x15min) followed by incubation for one hour in secondary antibodies, goat anti-mouse IgG+IgM conjugated to fluorescein (Boehringer-Mannheim; 1:100 dilution) and goat anti-rabbit IgG conjugated to rhodamine (Sigma; 1:100 dilution). Sections were given a final rinse in PBS (1x15min) and then mounted using buffered glycerol with p-phenylenediamine (Johnson and Nogueira Araujo, 1981). Sections were viewed using a Zeiss epifluorescence microscope equipped with rhodamine and fluorescein filter sets.

RESULTS

In all sections, antigen staining was clear with no apparent indiscriminate background staining. All control sections were clearly negative. No antigen staining was observed for J1-31 or GFAP anywhere in the telencephalon. In contrast, staining for both laminin and vimentin was apparent throughout the telencephalon. Laminin staining was seen as punctate stain similar to that shown previously (see Liesi, 1990), whereas fluorescence indicating vimentin appeared in larger quantities and more widely distributed. The amount of laminin and vimentin staining was high in the midline region but did not appear to be isolated to any

particular area or structure. Both antigens were present in the area of the pia membrane, but also directly adjacent to it, including in the areas where axon pathways were present, making it difficult to differentiate between cell types.

DISCUSSION

The lack of both J1-31 and GFAP staining indicates that neither antigen is expressed at E15.3 in $B6D2F_2$ mice, or is present at a level too low to be discerned. A masking effect due to the paraformaldehyde fixation is unlikely because both antigens have been detected in paraformaldehyde-fixed rat tissue (Predy *et al*, 1987). Despite the absence of GFAP, the abundance of vimentin and laminin would suggest that glial cells may yet be present in the midline region, however the comprehensive distribution of both laminin and vimentin throughout the midline region would suggest that neither are unique to glial cells at this age. Vimentin has been identified in both neural and glial cells early in development (Bignami *et al*, 1982; Cochard and Paulin, 1984) and has also been found in cells of both mesenchymal and non-mesenchymal origin (Schnitzer, Franke, and Schachner, 1981; Yen and Fields, 1981). Besides being an ECM glycoprotein, laminin is also a major component of basement membranes (Timpl, Rohde, Gehron Robey, Rennard, Foidart, and Martin, 1979) and has been used to identify blood vessel endothelium in the brain (Bignami, Chi, and Dahl, 1984).

Many other antigens have been identified in the guidance and support of axonal outgrowth. Perhaps the best known of these antigens is N-CAM (Rutishauser, Acheson, Hall, Mann, and Sunshine, 1988), however it is thought to be present in higher quantities

than laminin (Dodd and Jessell, 1988). Fibronectin (Rogers, Letourneau, Peterson, Furcht, and McCarthy, 1987), thrombospondin (O'Shea and Dixit, 1988; O'Shea, Rheinheimer, and Dixit, 1990), tenascin/cytotactin (Grierson, Petroski, Ling, and Geller, 1990; Faissner and Kruse, 1990), F3/F11 (Gennarini, Durbec, Boned, Rougon, and Goridis, 1991), axonin (Ruegg, Stoeckli, Lanz, Streit, and Sonderegger, 1989), and contactin (Moss and White, 1992) have all been implicated in the guidance and support of axons in the CNS and any or all may play a role in the guidance of commissural axons through the midline region.

There are several antigens which may have particular relevance in the investigation of HC and CC formation. Radial glial cells have been identified during the pre-GFAP expression period in embryos using RC-1 (Edwards, Yamamoto, and Caviness, 1990) and RC-2 (Misson *et al*, 1988) antibodies as early as E9-10 in mice and could therefore be used to identify the growth of cells into the medial septal region. RC-1 and RC-2 have been used by Silver *et al* (1993) to demonstrate the presence of glial boundaries existing at the telencephalic midplane within the mouse and cat brain which are thought to provide a repellent substrate for the guidance of commissural axons. Keratan and chondroitin sulfate proteoglycans inhibit axonal outgrowth and have also been identified in similar glial boundaries (Snow, Lemmon, Carrino, Kaplin, and Silver, 1990; Snow, Steinler, and Silver, 1990; Snow, Watanabe, Letourneau, and Silver, 1991). In the epichordal CNS of embryonic rodents, TAG-1 (Furley, Morton, Manalo, Karagogeos, Dodd, and Jessell, 1990) is expressed by commissural axons approaching the floor plate but is replaced by the expression of L1 after crossing through this area (Dodd, Morton, Karagogeos, Yamamoto, and Jessell, 1988). During this time, the floor plate cells express p35/LC1 (McKanna and Cohen, 1989;

McKanna, 1993a) and F-spondin (Klar, Baldassare, and Jessell, 1992) which may act as substrate adhesion molecules. Although the floor plate ends at the rhombencephalon - mesencephalon junction (Jessell, Bovolenta, Placzek, Tessier-Lavigne, and Dodd, 1989), LC1 has also been identified on glial cells during commissure formation in prechordal areas such as the optic chiasm and infundibular decussation (McKanna, 1993b). Another antigen, the limbic associated membrane protein (LAMP), has been found in the neuronal soma, dendrites and axons originating from regions in the limbic system (Levitt, 1984). The discovery of this antigen on developing axons and their target cells in embryonic rat suggests that it may play a role in initial pathway determination and has been implicated as one of the important molecular components necessary for the formation of proper connection between limbic system regions (Horton and Levitt, 1988; Zhukareva and Levitt, 1995).

The early outgrowth of hippocampal axons from the fornix columns towards the telencephalic midline suggests the presence of a chemoattractant factor. Several such chemotropic factors have been identified. Nerve growth factor (Johnson and Taniuchi, 1987) has been shown to affect the direction of regenerating axons (Gundersen and Barrett, 1979) but not developing (embryonic) axons (Davies, 1987; Hoyle, Mercer, Palmiter and Brinster, 1993). Netrins have been identified as attractant factors released by the floor plate to direct commissural axon growth towards the midline during development of the spinal cord (Serafini, Kennedy, Galko, Mirzayan, Jessell, and Tessier-Lavigne, 1994; Kennedy, Serafini, de la Torre, and Tessier-Lavigne, 1994) and hindbrain (Shirasaki, Tamada, Katsumata, and Murakami, 1995), and may also act as a repulsive factor on other axons to direct them away from the floor plate (Colamarino and Tessier-Lavigne, 1995). Similarly, cells of the septal

midline are thought to emit a diffusible chemorepellent that acts to prevent the passage of olfactory axons through this region (Fitzgerald *et al*, 1993; Pini, 1993).

The use of *in vitro* designs with the meninges or the medial septal cells may provide insight into their effect on axonal outgrowth. However, given the number of compounds that may play a role in the outgrowth of axons, any such investigation into the possible effectors of this growth would require an extensive amount of time and effort and should be considered as worthy of a separate thesis project, or indeed an entire research program.

EXPERIMENT 5

INTRODUCTION

Neural plasticity may effect functional recovery when structural morphology is altered during abnormal development of the brain. Congenital absence of the corpus callosum (CC) arises from a defect in the formation of the substrate that normally guides the callosal axons across the telencephalic midline (Silver *et al*, 1982; Wahlsten, 1987a; results from Experiment 1). Although this defect is hereditary, it is not developmentally fixed; instead, the plasticity in this developing system allows animals with identical genotypes to display a wide range of phenotypic expression. Hippocampal commissure (HC) formation in most embryos from acallosal strains is retarded, yet most adults demonstrate normal a HC structure, suggesting an ability to recover from these early structural deficits. In contrast, callosal structure in some mouse strains can range from decreased CC size to total callosal absence. Callosal axons that do not cross midline form a new structure, the Probst bundle (Probst, 1901), which runs longitudinally just lateral to the longitudinal fissure (Wahlsten, 1987a; Ozaki and Shimada, 1988).

Despite the absence of this large interhemispheric communication route, very few behavioural deficits are obvious both in animals (Lipp, Waanders, Berther, Glanzmann, and Bolla, 1989; Lipp and Waanders, 1990; Gruber, Waanders, Collins, Wolfer, and Lipp, 1991; Schmidt, Manhaes, and DeMoraes, 1991; Lipp and Wahlsten, 1992), and in humans

(Ettlinger, Blakemore, Milner, and Wilson, 1972; Ferris and Dorsen, 1975; Milner and Jeeves, 1979; Chiarello, 1980; Milner, 1983; Lassonde *et al*, 1991; Sauerwein *et al*, 1994). This is in contrast to surgical transection of the callosum, often used in the control of epileptic seizure activity in humans, which results in many readily discernible behavioural deficits including access to language centres (Sperry, Gazzaniga, and Bogen, 1969), memory decreases (Sass, Novelly, Spencer, and Spencer, 1988), reduced speed and accuracy of tactile discrimination (Lassonde, Sauerwein, Geoffroy, and Decarie, 1986), decreased motor performance and coordination (Preilowski, 1977; Chen, Campbell, Marshall, and Zaidel, 1990; Provinciali, DelPesce, Censori, Quattrini, Paggi, Ortenzi, Mancini, Papo, and Rychlicki, 1990), and reduced depth perception (Mitchell and Blakemore, 1970; Jeeves, 1991). Although some recovery from the effects of transection in adults is apparent due to neural plasticity and learned effects (Sperry, 1968; Lassonde, Ptito, and Lepore, 1990; Jinkins, 1991; Reeves, 1991), this deficit recovery does not result in the same level of deficit attenuation as expressed in callosal agenesis.

This difference in expressed behavioural deficit suggests that more effective compensatory mechanisms are employed in the developmental defect. In a study of human patients, Persson (1970) could not find any disturbance in the transfer of information between hemispheres despite complete agenesis and proposed that extracallosal pathways were used. Several researchers have suggested that the anterior commissure (AC) acts as this route in humans (Loeser and Alvord, 1968; Bossy, 1970; Ettlinger, Blakemore, Milner, and Wilson, 1974; Chiarello, 1980; Muente and Heinze, 1991). Monotremes and marsupials have no corpus callosum and the anterior commissure provides the main route of

interhemispheric communication (Ebner, 1967; Ebner, 1969; Heath and Jones, 1971; Granger *et al*, 1985). Hypertrophy of the AC in acallosal patients has been reported by Loeser and Alvord (1968), Geschwind (1974), Stefanko and Schenk (1979), and Fisher, Ryan, and Dobyns, (1992). Rauch and Jinkins (1994) reported an increase in AC area in 10% of patients with callosal agenesis but a decrease in AC area in another 10% of patients. In animal studies, Lent (1983) found that a few neocortical axons were present in the AC of hamsters with surgically induced agenesis, suggesting a reorganization of the interhemispheric connections in acallosal animals. However, no evidence for such reorganization has been found in mice with hereditary callosal absence (Wahlsten and Jones, 1983; Ozaki, *et al*, 1987; Ozaki and Wahlsten, 1993; Olavarria, Serra-Oller, Yee, and van Sluyters, 1988, 1994).

If the anterior commissure is being used to compensate for the loss of the corpus callosum, it would be expected that the number of axons in the AC would increase to manage the increased communication volume, thus increasing AC size. In this study, AC size, number of axons, and axon diameter have been compared between acallosal and normal mice using electron microscopy. The number of unmyelinated axons present in the anterior commissure of acallosal mice was found to be higher than that in normal mice but this higher axonal number did not significantly increase the overall size of the AC because of a decrease in the diameter of these axons.

METHODS

Animals

The subjects were the F_2 offspring from hybrid 129CF$_1$ parents (129/ReJ females x BALB/cWah1 males), bred and raised at the University of Alberta, and two recombinant inbred (RI) lines obtained from 129CF$_2$ pairings. The callosal defect is expressed variably in both BALB/cWah1 and 129/J mice (Wahlsten, 1982d; Wahlsten, 1987a; Ward *et al*, 1987; Livy and Wahlsten, 1991), and about 25% of their F_2 offspring express 100% total CC absence (Wahlsten and Schalomon, 1994, and unpublished observations). The recombinant inbred lines used were propagated at the University of Alberta and were in their sixth generation of inbreeding (Wahlsten and Sparks, 1995). RI Line #1 has complete absence of the CC similar to that seen in the strain I/LnJ (Lipp and Waanders, 1990; Livy and Wahlsten, 1991). RI Line #22 has consistently shown normal callosal structure. Normal CC and AC development was confirmed by comparison with the F_2 offspring from hybrid B6D2F$_1$ /J parents (C57BL/6J females x DBA/2J males) obtained from the Jackson Laboratories, Bar Harbor, Maine, at 7-8 weeks of age, then raised and bred at the University of Alberta. These mice have often been used to demonstrate normal development and have never been found to have any developmental defects in brain architecture (Wahlsten, 1987a; Wahlsten and Smith, 1989; Ozaki and Wahlsten, 1992; results from Experiment 1).

All mice were housed in 29 x 18 x 13 cm opaque plastic mouse cages with Aspen-Chip bedding (Northeastern Products Corp., Warrensburg, New York) with a few sheets of

tissue added. Mice were allowed free access to food (non-autoclaved Wayne Rodent Blox 8604) and tap water. Room temperature was maintained at approximately 23°C with a 12/12 hour light cycle (lights on at 6 am).

Histology and Microscopy

Adult mice (see Table 5.1) were euthanized with sodium pentobarbital (120 mg/kg, IP) and immediately perfused intracardially with about 10mL of 10mM phosphate-buffered saline (pH 7.6) followed by 80-100mL of fixative consisting of 3% paraformaldehyde, 1.5% glutaraldehyde and 0.02% $CaCl_2$ in 0.1M cacodylate buffer (pH 7.2). The brains were processed as two groups with slightly different methodologies. $B6D2F_2$ and $129CF_2$ brains were immediately extracted, trimmed, and weighed to the nearest mg (see Table 5.1). They were then post-fixed overnight in the same fixative. The following day the brains were blocked sagittally and 25-30μm sections were cut using a microslicer (DSK - DTK 1500E) and a sapphire knife. Sections were collected in 0.1M cacodylate buffer and immediately viewed to determine the midsagittal section. The sections immediately preceding and following the midsagittal section were removed and further processed for electron microscopy. The remaining sections were stained using gold chloride (Schmued, 1990) to determine the size of the CC and HC. Sections for EM were placed into 4% glutaraldehyde in 0.1M cacodylate buffer (pH 7.2) at 4°C overnight, then rinsed in 0.1M cacodylate buffer (3x15min) and placed on poly-L-lysine coated coverslips. They were then coated with 2% gelatin in 0.1M cacodylate buffer and the gelatin was allowed to set. The gelatin was fixed

using 4% glutaraldehyde in 0.1M cacodylate buffer for 30-45 minutes.

Brains from RI-1 and RI-22 mice were immediately extracted and postfixed overnight in the same fixative. The following day the brains were trimmed and weighed to the nearest mg (see Table 5.1). The brains were then bisected in the midsagittal plane. The left hemispheres were stained using gold chloride and measured using a Java video image analysis system (Jandel Scientific) to determine CC and HC midsagittal area. Right hemispheres were blocked parasagittally and further trimmed to reduce the cutting surface for the microslicer. Three sections, counted from the presence of the complete AC in the section, were cut at 50μm using a microslicer and steel knife into 0.1M cacodylate buffer. Sections were placed into fresh 0.1M cacodylate buffer for about 4 hours, and then on 1% gelatin (aq) coated coverslips. They were then coated with 2% gelatin in 0.1M cacodylate buffer and the gelatin allowed to set at 4°C for 4 hours. After trimming excess gelatin, the remaining gelatin was fixed using 4% glutaraldehyde and 0.02% $CaCl_2$ in 0.1M cacodylate buffer at 4°C overnight.

All sections were further trimmed to leave a small square containing the AC that would fit within the embedding mold, rinsed (2x10min) in 0.1M cacodylate buffer and postfixed with 1% OsO_4, 1.5% $K_3Fe(CN)_6$ and 0.02% $CaCl_2$ in 0.1M cacodylate buffer for 3 hours. This was followed by rinsing (3x10min) in acetate buffer (pH 5.2) and *en bloc* staining in 2% uranyl acetate (aq) in 0.1M sodium acetate for 45 minutes and then an additional acetate buffer wash (2x15min). Sections were then dehydrated through an ethanol series (1x10min 50%; 1x10min 70%; 2x10min 90%; 2x10min 95%; 2x15min 100%) and then rinsed in propylene oxide (2x15min). They were infiltrated with a graded series of

Epon 810 beginning with a 1:2 mixture of Epon and propylene oxide, and ending with pure Epon which was left on the sections for 24 hours and trimmed to the size of the gelatin block. Fresh Epon was then applied to the section and an embedding mold was lowered over each section and filled with fresh Epon which was allowed to cure for 48 hours at 60°C. After curing, the embedding mold was removed and the block dipped in liquid nitrogen to remove the coverslip from the block face.

Tissue blocks were trimmed to expose the anterior commissure and thick sections (about 1μm) were cut using glass knives on a Reichert-Jung Ultracut E ultramicrotome and stained using Toluidine blue O at 60°C for 15 seconds. A Leitz Laborlux microscope with a drawing tube attachment was used to make detailed tracings of the AC areas from these sections at a magnification of 400x (Fig. 5.1). Thin sections (90nm gold) were cut using a DuPont diamond knife in the same microtome. Sections obtained were picked up on 1,000 mesh copper grids and stained for 2 hours with 4% uranyl acetate (aq) and for 1 minute with Sato's lead citrate (aq).

Thin sections were viewed on a Philips 400 TEM at a magnification of 1,800x. Fifteen photos were taken of the anterior part of the AC (AAC) and 10 from the posterior part (PAC). Photos were shot using 35mm film at the approximate middle of the grid pore. Grid pores were selected to provide an evenly spaced distribution of the AC; care was taken to avoid the AC edges, the junction between the AAC and PAC and grid pores that contained tissue anomalies due to processing.

Fig. 5.1. Midsagittal Morphology of the Mouse Anterior Commissure. A midsagittal tracing of the anterior commissure of a $129CF_2$ mouse showing the relative sizing of the AAC and PAC areas, as well as the size and positioning of an unmyelinated axon field which may comprise part of the commissural section of the stria terminalis.

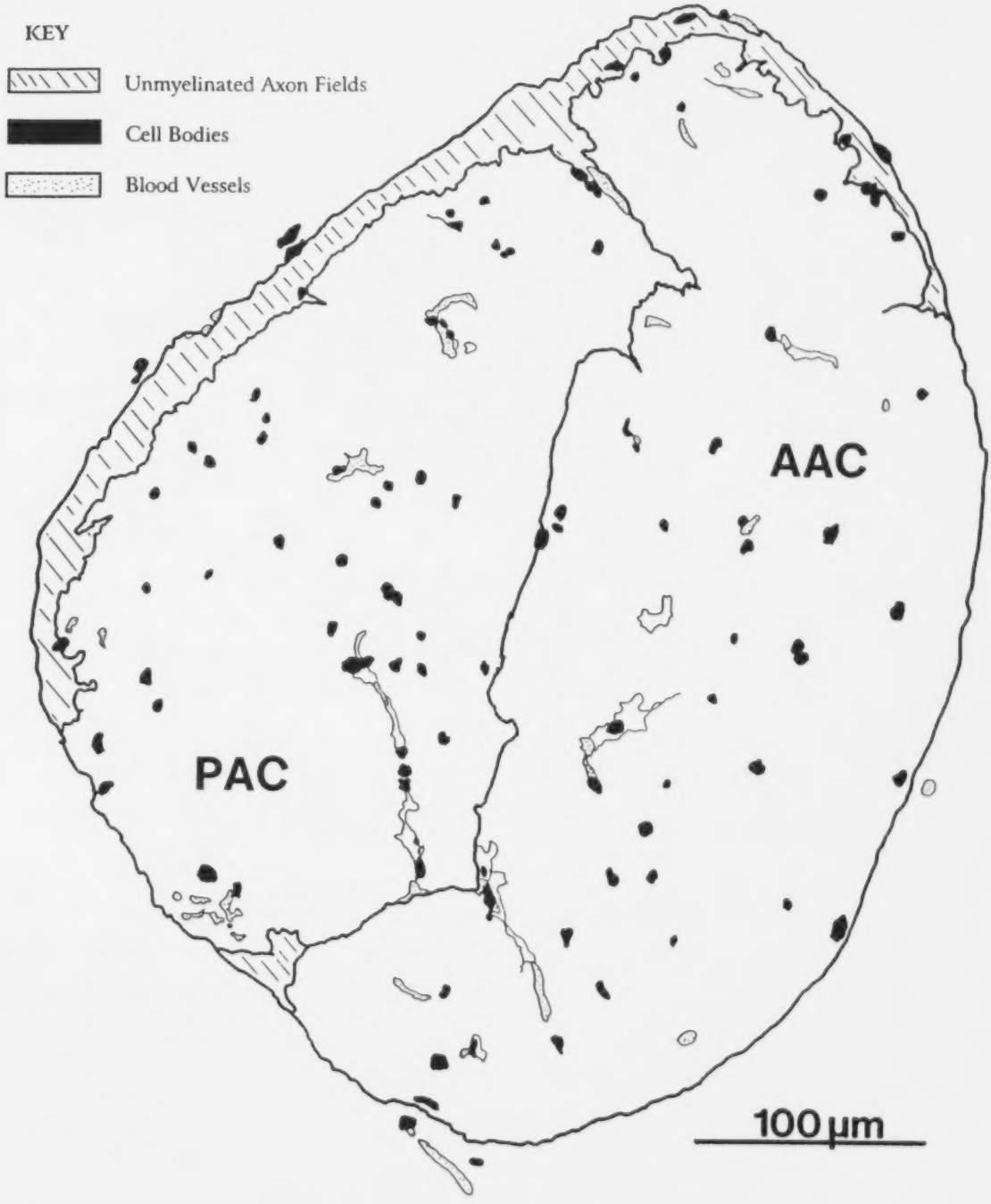
KEY
Unmyelinated Axon Fields
Cell Bodies
Blood Vessels
AAC
PAC
100 µm

Axon Counts and Measurements

Counts and diameters were measured blind to the identity of the mouse. Kodabrome RC III glossy paper developed in a Rapidoprint DD 5400 automated printer was used to produce 8x10 prints from the approximate middle of the negative at an enlargement factor of 9.2x. The counting region was outlined in the middle of the print using a 15.1cm x 20.1cm counting template and the number of myelinated and unmyelinated axons within the outline was counted. Of the axons touching the border of the template, only those touching the top or left border were included in the count.

Axon diameters were measured separately for myelinated and unmyelinated axons. Two 15.1cm x 20.1cm templates were prepared with fine wire producing a grid with 12 intersection points. These points differed for each template. A coin toss was used to determine which template was to be used, and this template was lain over the outline from the counting template. The diameter of the axon closest to the grid intersection was measured. The diameter of non-spherical cross-sections was considered to be the largest distance across the shorter of the axon's outline dimensions.

Statistics

Axon counts were extrapolated to the appropriate area to give a final count. Multiple regression was used with effect coding to test main effects of corpus callosum presence ($129CF_2$ acallosal and RI-1 mice vs. $129CF_2$ normal and RI-22 mice) and genetic background

($129CF_2$ vs. recombinant inbred), as well as their interaction, on morphometric and axon count data. Differences in axonal diameter were tested using t-tests with diameter means, and Mann-Whitney U nonparametric tests with the diameter distributions. All statistics were performed using SPSS for Windows v6.1.

RESULTS

A total of 15 mice were included in the study, 3 from $B6D2F_2$, 3 normal and 2 acallosal $129CF_2$ mice, 4 from RI-1, and 3 from RI-22 (see Table 5.1). Fixation quality was excellent in most animals, enabling the distinction between axonal type and extra-axonal tissue (Fig. 5.2a). Differentiation between the AAC and PAC was facilitated by the increased quantity of myelination in the AAC (see Fig. 5.2b; Sturrock, 1976). The external border of the AC was defined by an abrupt decrease in the presence of axons or by the presence of longitudinally running axons of the dorsal stria (DeOlmos and Ingram, 1972). In both normal and acallosal brains, very dense fields of unmyelinated axons were seen in certain areas around the perimeter of the AC (see Fig. 5.2c). These fields were quite distinct from the AC proper due to a lack of myelinated axons and by the consistency in the shape and size of the axons. Often, these axons overlapped the border between AAC and PAC. These fields of unmyelinated axons were not included in the area measurements or axon counts, because it is likely that they are part of the commissural division of the stria terminalis which crosses midline in close association with the AC (Sidman, Angevine, and Taber Pierce, 1971; DeOlmos and Ingram, 1972).

Table 5.1: Anterior Commissure Morphometric Data.

Strain	Sex	Age (days)	Body Weight (g)	Brain Weight (g)	CC Area (mm^2)	HC Area (mm^2)
$B6D2F_2$	F	99	24.8	0.401	0.684	0.160
$B6D2F_2$	F	99	24.5	0.427	0.909	0.160
$B6D2F_2$	F	99	24.9	0.413	0.619	0.134
$129CF_2$	F	68	21.7	0.442	0.922	0.226
$129CF_2$	F	67	21.0	0.503	1.079	0.293
$129CF_2$	M	67	29.3	0.436	0.757	0.318
$129CF_2$	M	69	24.3	0.448	0.000	0.181
$129CF_2$	M	68	20.3	0.398	0.000	0.061
RI-22	F	110	27.9	0.474	0.856	0.337
RI-22	M	110	31.6	0.460	1.003	0.309
RI-22	M	110	31.7	0.430	0.850	0.287
RI-1	F	109	31.1	0.465	0.000	0.046
RI-1	F	109	25.0	0.468	0.000	0.046
RI-1	M	109	26.0	0.436	0.000	0.137
RI-1	M	109	26.3	0.433	0.000	0.078

Fig. 5.2. Ultrastructure of the Mouse Anterior Commissure. *(a)* PAC area of a $B6D2F_2$ mouse showing fields of myelinated (m) and unmyelinated (u) axons, as well as an oligodendroglial cell (o). *(b)* AAC area from the same mouse showing the higher proportion of myelinated axons. The fields of unmyelinated axons seen around the perimeter of the AC are shown in *(c)*. Note the consistent size and shape of these axons; these axons are likely part of the commissural division of the stria terminalis. (Scale: 1μm)

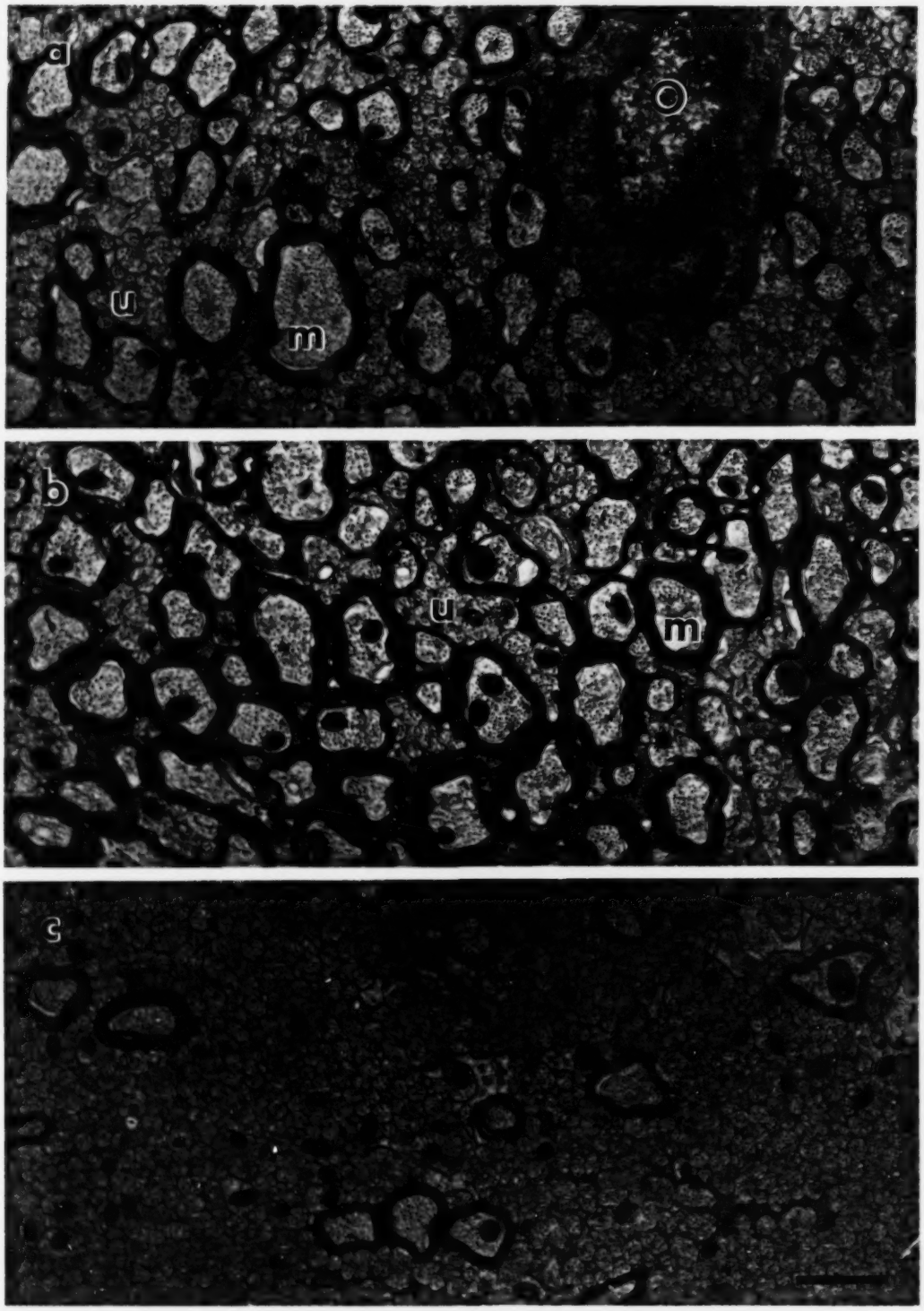
a
u
m
b
u
m
c

Morphometric Measurements

Multiple regression was used to test for a main effect of sex on AC morphology and axon count data; no significant effect of sex was found so mice were pooled in two groups as follows:

normals - $129CF_2$ normals + RI-22

acallosals - $129CF_2$ acallosals + RI-1

A comparison of midsagittal AC area and total AC axon number between the normals and the $B6D2F_2$ mice indicated these two groups did not differ and therefore it was assumed that the normal group provided an adequate estimation of normal development for comparison to the acallosal group.

Brain weight of $B6D2F_2$ mice was lower than in the normals ($p=0.037$) but this was reflective of the smaller body size of these mice and did not result in a significant difference in corpus callosum area (see Table 5.1). No difference in brain weight was evident between the normals and acallosals; however an expected decrease in HC area was found in the acallosal animals ($p<0.0001$). Callosal agenesis may result from a defect in the traverse of the telencephalic midline by hippocampal axons forming the hippocampal commissure and therefore animals with callosal absence are often accompanied by a defect in HC structure (Livy and Wahlsten, 1991; Wahlsten and Bulman-Fleming, 1994).

AC measures were not corrected for the shrinkage caused by the rigorous fixation

protocol required for electron microscopy. AC tissue from both acallosals and normals underwent identical fixation protocols, and area measures obtained were compared between the two groups. No difference in midsagittal AC area was found between the normals and acallosals (Table 5.2). Similarly, no significant differences were found between the normals and acallosals in mid-sagittal AAC area (Table 5.3) or in mid-sagittal PAC area (Table 5.4).

Axon Numbers

Axon counts from the entire AC are shown in Table 5.2. The total number of axons in the acallosal animals was 15.7% higher than in the normal animals (529,073 vs. 457,381; p=0.0003). This difference was specific for the number of unmyelinated axons (419,271 vs. 353,539; p<0.0001). Although the $129CF_2$ acallosals had a greater number of myelinated axons than the $129CF_2$ normals, as a group the acallosals did not differ significantly from the normals. RI mice did have more myelinated axons than the $129CF_2$ mice (113,517 vs. 97,448; p=0.02); however Sturrock (1976) has reported an increase in the number of myelinated axons in older animals. A corresponding increase in unmyelinated axon number was found in the $129CF_2$ animals (408,495 vs. 370,627; p=0.0012).

Because the AAC and PAC arise from different origin sites (Jouandet and Hartenstein, 1983), it is possible that the difference in axon number may be present in only one of these areas. Axon numbers for the anterior part of the AC are shown in Table 5.3. The differences found in the AAC were similar to those found in the total AC. Acallosal animals had a 17% greater total number of axons (256,203 vs. 219,040; p=0.0026) and this

Table 5.2: Mean and Standard Deviation (italics) of Areas and Axon Numbers in the Total Anterior Commissure.

Strain	Total AC Area (μm^2)	Total Axon #	Myelinated Axon #	Unmyelinated Axon #
$B6D2F_2$	92,520 *2,910*	489,200 *19,800*	95,850 *7,320*	393,300 *12,800*
$129CF_2$ Normal	103,200 *12,100*	476,500 *36,200*	93,920 *17,700*	382,600 *18,500*
$129CF_2$ Acallosal	109,200 *4,190*	550,100 *27,800*	102,700 *5,870*	447,400 *21,900*
RI-22	115,600 *10,700*	438,300 *44,700*	113,800 *9,400*	324,500 *35,300*
RI-1	124,000 *6,900*	518,500 *17,300*	113,300 *4,700*	405,200 *16,600*

difference was again specific for the number of unmyelinated axons (188,619 vs. 155,122; p=0.0004). An effect of genetic background was only present in the comparison of unmyelinated axon numbers, $129CF_2$ animals having a greater number than the RI strains (184,210 vs. 163,056; p=0.0064).

Axon numbers for the posterior part of the AC are shown in Table 5.4. Acallosal animals had a 15.3% greater total number of axons than the normals (275,841 vs. 239,324; p=0.034). No difference in myelinated axon number was found between the acallosals and normals, but was again found between the RI strains and the $129CF_2$ animals (p=0.018). A significant interaction between genetic background and callosal absence was found for the number of unmyelinated axons (p=0.041); axon number was similar in the $129CF_2$ normals and acallosals, but in the RI strains, RI-1 mice had a much larger number of axons than the RI-22 mice.

Reliability Measures

Two series of blind axon recounts of myelinated and unmyelinated axons were made to determine the reliability of the counting protocol. For both series of recounts, fifteen photographs were selected (one from each brain) to cover a range of original axon counts; different photographs were selected for each series. In the first series, recounts were performed using the same area outline to determine if the criteria used to differentiate between axon types and extracellular material was reliable. The correlation between the original counts and the recounts for myelinated axons was 0.995 and for unmyelinated axons

Table 5.3: Mean and Standard Deviation (italics) of Areas and Axon Numbers in the Anterior Part of the Anterior Commissure.

Strain	AAC Area (μm^2)	AAC Axon #	Myelinated Axon #	Unmyelinated Axon #
$B6D2F_2$	57,070 *3,180*	250,300 *10,900*	62,790 *6,850*	187,500 *7,590*
$129CF_2$ Normal	59,150 *6,610*	220,600 *27,700*	56,920 *10,900*	163,600 *18,300*
$129CF_2$ Acallosal	66,620 *2,940*	284,200 *3,110*	69,140 *3,000*	215,100 *6,100*
RI-22	68,100 *6,860*	217,500 *18,000*	70,920 *3,780*	146,600 *14,200*
RI-1	70,330 *4,750*	242,200 *13,700*	66,810 *3,270*	175,400 *12,300*

Table 5.4: Mean and Standard Deviation (italics) of Areas and Axon Numbers in the Posterior Part of the Anterior Commissure.

Strain	PAC Area (μm^2)	PAC Axon #	Myelinated Axon #	Unmyelinated Axon #
$B6D2F_2$	35,210 *489*	233,700 *13,500*	33,120 *1,610*	200,500 *12,000*
$129CF_2$ Normal	43,440 *7,510*	258,600 *33,500*	36,190 *8,610*	222,400 *26,300*
$129CF_2$ Acallosal	42,400 *1,350*	262,800 *29,800*	33,770 *3,000*	229,100 *26,800*
RI-22	47,000 *3,830*	220,100 *28,600*	42,150 *6,260*	177,900 *22,400*
RI-1	53,420 *2,670*	282,300 *4,450*	45,920 *1,880*	236,400 *5,590*

was 0.978, indicating an excellent count-recount reliability. In the second recount series, the area outline from which the counts were made was moved to a different location of the photograph to determine if the axons counts obtained for each brain was a reliable estimation of the actual axon number. Again, the correlations between the original counts and recounts were high, 0.971 for myelinated axons and 0.984 for unmyelinated axons, indicating that the counts obtained were indeed excellent estimates of the actual number of axons contained within each area being measured.

Axon Densities

Axon density removes any possible effect of area as a covariate. Table 5.5 shows the axon densities of the AC as a whole. The results support those from the axon counts, with acallosal mice having a higher density of unmyelinated axons than normal mice ($p = 0.026$); no differences in myelinated axon density were apparent. Similarly, the unmyelinated axon density in the AAC (Table 5.6) was higher in acallosal mice that in normal mice ($p = 0.021$). A similar pattern was seen in the PAC (Table 5.7), but the difference was not significant. It is interesting to note that the effect of genetic background was greater in the axon density data than in the axon count data, with a higher density usually present in the $129CF_2$ mice.

Axon Diameters

One explanation for the existence of more axons in the anterior commissure of

Table 5.5: Mean and Standard Deviation (italics) of Combined, Myelinated, and Unmyelinated Axon Density in the Total Anterior Commissure.

Strain	Combined Axon Density (#/1000μm^2)	Myelinated Axon Density (#/1000μm^2)	Unmyelinated Axon Density (#/1000μm^2)
$B6D2F_2$	5,288 *169*	1,036 *72*	4,252 *100*
$129CF_2$ Normal	4,630 *212*	905 *73*	3,725 *253*
$129CF_2$ Acallosal	5,039 *61*	941 *18*	4,098 *44*
RI-22	3,794 *254*	985 *53*	2,808 *204*
RI-1	4,187 *171*	915 *32*	3,272 *164*

Table 5.6: Mean and Standard Deviation (italics) of Combined, Myelinated, and Unmyelinated Axon Density in the Anterior Part of the Anterior Commissure.

Strain	Combined Axon Density (#/1000μm^2)	Myelinated Axon Density (#/1000μm^2)	Unmyelinated Axon Density (#/1000μm^2)
$B6D2F_2$	4,387 *52*	1,099 *90*	3,289 *115*
$129CF_2$ Normal	3,728 *212*	956 *82*	2,771 *207*
$129CF_2$ Acallosal	4,271 *235*	1,037 *0.85*	3,233 *234*
RI-22	3,198 *74*	1,045 *50*	2,153 *39*
RI-1	3,449 *175*	951 *33*	2,498 *168*

Table 5.7: Mean and Standard Deviation (italics) of Combined, Myelinated, and Unmyelinated Axon Density in the Posterior Part of the Anterior Commissure.

Strain	Combined Axon Density (#/1000μm^2)	Myelinated Axon Density (#/1000μm^2)	Unmyelinated Axon Density (#/1000μm^2)
$B6D2F_2$	6,638 *425*	941 *48*	5,697 *380*
$129CF_2$ Normal	5,982 *313*	828 *64*	5,154 *375*
$129CF_2$ Acallosal	6,190 *506*	795 *45*	5,395 *461*
RI-22	4,687 *565*	897 *116*	3,790 *452*
RI-1	5,294 *256*	860 *33*	4,434 *247*

acallosal animals without a corresponding increase in AC size, is a reduction in the diameter of the axons in these animals. Mean axonal diameters are shown in Table 5.8. Examination using one-tail t-tests indicated that unmyelinated axon mean diameters were indeed lower in the acallosal animals than in the normals ($t=2.59$, $df=10$, $p=0.014$), a difference that was maintained for both the AAC ($t=2.37$, $df=10$, $p=0.020$) and the PAC ($t=1.89$, $df=10$, $p=0.044$). No differences were found in the diameter of myelinated axons.

The distributions of myelinated and unmyelinated axon diameters for both the acallosal and normal animals are shown in Figs. 5.3 and 5.4 respectively. The group distributions were created by adding, or overlaying, the distributions of individual animals within a group. A relatively high proportion of axons was of smaller diameter, producing diameter distributions that were positively skewed. As reported by Sturrock (1976), no axons less than 0.24μm in diameter were myelinated; however about 4% of the unmyelinated axons were larger than 0.6μm, the largest being 1.5μm. A visual analysis of the distributions indicates no apparent differences between acallosal and normal animals for the distribution of myelinated axons, a result supported by Mann-Whitney U nonparametric tests. In contrast, Mann-Whitney U analysis indicated that the distribution of unmyelinated axons in the acallosal animals is shifted toward the range of smaller diameters ($p<0.0001$), a difference that is maintained in both the AAC ($p=0.0007$) and PAC ($p=0.0004$). These differences support the t-test results, suggesting that the diameters of the unmyelinated axons in the acallosal animals are reduced.

Table 5.8: Mean and Standard Deviation of Axon Diameters.

Strain	Myelinated Axon Diameters (μm)			Unmyelinated Axon Diameters (μm)		
	AC	AAC	PAC	AC	AAC	PAC
129CF$_2$ Normal	0.7860 *0.030*	0.8077 *0.022*	0.7533 *0.052*	0.2547 *0.025*	0.2457 *0.013*	0.2683 *0.044*
129CF$_2$ Acallosal	0.7989 *0.006*	0.8253 *0.049*	0.7594 *0.060*	0.2430 *0.018*	0.2455 *0.009*	0.2385 *0.032*
RI-22	0.7981 *0.035*	0.8165 *0.043*	0.7706 *0.021*	0.2713 *0.006*	0.2787 *0.009*	0.2603 *0.017*
RI-1	0.7951 *0.019*	0.8232 *0.036*	0.7531 *0.034*	0.2340 *0.016*	0.2360 *0.013*	0.2313 *0.028*

Fig. 5.3. Myelinated AC Axon Diameters. The average distribution of myelinated axon diameters is shown in normal CC (top) and acallosal (bottom) mice. A mean-centered normal curve is superimposed on the distributions to assist the comparison between the normal and acallosal mice. The shape and position of the average diameter distributions of myelinated axons are similar in both normal and acallosal mice, suggesting no difference between them, which was supported by statistical testing.

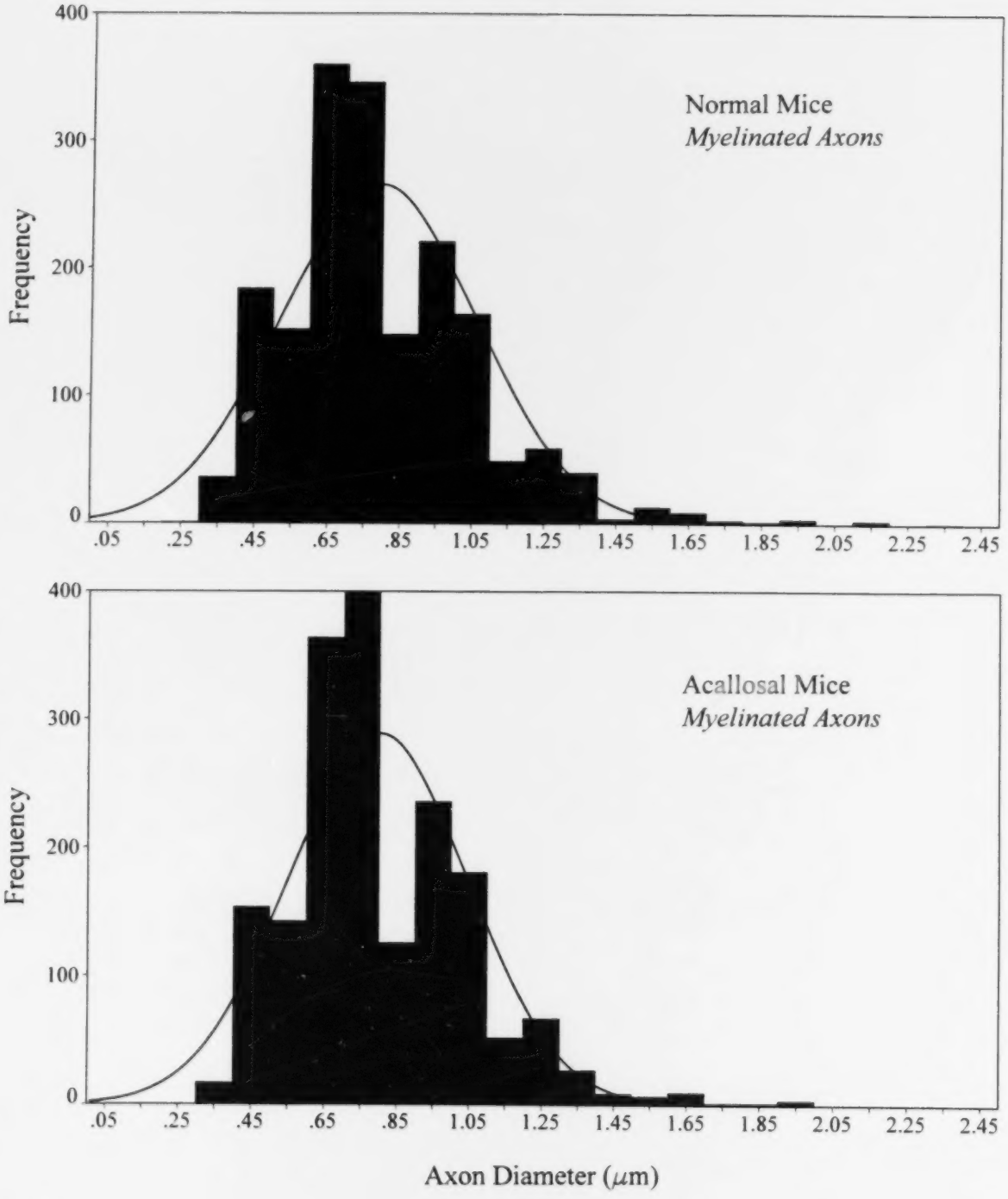
Normal Mice
Myelinated Axons
Frequency
400
300
200
100
0
.05
.25
.45
.65
.85
1.05
1.25
1.45
1.65
1.85
2.05
2.25
2.45
Acallosal Mice
Myelinated Axons
Frequency
400
300
200
100
0
.05
.25
.45
.65
.85
1.05
1.25
1.45
1.65
1.85
2.05
2.25
2.45
Axon Diameter (μm)

Fig. 5.4. Unmyelinated AC Axon Diameters. The average distribution of unmyelinated axon diameters is shown in normal (top) and acallosal (bottom) mice. A mean-centered normal curve is superimposed on the distributions to assist the comparison between the normal and acallosal mice. The extrapolation of axon diameter measurements resulted in no axons measuring within the 0.25μm range resulting in the gap seen in the histograms, however as this is consistent for both normal and acallosal mice, this does not affect the comparison of their distributions. The average diameter distribution of unmyelinated axons in acallosal mice shows more kurtosis than that shown in the normal mice and is also shifted towards the range of smaller diameters. This smaller diameter of unmyelinated axons in the acallosal mice may enable more axons to pass through the AC without significantly increasing the AC area.

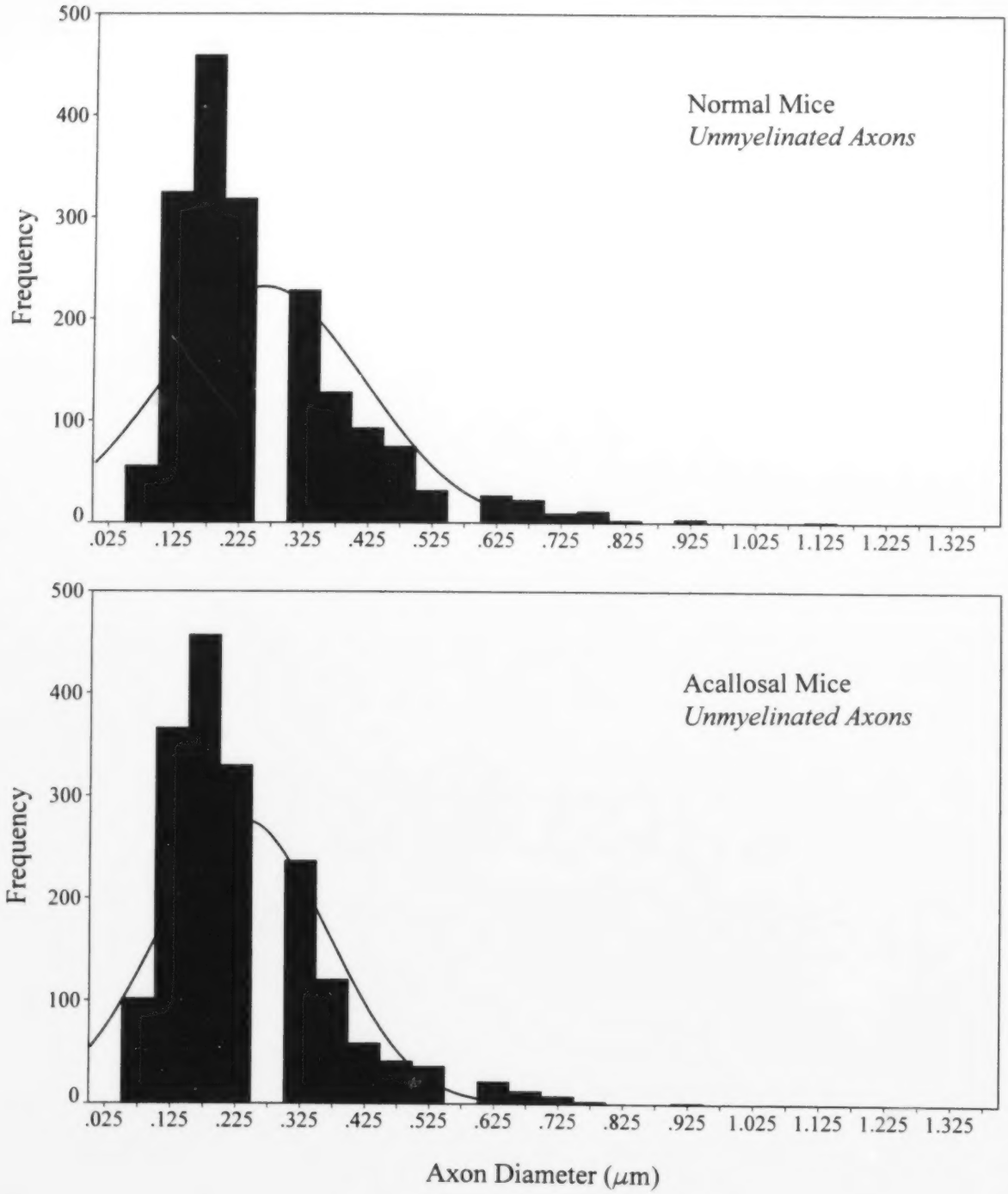
Normal Mice
Unmyelinated Axons
Acallosal Mice
Unmyelinated Axons
Frequency
Frequency
0
100
200
300
400
500
.025
.125
.225
.325
.425
.525
.625
.725
.825
.925
1.025
1.125
1.225
1.325
Axon Diameter (μm)

DISCUSSION

The results clearly show a large increase in the number of axons in the anterior commissure of acallosal mice. Although this increase was specific for unmyelinated axons, it was found in both the anterior and posterior halves of the AC. The increase in the number of unmyelinated axons was accompanied by a decrease in the diameter of these axons, resulting in no net increase in AC size. Although some differences were noted in the number of myelinated axons, none were statistically significant. Similarly, no differences were noted in myelinated axon density, although unmyelinated axon densities were higher in the acallosal animals.

The increase seen in unmyelinated axon number is far less than the number of interhemispheric axons lost due to the absence of the corpus callosum. Tomasch and MacMillan (1957) estimated the total number of callosal axons to be 300,000 in the white mouse but this estimate was severely compromised by the lack of resolution afforded by light microscopy. Extrapolating the number of callosal axons in the rat (12 million in 2.563mm^2, Gravel *et al*, 1990) to the mouse provides an estimate of 3.5 million in B6D2F$_2$ mice and 4.3 million in 129CF$_2$ mice; a rough estimate using direct callosal axon counts found about 7.1 million in a 42 day old female B6D2F$_2$ mouse (see Appendix A).

The increase in unmyelinated axons through the AC may help to compensate for this loss of callosal axons by improving the efficiency of information transfer between the hemispheres in the acallosal animals. However, the large net loss in commissural axon numbers, particularly myelinated axons, may explain the increased time required for

information transfer between hemispheres in humans (Jeeves, 1969; Milner, Jeeves, Silver, Lines, and Wilson, 1985; Jeeves, Silver, and Jacobsen, 1988).

The critical question of where these "extra" axons come from still remains. Although the higher numbers may be suggestive of re-routing by callosal axons through the anterior commissure, a recent study using retrograde labelling of AC axons in acallosal mice has not shown this to occur (Lent, personal communication), supporting previous findings by Wahlsten and Jones (1983), Olavarria *et al* (1988) and Ozaki and Wahlsten, (1992). All labelled axons were traced back to normal sites of AC origin, showing qualitatively normal patterns of labelling, except in the anterior piriform cortex where a clear deficit was shown in both BALB and $129CF_2$ mice, regardless of callosal size.

The plasticity in the number of AC axons may be due to transient branching of fibres within the AC, similar to that shown by callosal axons in the hamster (Khadim, Bhide, and Frost, 1993). Alternatively, the results could be explained by a decrease in the amount of axon elimination after an initial period of overabundant proliferation. Axon elimination following a period of rapid axon production during early development has been shown in the corpus callosum of the rat (Gravel and Hawkes, 1990; Gravel *et al*, 1990), cat (Berbel and Innocenti, 1988), and monkey (LaMantia and Rakic, 1990b). Similarly, a developmental elimination of AC axons has been reported in monkeys (LaMantia and Rakic, 1994) and opposums (Cabana and Martin, 1985). However, in both rats (Berbel, Guadaño-Ferraz, Angulo, and Cerezo, 1994; Guadaño-Ferraz, Escobar del Rey, Escobar, Innocenti, and Berbel, 1994) and hamsters (Lent and Guimarães, 1991) this elimination of AC axons was not apparent; this may have been due to a simultaneous production and elimination of axons

resulting in no net change in axonal number, similar to the pattern of development seen in the rat CC (Gravel and Hawkes, 1990). In the mouse, the mid-sagittal area of the AC increases rapidly during development to about 6 days after birth (Wahlsten, 1984). Sturrock (1976) found that myelination of AC axons starts at about P8 - P9 in ASH/TO mice, and continues rapidly to about P50. During this time, the size of the AC remains relatively stable; although there is a doubling of axonal diameter due to myelination, which occurs in 12% of axons in the PAC and in 27% of axons in the AAC, there is also a gradual decrease in axon number from P6 - P30. This suggests that the mouse also undergoes an elimination of AC axons during normal development, and it is possible that the number of axons eliminated is reduced when the CC is absent.

The AC in primates and marsupials is mainly of neocortical origin, while in rodents the AC is mainly of paleocortical origin, and therefore the occurrence of axon elimination may be a developmental process that is unique to the neocortex (Lent and Guimarães, 1991; Lent, 1992). However, Hedin-Pereira, Uziel, and Lent, (1992) described the presence of bicommissural axons from the lateral cortex of developing hamsters which project through both the corpus callosum and the anterior commissure. These bifurcating axons are not seen in the adult, suggesting that one branch is eliminated during development. It is possible that callosal agenesis would favour the survival of the axonal branch travelling through the AC.

The anterior commissure provides interhemispheric transfer of visual, auditory, olfactory, and mnemonic information in animals (Black and Myers, 1964; Pandya, Hallett, and Mukherjee, 1969; Sullivan and Hamilton, 1973; Butler, 1979; King and Hall, 1990; Kucharski, Burka, and Hall, 1990) and humans (Risse, LeDoux, Springer, Wilson, and

Gazzaniga, 1978 - but see McKeever, Sullivan, Ferguson, and Rayport, 1981). Although similar functions are performed by the corpus callosum, cortical areas served by these two commissures have in some cases been found to be distinct (Zeki, 1973). The unique use of the anterior commissure as an extracallosal commissural pathway would not provide the level of compensation generally seen in acallosals, and it is probable that the uses of all other commissures are also enhanced. Ettlinger and Blakemore (1969) suggested that the posterior commissure and superior colliculus mediate the interhemispheric transfer of colour and intensity discrimination in cats and monkeys. Work by Sergent (1986, 1990) and Milner (1994) has indicated the importance of subcortical pathways for the transfer of visual information. An increased bilateral representation of function in the brain, an increased use of ipsilateral pathways, and the use of behavioural cross-cuing have also been proposed to assist in the compensation of interhemispheric function (Jeeves, 1992). No one form of compensation appears to be sufficient to explain the extent of recovery of function displayed in acallosals, and Chiarello (1980) has suggested that all four mechanisms may be involved. These may be accompanied by a general re-organization of cortical communication to improve the efficiency of interhemispheric transfer. Surgical lesion often produces a reorganization of axonal and dendritic connections leading to some form of functional recovery (Steward, 1984) and it is possible that the loss of connections by a more natural occurrence may elicit the same effect. In fact, Wolff and Zaborszky (1979) have demonstrated functional recovery after surgical lesion due to the plasticity of callosal connections in the rat cortex.

Electron microscopy has shown that the number of AC axons is higher in mice with

complete absence of the CC. This is the first direct and consistent morphological evidence supporting a compensatory role for the anterior commissure in callosal agenesis. AC axon counts in mice with callosal dysgenesis will indicate whether a total absence of callosal fibres is necessary for the increase in AC axon number, or whether the few callosal axons that do manage to cross midline are sufficient to maintain effective interhemispheric communication. Olavarria *et al* (1988) have shown that the abnormally small callosum that forms in callosal dysgenesis maintains the topographic pattern of connectivity seen in normal development, permitting interhemispheric communication in all areas of the cortex. However a large net loss of axons would still be evident and further investigation would determine whether the increase in AC axon number is maintained in animals with callosal dysgenesis or whether there is a smaller increase in number that is correlated with the size of the callosal remnant. Similarly, a developmental series of axon counts in both normal and acallosal mice would be useful for comparing the patterns of proliferation of AC axons to determine when the axonal increase occurs in relation to the callosal defect and to determine whether there is a critical period for the effect of callosal absence to affect AC morphology, similar to the critical period during which callosal absence affects visual cortex development (Elberger, 1988). Such information would provide insight into the brain's ability to alter its structure in response to developing anomalies.

SUMMARY AND CONCLUSIONS

Agenesis of the corpus callosum has been used as a model to study the guidance of commissural axons during their traverse of the interhemispheric region in the brain and the plasticity that is displayed by these axons when their normal mechanisms of guidance are disrupted. Several important and unique discoveries have been described within the scope of the present research.

In Experiment 1, the route and timing of axonal traverse by axons of the hippocampal commissure were described in both normal and acallosal strains of mice. Axons of this commissure cross midline immediately prior and ventral to axons of the corpus callosum, and the HC has been suggested as a possible substrate for callosal axons during their midline traverse. Therefore, the interaction between hippocampal and callosal axons was also observed in normal mice. In normal B6D2F_2 mice, the hippocampal axons cross the telencephalic midline at the base of the longitudinal fissure in association with the pia membrane at about 0.35g body weight. These axons were initially prevented from crossing due to the presence of the interhemispheric fissure which extended deep into the septal region. Callosal axons were first seen crossing midline at 0.62g body weight, approximately 29 hours after the HC axons. These early callosal axons were identified fasciculating along and between existing hippocampal axons at the dorsal surface of the hippocampal commissure. It is important to stress that this is the first time direct evidence has been demonstrated to support the use of the hippocampal axons by early callosal axons to cross

midline in normal mice. No callosal axons were seen to cross midline on top of a cellular bridge spanning midline rostral to the HC during this early phase of corpus callosum formation.

In acallosal strains, the continued presence of the interhemispheric fissure deep within the septal region blocked the normal route of passage across midline by the hippocampal axons for an extended period of time. The delay in fissure fusion and subsequently of midline crossing by HC axons was found to be longer in strains with a higher incidence of callosal defect. These results suggest that callosal agenesis may be a secondary defect resulting from a primary defect occurring during the time of HC formation.

The delay in HC formation in acallosal mice was related to the continued presence of the interhemispheric fissure at midline. An attempt was made to determine the cause of this delay in fissure fusion in Experiment 3. Although Wahlsten and Bulman-Fleming (1994) did find a retardation in the rate of rostral growth of the septal region in acallosal strains, results from the present study indicated that this retarded growth was not the result of a difference between normal and acallosal mice in the number of cells in mitosis in the neuroepithelium of the third ventricle. Qualitative observation suggested a similar lack of difference between strains within the medial neuroepithelium of the lateral ventricles and in general cytoarchitecture.

These experiments described the structure of the midline region and the activity and interactions of the commissural axons as they approached and crossed the telencephalic midline. In Experiment 5, the consequence of the failure of CC axons to cross midplane was addressed. The absence of the corpus callosum represents the loss of a large

interhemispheric communication route, yet it produces relatively few behavioural deficits. The plasticity inherent in developing systems suggests that structural morphology could be altered to compensate for this loss of axons. In non-placental mammals the anterior commissure provides the largest route for interhemispheric axon travel and has been suggested to act as a compensatory route for interhemispheric communication in placental mammals lacking a corpus callosum. Therefore, the structure of the AC at midline was compared between normal and acallosal mice.

The number of axons in the AC of acallosal mice was higher than that in normal mice, a difference specific for the number of unmyelinated axons. Despite this higher number of axons, the midsagittal area of the AC in acallosal mice did not differ significantly from that in normal hybrids. This was likely possible due to a smaller diameter of the unmyelinated axons in the acallosal mice. Again it should be stressed that this is the first time that direct and conclusive evidence has been reported for use of the AC as a mechanism to compensate for the loss of the callosal communication route.

Despite the importance of these observations, several issues remain unresolved. Early callosal axons were observed crossing midline on top of the hippocampal commissure but it is possible that they may cross elsewhere in some normal brains. Indeed, callosal axons did not cross as a bundle in one location but rather were dispersed in different locations on top of the HC. In more mature brains, a main bundle of callosal axons was observed rostral and dorsal to the HC which brings into question the role of those axons atop the HC; these axons may serve to guide following callosal axons, they may signal the readiness of the midline region to accept crossing axons, or their presence may be unrelated

to the crossing of following callosal axons. Although an attempt was made to maximize the number of callosal axons labelled, it is possible that such labelling was incomplete. A more extensive labelling protocol would ensure that all callosal axons are labelled to help dispel doubts pertaining to present, but unlabelled, callosal axons.

Intimate contact between the early callosal axons and HC axons was directly observed in only one brain; although certainly suggestive of a facilitatory role for HC axons, this observation will have to be repeated to determine whether this is the usual method of crossing. It is also possible that this intimate contact was mediated by glial processes. Glial structures identified at the midline of the developing brain and spinal cord are thought to provide a guiding substrate for commissural axons (Silver, 1993). The use of existing axons by callosal axons during their traverse of midline is a major departure from this guidance mechanism that is apparently well-utilized by other commissural axons. Glial cells likely guide early callosal axons towards the midline; cell bodies were not identified to form a ventral bridge across the midline region but this does not preclude the existence of glial processes which may extend between the hemispheres as a guiding substrate (see Silver *et al*, 1993).

Similar questions remain regarding the specific substrate utilized by early hippocampal axons during their traverse of midline, which appeared in close apposition with the pia membrane lining the longitudinal fissure. The nature of this relationship, and that between the HC and early CC axons, was examined in Experiment 2 using electron microscopy but did not produce definitive results. Repetition of this study with the use of a refined technique (see Experiment 5) may provide more information about these

relationships. Immunofluorescent techniques were used in Experiment 4 to identify the presence of some of the more common antigens (laminin, GFAP, and vimentin) which have been identified in axon guidance, as well as one (J1-31) which has been identified at CNS trauma sites. Both laminin and vimentin were present at the midline in abundant quantities, but did not appear to be present in any form of substrate that might be specific for the guidance of the commissural axons. The absence of GFAP in the midline region likely indicates that the age of these animals was too young to demonstrate the presence of GFAP antigen (Bignami and Dahl, 1974; Raju *et al*, 1981; Valentino *et al*, 1983). The absence of J1-31 may indicate the lack of any trauma response at midline resulting from the fusion of the interhemispheric fissure. Many other antigens have been identified to be involved with the guidance of axons and a thorough investigation into the presence of these antigens is critical for understanding their potential role in the guidance of hippocampal and callosal axons through the midline region. Of particular interest is whether glial processes may be present at midline for these axons to utilize as a guiding substrate.

The continued presence of the deep cleft extending into the septal region appears to be the cause of the delay in the traverse of midline by the hippocampal axons in acallosal strains, but the reason for this continued presence remains unclear. A decrease in septal growth may result in a delay in hemispheric fusion and the amplification of differential growth rates between adjacent tissues in the septal region, both of which may serve to retard the midline development. A decrease in the mitotic index of neuroepithelial cells from the lateral ventricles would result in a decrease in septal growth, however a precise method of determining coronal position will be required to provide an accurate comparison of this

measure between normal and acallosal mice. Septal growth may also be affected by an aberrant migration pattern of post-mitotic cells from the third and lateral ventricles toward the midline region. As described in Experiment 3, the use of BrdU to observe cell migration was not found to be suitable for the present study; however, BrdU-labelling did prove to be an effective marker for identifying cell position and movement and may be considered to be superior to such methods as cell-marking with ^{3}H-thymidine due to the possibility of its use in conjunction with immunofluorescent applications to other antigens.

The increase in the number of AC unmyelinated axons in acallosal mice occurred in the absence of a significant concurrent increase in AC size. This increase in number was accompanied by a decrease in mean axonal diameter, yet it is possible that this decrease in axonal diameter does not adequately compensate for the higher number of axons and that differences must also be present in the amount extra-axonal tissue present in the AC. However, a rough estimate using mean values for axon number and diameter indicates that unmyelinated axons occupy 18,400μm^2 in the acallosals and 19,100μm^2 in the normals; this difference is only 4% but in favour of the acallosals, suggesting that the decrease in axonal diameter in the acallosals may indeed account for their higher number of axons.

Determining axon counts from other commissures in acallosal brains will indicate whether this increase in axon number is unique to the anterior commissure. It is also important to understand the timing of this increase relative to the development of the CC; a critical period may be present within which the AC can respond to the loss of callosal axons. Similarly, the AC may respond in a graduated fashion, altering axon number relative to the number of callosal axons that are able to cross midline. However, such differences, if

present, are likely to be very subtle and will require much larger sample sizes for their determination.

Juraska and Kopcik (1988) reported a difference between sexes in the number of axons in the splenium of the rat corpus callosum, however a recent study by Kim, Ellman, and Juraska (1996) found that sex differences were only present for the number of myelinated axons. This recent result was obtained using a more accurate method of selecting areas for sampling axon number. Axon density varies throughout the CC (Berbel and Innocenti, 1988; Gravel *et al*, 1990; LaMantia and Rakic, 1990b; Aboitiz *et al*, 1992) and therefore sampling error may not provide an accurate reflection of axon complement. The sampling method employed in Experiment 5 was used to provide equal representation from all areas within the AC and thus help to eliminate this problem. It is interesting to note that sex differences were not apparent for the number of axons within the AC. However it is possible that such differences were masked by the effect of callosal absence; larger sample sizes would be required for a more accurate assessment of sex effect on AC axon number.

The results that have been presented here redirect the focus of attention to the time of HC formation in order to understand the mechanisms responsible for callosum absence. Indeed, if the defect is severe enough, it should be possible to identify some mice, or potentially a strain of mouse, which consistently show HC absence or a severe reduction in HC size. If the defect is the product of only two genes, recombinant inbreds (RI) produced from acallosal inbreds should isolate at least one strain with HC absence or at least a consistently severe HC defect. Wahlsten *et al* (1996) recently developed a series of recombinant inbred strains from 129 x BALB F_2 parents and demonstrated that certain of

these RI strains do indeed express severe HC defect in every mouse.

The continued study of these RI strains may provide further insight into anomalous HC formation. In many ways, questions regarding the loss of HC axons mirror those concerning the loss of callosal connections. Results from Experiment 1 indicated that hippocampal axons unable to cross midline return to the fornix, but it was not possible to continue the observation of these axons during their subsequent growth. Of interest is whether these axons remain viable to make connections in the septal region and mamillary bodies and thus increase the functional capacity of the fornix columns. If these HC connections are indeed "lost", questions are obviously raised as to the presence of functional deficits or the possible mechanisms of compensation to overcome deficits.

The Wahlsten *et al* (1996) study also indicated that the mode of inheritance of the defect appears to fit a two-gene model with a threshold. The presence of a threshold in this defect may explain the variability in the expression of the defect. Although a difference of two alleles may alter the level of penetrance of the defect, the severity of the defect differs within different mice of the same strain. It would be easy to consider that all offspring from an inbred pairing should be identical because all offspring have an identical genotype and all are exposed to the same uterine environment. Although it is possible that the uterus may contain microenvironments that may affect each embryo in a unique manner, it is difficult to presume that such subtle differences could cause such a drastic range of differences in phenotype.

This leaves the strong suggestion of a third source of variability to account for the individual differences observed within a strain. Stochastic differences within (Spudich and

Koshland, 1976) and between (Wahlsten, 1987b) cells at early stages of growth have been suggested to create larger differences later in development. Stochastic differences and uterine microenvironments may create small differences in facial morphology which can result in nonsyndromic cleft lip with or without cleft palate in A strain mouse embryos (Juriloff, 1995); embryos that are able to surpass this developmental threshold go on to develop normal facial morphology. Monk (1995) has proposed that the relative positioning of a differentiating cell during gastrulation will add to phenotypic variability by permanently altering the future genetic activity of that cell. Such subtle differences in cell positioning are likely due to random fluctuations in the interactions and movements of cells. Computer modelling has demonstrated the amplified result of such subtle changes in early cell configurations through a period of simulated growth (Kurnit, Layton, and Matthysse, 1987), which may very well serve as a model to describe the variations observed within the developing telencephalic midline of the acallosal mouse strains.

The research described herein has provided a unique contribution to the study of callosal agenesis in particular, but also to the general study of neural system development. The developmental defect labelled agenesis of the corpus callosum does not appear to be a defect of the corpus callosum *per se*, but rather occurs due to a defect that manifests during the formation of the hippocampal commissure. Although the cause of this defect remains unknown, significant evidence has been provided to indicate its association with the continued presence of the interhemispheric fissure at the septal midline. Present results suggest that early callosal axons may use glial cells to guide them toward midline, but then use existing axons of the hippocampal commissure during the actual traverse. Such a

developmental strategy is a departure from the exclusive use of glial tissue which is thought to provide guiding support for most other commissural pathways examined but is certainly a very plausible mechanism.

The development of the three commissural pathways studied is not fixed. Instead, these pathways have demonstrated a large amount of developmental plasticity even within mice with identical genotypes, ranging from the recovery of severe structural delays in the hippocampal commissure, to the increase in axonal complement in the anterior commissure when the callosum is absent. This is further evidence to refute the idea of a "hard-wired", regimented developmental process, suggesting instead that neural systems have the capability to respond to subtle changes in their environment and effect compensatory changes to maintain the functionality of these systems.

REFERENCES

Abbey H, and Howard E (1973). Statistical procedure in developmental studies on species with multiple offspring. *Dev. Psychobiol. 6:* 329-335.

Aboitiz F, Scheibel AB, Fisher RS, and Zaidel E (1992). Fiber composition of the human corpus callosum. *Brain Res. 598:* 143-153.

Aicardi J, Chevrie JJ, and Baraton J (1987). Agenesis of the corpus callosum. *In:* Handbook of Clinical Neurology, vol. 6(50): Malformations. Myrianthopoulous NC (Ed.), New York: Elsevier. pp. 149-173.

Altman J, and Bayer SA (1990). Vertical compartmentation and cellular transformations in the germinal matrices of the embryonic rat cerebral cortex. *Exp. Neurol. 107:* 23-35.

Amaral DG, Insausti R, and Cowan WM (1984). The commissural connections of the monkey hippocampal formation. *J. Comp. Neurol. 224:* 307-336.

Auladell C, Martinez A, Alcantara S, Supèr H, and Soriano E (1995). Migrating neurons in the developing cerebral cortex of the mouse send callosal axons. *Neuroscience 64:* 1091-1103.

Austin CP, and Cepko CL (1990). Migration patterns in the developing mouse cortex. *Development 110:* 713-732.

Balaban E, Teillet M-A, and Le Douarin N (1988). Application of the quail-chick chimera system to the study of brain development and behavior. *Science 241:* 1339-1342.

Barr M Jr., Jensch RP, and Brent RL (1970). Prenatal growth in the albino rat: Effects of number, intrauterine position and resorptions. *Am. J. Anat. 128:* 413-428.

Bastiani MJ, and Goodman CS (1986). Guidance of neuronal growth cones in the grasshopper embryo. III. Recognition of specific glial pathways. *J. Neurosci. 6:* 3542-3551.

Berbel P, and Innocenti GM (1988). The development of the corpus callosum in cats: A light- and electron-microscopic study. *J. Comp. Neurol. 276:* 132-156.

Berbel P, Guadaño-Ferraz A, Angulo A, and Cerezo JR (1994). Role of thyroid hormones in the maturation of interhemispheric connections in rats. *Behav. Brain Res. 64:* 9-14.

Berrebi AS, Fitch RH, Ralphe DL, Denenberg JO, Friedrich VL Jr, and Denenberg

VH (1988). Corpus callosum: region-specific effects of sex, early experience and age. *Brain Res. 438:* 216-224.

Bhide PG, and Frost DO (1991). Stages of growth of hamster retinofugal axons: implications for developing axonal pathways with multiple targets. *J. Neurosci. 11:* 485-504.

Bignami A, and Dahl D (1974). Astrocyte-specific protein and neuroglial differentiation. An immunofluorescence study with antibodies to the glial fibrillary acidic protein. *J. Comp. Neurol. 153:* 27-38.

Bignami A, Raju T, and Dahl D (1982). Localization of vimentin, the nonspecific intermediate filament protein, in embryonal glia and in early differentiating neurons. *Dev. Biol. 91:* 286-295.

Bignami A, Chi NH, and Dahl D (1984). First appearance of laminin in peripheral nerve, cerebral blood vessels and skeletal muscle of the rat embryo. *Int. J. Dev. Neurosci. 2:* 367-376.

Bishop KM, and Wahlsten D (1996). Sex differences in human corpus callosum: myth or reality? *Neurosci. Biobehav. Rev.*, in press.

Black P, and Myers RE (1964). Visual function of the forebrain commissures in the chimpanzee. *Science 146:* 799-800.

Blackstad, TW (1956). Commissural connections of the hippocampal region in the rat, with special reference to their mode of termination. *J. Comp. Neurol. 105:* 417-537.

Blakemore WF (1969). The ultrastructure of the subependymal plate in the rat. *J. Anat. 104:* 423-433.

Bossy JG (1970). Morphological study of a case of complete, isolated, and asymptomatic agenesis of the corpus callosum. *Arch. Anat. Histol. Embryol. 53:* 289-340.

Boulder Committee (1970). Embryonic vertebrate central nervous system: revised terminology. *Anat. Rec. 166:* 257-262.

Bovolenta P, and Dodd J (1990). Guidance of commissural growth cones at the floor plate in embryonic rat spinal cord. *Development 109:* 435-447.

Bovolenta P, and Dodd J (1991). Perturbation of neuronal differentiation and axon guidance in the spinal cord of mouse embryos lacking a floor plate: analysis of Danforth's short-tail mutation. *Development 113:* 625-639.

Bovolenta P, and Mason C (1987). Growth cone morphology varies with position in the developing mouse visual pathway from retina to first targets. *J. Neurosci. 7:* 1447-1460.

Buchhalter JR, Fieles A, and Dichter MA (1990). Hippocampal commissural connections in the neonatal rat. *Dev. Brain Res. 56:* 211-216.

Bulman-Fleming B, and Wahlsten D (1988). Effects of a hybrid maternal environment on brain growth and corpus callosum defects of inbred BALB/c mice: A study using ovarian grafting. *Exp. Neurol. 99:* 636-646.

Bulman-Fleming B, and Wahlsten D (1991). The effects of intrauterine position on the degree of corpus callosum deficiency in two substrains of BALB/c mice. *Dev. Psychobiol. 24:* 395-412.

Bulman-Fleming B, Wainwright PE, and Collins RL (1992). The effects of early experience on callosal development and functional lateralization in pigmented BALB/c mice. *Behav. Brain Res. 50:* 31-42.

Butler SR (1979). Interhemispheric transfer of visual information via the corpus callosum and anterior commissure in the monkey. *In:* Structure and Function of the Cerebral Commissures. Steele Russel I, Van Hof M, and Berlucchi G (Eds.). New York: MacMillan. pp: 343-357.

Cabana T, and Martin GF (1985). The development of commissural connections of somatic motor-sensory areas of neocortex in the North American opossum. *Anat. Embryol. 171:* 121-128.

Cassells B, and Wahlsten D (1989). Heredity of collisions between anterior commissure and columns of the fornix in mouse brain. *Soc. Neurosci. Abstr. 15:* 875.

Cassells B, Wainwright P, and Blom K (1987). Heredity and alcohol-induced brain anomalies: Effects of alcohol on anomalous prenatal development of the corpus callosum and anterior commissure in BALB/c and C57BL/6 mice. *Exp. Neurol. 95*: 587-604.

Chen YP, Campbell R, Marshall JC, and Zaidel DW (1990). Learning a unimanual motor skill by partial commissurotomy patients. *J. Neurol. Neurosurg. Psych. 53:* 785-788.

Chiarello C (1980). A house divided? Cognitive functioning with callosal agenesis. *Brain Lang. 11:* 128-158.

Cochard P, and Paulin D (1984). Initial expression of neurofilaments and vimentin in the central and peripheral nervous system of the mouse embryo in vivo. *J. Neurosci. 4:*

2082-2094.

Colamarino SA, and Tessier-Lavigne M (1995). The axonal chemoattractant netrin-1 is also a chemorepellent for trochlear motor axons. *Cell 81:* 621-629.

Crandall JE, and Caviness VS Jr. (1984). Axon strata of the cerebral wall in embryonic mice. *Dev. Brain Res. 14:* 185-195.

Crespo D, O'Leary DDM, and Cowan WM (1985). Changes in the numbers of optic nerve fibers during late prenatal and postnatal development in the albino rat. *Dev. Brain Res. 19:* 129-134.

Dahl D (1981). The vimentin-GFA protein transition in rat neuroglia cytoskeleton occurs at the time of myelination. *J. Neurosci. Res. 6:* 741-748.

Dahl D, Rueger DC, Bignami A, Weber K, and Osborn M (1981). Vimentin, the 57,000 dalton protein of fibroblast filaments, is the major cytoskeletal component in immature glia. *Eur. J. Cell Biol. 24:* 191-196.

Davies AM (1987). Molecular and cellular aspects of patterning sensory neurone connections in the vertebrate nervous system. *Development 101:* 185-208.

Dehay C, Kennedy H, and Bullier J (1988). Characterization of transient cortical projections from auditory, somatosensory, and motor cortices to visual areas 17, 18 and 19 in the kitten. *J. Comp. Neurol. 272:* 68-89.

DeLacoste-Utamsing C, and Holloway RL (1982). Sexual dimorphism in the human corpus callosum. *Science 216:* 1431-1432.

Demeter S, Rosene DL, and van Hoesen GW (1985). Interhemispheric pathways of the hippocampal formation, presubiculum, and entorhinal and posterior parahippocampal cortices in the Rhesus monkey: the structure and organization of the hippocampal commissures. *J. Comp. Neurol. 233:* 30-47.

Demeter S, Rosene DL, and van Hoesen GW (1990). Fields of origin and pathways of the interhemispheric commissures in the temporal lobe of Macaques. *J. Comp. Neurol. 302:* 29-53.

De Olmos JS, and Ingram WR (1972). The projection field of the stria terminalis in the rat brain. An experimental study. *J. Comp. Neurol. 146:* 303-334.

Dodd J, and Jessell TM (1988). Axon guidance and the patterning of neuronal projections in vertebrates. *Science 242:* 692-699.

Dodd J, Morton SB, Karagogeos D, Yamamoto M, and Jessell TM (1988). Spatial regulation of axonal glycoprotein expression on subsets of embryonic spinal neurons. *Neuron 1:* 105-116.

Ebner FF (1967). Afferent connections to neocortex in the opossum *(Didelphis virginiana). J. Comp. Neurol. 129:* 241-268.

Ebner FF (1969). A comparison of primitive forebrain organization in metatherian and eutherian mammals. *Ann. N.Y. Acad. Sci. 167:* 241-257.

Edwards MA, Schneider GE, and Caviness VS Jr (1986). Development of the crossed retinocollicular projection in the mouse. *J. Comp. Neurol. 248:* 410-421.

Edwards MA, Crandall JE, Wood JN, Tanaka H, and Yamamoto M (1989). Early axonal differentiation in mouse CNS delineated by an antibody recognizing extracted neurofilaments. *Dev. Brain Res. 49:* 185-204.

Edwards MA, Yamamoto M, and Caviness VS Jr (1990). Organization of radial glia and related cells in the developing murine CNS. An analysis based upon a new monoclonal antibody marker. *Neuroscience 36:* 121-144.

Elberger AJ (1982). The corpus callosum is a critical factor for developing maximum visual acuity. *Dev. Brain Res. 5:* 350-353.

Elberger AJ (1984). The existence of a separate, brief critical period for the corpus callosum to affect visual development. *Behav. Brain Res. 11:* 223-231.

Elberger AJ (1988). Developmental interactions between the corpus callosum and the visual system in cats. *Behav. Brain Res. 30:* 119-134.

Elberger AJ (1993). Distribution of transitory corpus callosum axons projecting to developing cat visual cortex revealed by DiI. *J. Comp. Neurol. 333:* 326-342.

Elberger AJ, and Honig MG (1990). Double-labeling of tissue containing the carbocyanine dye DiI for immunocytochemistry. *J. Histochem. Cytochem. 38:* 735-739.

Elberger AJ, and Smith EL 3rd (1985). The critical period for corpus callosum section to affect cortical binocularity. *Exp. Brain Res. 57:* 213-223.

Eng LF (1988). Regulation of glial intermediate filaments in astrogliosis. *In:* The Biochemical Pathology of Astrocytes. Norenberg MD, Hertz L, and Schousboe A (Eds.). New York: Alan R. Liss. pp. 79-90.

Ettlinger G, and Blakemore CB (1969). The behavioural effects of commissure section. *In:* Contributions to Clinical Neuropsychology. Benton AL (Ed.). Chicago: Aldine. pp. 243.

Ettlinger G, Blakemore CB, Milner AD, and Wilson J (1972). Agenesis of the corpus callosum: A behavioural investigation. *Brain 95:* 327-346.

Ettlinger G, Blakemore CB, Milner AD, and Wilson J (1974). Agenesis of the corpus callosum: A further behavioural investigation. *Brain 97:* 225-234.

Faissner A, and Kruse J (1990). J1/Tenascin is a repulsive substrate for central nervous system neurons. *Neuron 5:* 627-637.

Faivre-Bauman A, Puymirat J, Loudes C, Barret A, and Tixier-Vidal A (1984). Laminin promotes attachment and neurite elongation of fetal hypothalamic neurons grown in serum-free medium. *Neurosci. Lett. 44:* 83-89.

Fawcett JW, Rokos J, and Bakst I (1989). Oligodendrocytes repel axons and cause axonal growth cone collapse. *J. Cell Sci. 92:* 93-100.

Ferris GS, and Dorsen MM (1975). Agenesis of the corpus callosum. I: Neuropsychological studies. *Cortex 11:* 95-122.

Fike JR, Gobbel GT, Chou D, Wijnhoven BP, Bellinzona M, Nakagawa M, and Seilhan TM (1995). Cellular proliferation and infiltration following interstitial irradiation of normal dog brain is altered by an inhibitor of polyamine synthesis. *Int. J. Rad. Oncol. Biol. Phys. 32:* 1035-1045.

Fischer M, Ryan SB, and Dobyns WB (1992). Mechanisms of interhemispheric transfer and patterns of cognitive function in acallosal patients of normal intelligence. *Arch. Neurol. 49:* 271-277.

Fishell G, Mason CA, and Hatten ME (1993). Dispersion of neural progenitors within the germinal zones of the forebrain. *Nature 362:* 636-638.

Fitch RH, Berrebi AS, and Denenberg VH (1987). Corpus callosum: masculinized via perinatal testosterone. *Soc. Neurosci. Abstr. 13:* 689.

Fitzgerald M, Kwiat GC, Middleton J, and Pini A (1993). Ventral spinal cord inhibition of neurite outgrowth from embryonic rat dorsal root ganglia. *Development 117:* 1377-1384.

Furley AJ, Morton SB, Manalo D, Karagogeos D, Dodd J, and Jessell TM (1990).

The axonal glycoprotein TAG-1 is an immunoglobulin superfamily member with neurite outgrowth-promoting activity. *Cell 61:* 157-170.

Gadisseux JF, Evrard P, Misson JP, and Caviness VS (1989). Dynamic structure of the radial glial fiber system of the developing murine cerebral wall. An immunocytochemical analysis. *Dev. Brain Res. 50:* 55-67.

Gadisseux JF, Kadhim HJ, van den Bosch de Aguilar P, Caviness VS, and Evrard P (1990). Neuron migration within the radial glial fiber system of the developing murine cerebrum: an electron microscopic autoradiographic analysis. *Dev. Brain Res. 52:* 39-56.

Gambetti P, Autilio-Gambetti L, and Papasozomenos SC (1981). Bodian's silver method stains neurofilament polypeptides. *Science 213:* 1521-1522.

Gennarini G, Durbec P, Boned A, Rougon G, and Goridis C (1991). Transfected F3/F11 neuronal cell surface protein mediates intercellular adhesion and promotes neurite outgrowth. *Neuron 6:* 595-606.

Geschwind N (1974). Late changes in the nervous system: an overview. *In:* Plasticity and Recovery of Function in the Central Nervous System. Stein DG, Rosen JJ, and Butters N (Eds.). New York: Academic Press. pp: 467-508.

Ghosh A, and Shatz CJ (1992). Pathfinding and target selection by developing geniculocortical axons. *J. Neurosci. 12:* 39-55.

Glas P (1975). *Onderzoek naar de vroege ontwikkeling van de commissuren in het mediane gebied van het telencephalon bij de witte muis.* Groningen: Drukkerij Van Denderen B.V.

Gloor P, Salanova V, Olivier A, and Quesney LF (1993). The human dorsal hippocampal commissure. An anatomically identifiable and functional pathway. *Brain 116:* 1249-1273.

Godement P, Vanselo J, Thanos S, and Bonhoeffer F (1987). A study in developing visual systems with a new method of staining neurones and their processes in fixed tissue. *Development 101:* 697-713.

Godement P, Wang L-C, and Mason CA (1994). Retinal axon divergence in the optic chiasm: Dynamics of growth cone behavior at the midline. *J. Neurosci. 14:* 7024-7039.

Goodrum GR, and Jacobson AG (1981). Cephalic flexure formation in the chick embryo. *J. Exp. Zool. 216:* 399-408.

Gottlieb DI, and Cowan WM (1973). Autoradiographic studies of the commissural and ipsilateral association connections of the hippocampus and dentate gyrus of the rat. I. The commissural connections. *J. Comp. Neurol. 149:* 393-422.

Granger EM, Masterton RB, and Glendenning KK (1985). Origin of interhemispheric fibers in acallosal opossum (with a comparison to callosal origins in rat). *J. Comp. Neurol. 241:* 82-98.

Gratzner HG (1982). Monoclonal antibody to 5-bromo- and 5-iododeoxyuridine: a new reagent for detection of DNA replication. *Science 218:* 474-475.

Gravel C, and Hawkes R (1990). Maturation of the corpus callosum of the rat: I. Influence of thyroid hormones on the topography of callosal projections. *J. Comp. Neurol. 291:* 128-146.

Gravel C, Sasseville R, and Hawkes R (1990). Maturation of the corpus callosum of the rat: II. Influence of thyroid hormones on the number and maturation of axons. *J. Comp. Neurol. 291:* 147-161.

Green EL (1981). Breeding systems. *In:* The Mouse in Biomedical Research, vol. 1. Foster HL, Small JD, and Fox JG (Eds.). New York: Academic Press. pp: 91-104.

Grierson JP, Petroski RE, Ling DSF, and Geller HM (1990). Astrocyte topography and tenascin/cytotactin expression: correlation with the ability to support neuritic outgrowth. *Dev. Brain Res. 55:* 11-19.

Gruber D, Waanders R, Collins RL, Wolfer DP, and Lipp H-P (1991). Weak or missing paw lateralization in a mouse strain (I/LnJ) with congenital absence of the corpus callosum. *Behav. Brain Res. 46:* 9-16.

Guadaño-Ferraz A, Escobar del Ray F, Escobar GM, Innocenti GM, and Berbel P (1994). The development of the anterior commissure in normal and hypothyroid rats. *Dev. Brain Res. 81:* 293-308.

Gundersen RW, and Barrett JN (1979). Neuronal chemotaxis: chick dorsal-root axons turn toward high concentrations of nerve growth factor. *Science 206:* 1079-1080.

Gupta JK, and Lilford RJ (1995). Assessment and management of fetal agenesis of the corpus callosum. *Prenatal Diag. 15:* 301-312.

Hall DE, Neugebauer KM, and Reichardt LF (1987). Embryonic neural retinal cell response to extracellular matrix proteins: developmental changes and effects of the cell substratum attachment antibody (CSAT). *J. Cell Biol. 104:* 623-634.

Hall DH, and Russell RL (1991). The posterior nervous system of the Caenorhabditis elegans: serial reconstruction of identified neurons and complete pattern of synaptic interactions. *J. Neurosci. 11:* 1-22.

Halloran MC, and Kalil K (1994). Dynamic behaviors of growth cones extending in the corpus callosum of living cortical brain slices observed with video microscopy. *J. Neurosci. 14:* 2161-2177.

Hammarback JA, Palm SL, Furcht LT, and Letourneau PC (1985). Guidance of neurite outgrowth by pathways of substratum-adsorbed laminin. *J. Neurosci. Res. 13:* 213-220.

Hankin MH, and Silver J (1986). Mechanisms of axonal guidance. The problem of intersecting fiber systems. *In:* Developmental Biology, vol. 2. Browder LW (Ed.), New York: Plenum Press, pp. 565-604.

Hankin MH, and Silver J (1988). Development of intersecting CNS fiber tracts: the corpus callosum and its perforating fiber pathway. *J. Comp. Neurol. 272:* 177-190.

Hankin MH, Schneider BF, and Silver J (1988). Death of the subcallosal sling is correlated with formation of the cavum septi pellucidi. *J. Comp. Neurol. 272:* 191-202.

Harrelson AL, and Goodman CS (1988). Growth cone guidance in insects: Fasciclin II is a member of the immunoglobulin superfamily. *Science 242:* 700-708.

Hatten ME (1990). Riding the glial monorail: a common mechanism for glial-guided neuronal migration in different regions of the developing mammalian brain. *Trends Neurosci. 13:* 179-184.

Hatten ME, Fishell G, Stitt TN, and Mason CA (1990). Astroglia as a scaffold for development of the CNS. *Sem. Neurosci. 2:* 455-465.

Hayat MA (1981). *Fixation for Electron Microscopy.* New York: Academic Press. pp. 39-182.

Healy MJR, McLaren A, and Michie D (1960). Foetal growth in the mouse. *Proc. Roy. Soc. Lon. B 153:* 367-379.

Heath CJ, and Jones EG (1971). Interhemispheric pathways in the absence of a corpus callosum. An experimental study of commissural connexions in the marsupial phalanger. *J. Anat. 109:* 253-270.

Hedin-Pereira C, Uziel D, and Lent R (1992). Bicommissural neurones in the

cerebral cortex of developing hamsters. *Neuroreport 3:* 873-876.

Heffner CD, Lumsden AGS, and O'Leary DDM (1990). Target control of collateral extension and directional axon growth in the mammalian brain. *Science 247:* 217-220.

Honig MG, and Hume RI (1989). DiI and DiO: versatile fluorescent dyes for neuronal labelling and pathway tracing. *Trends Neurosci. 12:* 337-341.

Horton HL, and Levitt P (1988). A unique membrane protein is expressed on early developing limbic system axons and cortical targets. *J. Neurosci. 8:* 4653-4661.

Hoyle GW, Mercer EH, Palmiter RD, and Brinster RL (1993). Expression of NGF in sympathetic neurons leads to excessive axon outgrowth from ganglia but decreased terminal innervation within tissues. *Neuron 10:* 1019-1034.

Humason GL (1972). *Animal Tissue Techniques (Third Edition).* San Fransisco: W.H. Freeman and Co.

Hynes RO, and Lander AI (1992). Contact and adhesive specificities in the associations, migrations, and targeting of cells and axons. *Cell 68:* 303-322.

Innocenti GM, and Clarke S (1984). The organization of immature callosal connections. *J. Comp. Neurol. 230:* 287-309.

Ivy GO, and Killackey HP (1981). The ontogeny of the distribution of callosal projection neurons in the rat parietal cortex. *J. Comp. Neurol. 195:* 367-389.

Jacobs JR, and Goodman CS (1989). Embryonic development of axon pathways in the Drosophila CNS. I. A glial scaffold appears before the first growth cones. *J. Neurosci. 9:* 2402-2411.

Jeeves MA (1969). A comparison of interhemispheric transmission times between acallosals and normals. *Psychon. Sci. 16:* 245-246.

Jeeves MA (1991). Stereo perception in callosal agenesis and partial callosotomy. *Neuropsychology 29:* 19-34.

Jeeves MA (1992). Compensatory mechanisms - neural and behavioural: Evidence from prenatal damage to the forebrain commissures. *In:* Recovery from Brain Damage. Rose FD, and Johnson DA (Eds). New York: Plenum Press. pp. 153-168.

Jeeves MA, Silver P, and Jacobsen I (1988). Bimanual co-ordination in callosal agenesis and partial commissurotomy. *Neuropsychology 26:* 833-850.

Jessell TM, Bovolenta P, Placzek M, Tessier-Lavigne M, and Dodd J. (1989). Polarity and patterning in the neural tube: the origin and function of the floor plate. *Ciba Found. Symp. 144:* 255-276.

Jinkins JR (1991). The MR equivalents of cerebral hemispheric disconnection: A telencephalic commissuropathy. *Comp. Med. Imag. Graph. 15:* 323-331.

Johnson EM Jr, and Taniuchi M (1987). Nerve growth factor (NGF) receptors in the central nervous system. *Biochem. Pharmacol. 36:* 4189-4195.

Johnson GD, and Nogueira Araujo GM de C (1981). A simple method of reducing the fading of immunofluorescence during microscopy. *J. Immunol. Meth. 43:* 349-350.

Jouandet ML, and Hartenstein V (1983). Basal telencephalic origins of the anterior commissure of the rat. *Exp. Brain Res. 50:* 183-192.

Juraska JM, and Meyer M (1985). Environmental, but not sex, differences exist in the gross size of the rat corpus callosum. *Soc. Neurosci. Abstr. 11:* 258.

Juraska JM, and Kopcik JR (1988). Sex and environmental influences on the size and ultrastructure of the rat corpus callosum. *Brain Res. 450:* 1-8.

Juriloff DM (1995). Genetic analysis of the construction of the AEJ.A congenic strain indicates that nonsyndromic CL(P) in the mouse is caused by two loci with epistatic interaction. *J. Craniofac. Genet. Dev. Biol. 15:* 1-12.

Juriloff DM, and Harris MJ (1985). Thyroxine-induced differential mortality of cleft lip mouse embryos: dose- and time-response studies of the A/WySn strain. *Teratology 31:* 319-329.

Kalter H (1975). Prenatal epidemiology of spontaneous cleft lip and palate, open eyelid, and embryonic death in A/J mice. *Teratology 12:* 245-258.

Katz MJ, Lasek RJ, and Silver J (1983). Ontophyletics of the nervous system: Development of the corpus callosum and evolution of axon tracts. *Proc. Nat. Acad. Sci. USA 80:* 5936-5940.

Kaufman MH (1992). *The Atlas of Mouse Development.* Academic Press, Inc., San Diego, Ca. pp. 5-8.

Keeler CE (1933). Absence of the corpus callosum as a Mendelizing character in the house mouse. *Proc. Nat. Acad. Sci. USA 19*: 609-611.

Kennedy TE, Serafini T, de la Torre JR, and Tessier-Lavigne M (1994). Netrins are diffusible chemotropic factors for commissural axons in the embryonic spinal cord. *Cell 78:* 425-435.

Kertesz A, Polk M, Howell J, and Black SE (1987). Cerebral dominance, sex, and callosal size in MRI. *Neurology 37:* 1385-1388.

Khadim HJ, Bhide PG, and Frost DO (1993). Transient axonal branching in the developing corpus callosum. *Cereb. Cort. 3:* 551-566.

Kim JHY, Ellman A, and Juraska JM (1996). A re-examination of sex differences in axon density and number in the splenium or the rat corpus callosum. *Submitted.*

King LS (1936). Hereditary aspects of the corpus callosum in the mouse, *Mus musculus*. *J. Comp. Neurol. 64:* 337-363.

King LS, and Keeler CE (1932). Absence of the corpus callosum, a hereditary brain anomaly of the house mouse. Preliminary report. *Proc. Nat. Acad. Sci. USA 18:* 525-528.

King C, and Hall WG (1990). Developmental change in unilateral olfactory habituation is mediated by anterior commissure maturation. *Behav. Neurosci. 104:* 796-807.

Klar A, Baldassare M, and Jessell TM (1992). F-spondin: A gene expressed at high levels in the floor plate encodes a secreted protein that promotes neural cell adhesion and neurite extension. *Cell 69:* 95-110.

Koester SE, and O'Leary DDM (1992). Functional classes of cortical projection neurons develop dendritic distinctions by class-specific sculpting of an early common pattern. *J. Neurosci. 12:* 1382-1393.

Koester SE, and O'Leary DDM (1994). Axons of early generated neurons in cingulate cortex pioneer the corpus callosum. *J. Neurosci. 14:* 6608-6620.

Koppel H, and Innocenti GM (1983). Is there a genuine exuberancy of callosal projections in development? A quantitative electron microscopic study in the cat. *Neurosci. Lett. 41:* 33-40.

Kucharski D, Burka N, and Hall WG (1990). The anterior limb of the anterior commissure is an access route to contralaterally stored olfactory preference memories. *Psychobiology 18:* 195-204.

Kurnit DM, Layton WM, and Matthysse S (1987). Genetics, chance, and morphogenesis. *Am. J. Hum. Gen. 41:* 979-995.

Kuwada JY, Bernhardt RR, and Chitnis AB (1990). Pathfinding by identified growth cones in the spinal cord of zebrafish embryos. *J. Neurosci. 10:* 1299-1308.

LaMantia A-S, and Rakic P (1990a). Cytological and quantitative characteristics of four cerebral commissures in the Rhesus monkey. *J. Comp. Neurol. 291:* 520-537.

LaMantia A-S, and Rakic P (1990b). Axon overproduction and elimination in the corpus callosum of the developing Rhesus monkey. *J. Neurosci. 10:* 2156-2175.

LaMantia A-S, and Rakic P (1994). Axon overproduction and elimination in the anterior commissure of the developing Rhesus monkey. *J. Comp. Neurol. 340:* 328-336.

Lassonde M, Ptito M, and Lepore F (1990). La plasticite du systeme calleux. *Rev. Can. Psych. 44:* 166-179.

Lassonde M, Sauerwein H, Geoffroy G, and Decarie M (1986). Effects of early and late transection of the corpus callosum in children. *Brain 109:* 953-967.

Lassonde M, Sauerwein H, Chicone A-J, and Geoffroy G (1991). Absence of disconnexion syndrome in callosal agenesis and early callosotomy: Brain reorganization or lack of structural specificity during ontogeny? *Neuropsychology 29:* 481-495.

Laurberg S (1979). Commissural and intrinsic connections of the rat hippocampus. *J. Comp. Neurol. 184:* 685-708.

Lazarides E (1980). Intermediate filaments as mechanical integrators of cellular space. *Nature 283:* 249-256.

Lefkowitz M, Durand D, Smith G, and Silver J (1991). Electrical properties of axons within Probst bundles of acallosal mice and callosi that have reformed upon glial-coated polymer implants. *Exp. Neurol. 113:* 306-314.

Lent R (1983). Cortico-cortical connections reorganize in hamsters after neonatal transection of the corpus callosum. *Dev. Brain Res. 11:* 137-142.

Lent R (1984). Neuroanatomical effects of neonatal transection of the corpus callosum in hamsters. *J. Comp. Neurol. 223:* 548-555.

Lent R (1992). Different developmental strategies of the telencephalic commissures: A comparison between the ontogeneses of visual callosal connections and of olfactory commissural connections in rodents. *In:* The Visual System, from Genesis to Maturity. Lent R (Ed.). Boston: Birkhauser, pp. 131-146.

Lent R, and Guimarães RZP (1991). Development of paleocortical projections through the anterior commissure of hamsters adopts progressive, not regressive, strategies. *J. Neurobiol. 22:* 475-498.

Lent R, and Schmidt SL (1986). Dose-dependent occurrence of the aberrant longitudinal bundle in the brains of mice born acallosal after prenatal gamma irradiation. *Dev. Brain Res. 25:* 127-132.

Lent R, Hedin-Pereira C, Menezes JRL, and Jhaveri S (1990). Neurogenesis and development of callosal and intracortical connections in the hamster. *Neuroscience 38:* 21-37.

Levison SW, and Goldman JE (1993). Both oligodendrocytes and astrocytes develop from progenitors in the subventricular zone of postnatal rat forebrain. *Neuron 10:* 201-212.

Levitt P (1984). A monoclonal antibody to limbic system neurons. *Science 223:* 299-301.

Liesi P (1990). Extracellular matrix and neuronal movement. *Experientia 46:* 900-907.

Liesi P, Dahl D, and Vaheri A (1983). Laminin is produced by early rat astrocytes in primary culture. *J. Cell Biol. 96:* 920-924.

Liesi P, Dahl D, and Vaheri A (1984). Neurons cultured from developing rat brain attach and spread preferentially on laminin. *J. Neurosci. Res. 11:* 241-251.

Liesi P, and Silver J (1988). Is glial laminin involved in axon guidance in the mammalian CNS? *Dev. Biol. 130:* 774-785.

Lipp HP, and Waanders R (1990). The acallosal mouse strain I/Ln: behavioral comparisons and effects of cross-breeding. *Behav. Gen. 20:* 728-729.

Lipp H-P, and Wahlsten D (1992). Absence of the corpus callosum. *In:* Genetically Defined Animal Models of Neurobehavioral Dysfunctions. Driscoll P (Ed.). Boston: Birkhauser. pp. 217-252.

Lipp H-P, Waanders R, Berther R, Glanzmann P, and Bolla C (1989). Two-way avoidance learning and swimming navigation in acallosal mice. *Eur. J. Neurosci. 2(suppl.):* 29

Lipp H-P, Schwegler H, Crusio WE, Wolfer DP, Leisinger-Trigona M-C, Heimrich B, and Driscoll P (1989). Using genetically-defined rodent strains for the identification of

hippocampal traits relevant for two-way avoidance behavior: a non-invasive approach. *Experientia 45:* 845-859.

Livy DJ, and Wahlsten D (1991). Tests of genetic allelism between four inbred mouse strains with absent corpus callosum. *J. Hered. 82:* 459-464.

Loeser JD, and Alvord EC Jr (1968). Clinicopathological correlations in agenesis of the corpus callosum. *Neurology 18:* 745-756.

Lois C, and Alvarez-Buylla A (1993). Proliferating subventricular zone cells in the adult mammalian forebrain can differentiate into neurons and glia. *Proc. Nat. Acad. Sci. USA 90:* 2074-2077.

Lomber SG, Payne BR, and Rosenquist AC (1992). The spatial relationship between the cerebral cortex and fiber trajectory through the corpus callosum. *Proceedings of the "Workshop on the Corpus Callosum and Interhemispheric Transfer".* Priorij Corsendonk, Belgium.

Looney GA, and Elberger AJ (1986). Myelination of the corpus callosum in the cat: Time course, topography, and functional implications. *J. Comp. Neurol. 248:* 336-347.

Malhotra SK, Svensson M, Aldskogius H, Bhatnagar R, Das GD, and Shnitka TK (1992). Diversity among reactive astrocytes: Proximal reactive astrocytes in lacerated spinal cord preferentially react with monoclonal antibody J1-31. *Brain Res. Bull. 30:* 395-404.

Marcus RC, Mason CA (1995). The first retinal axon growth in the mouse optic chiasm: Axon patterning and the cellular environment. *J. Neurosci. 15:* 6389-6402.

Marcus RC, Blazeski R, Godement P, Mason CA (1995). Retinal axon divergence in the optic chiasm: Uncrossed axons diverge from crossed axons within a midline glial specialization. *J. Neurosci. 15:* 3716-3729.

Martínez-Frías M-L (1995). Primary midline developmental field. I. Clinical and epidemiological characteristics. *Am. J. Med. Gen. 56:* 374-381.

Matsunaga M, Hatta K, Nagafuchi A, and Takeichi M (1988). Guidance of optic nerve by N-cadherin adhesion molecules. *Nature 334:* 62-64.

McConnell SK (1992). The genesis of neuronal diversity during development of cerebral cortex. *Sem. Neurosci. 4:* 347-356.

McConnell SK, and Kaznowski CE (1991). Cell cycle dependence of laminar determination in developing neocortex. *Science 254:* 282-285.

McConnell SK, Ghosh A, and Shatz CJ (1994). Subplate pioneers and the formation of descending connections from cerebral cortex. *J. Neurosci. 14:* 1892-1907.

McDermott KWG, and Lantos PL (1990). Cell proliferation in the subependymal layer of the postnatal marmoset, *Callithrix jacchus*. *Dev. Brain Res. 57:* 269-277.

McKanna JA (1993a). Primitive glial compartments in the floor plate of mammalian embryos: distinct progenitors of adult astrocytes and microglia support the notoplate hypothesis. *Perspect. Dev. Neurobiol. 1:* 245-255.

McKanna JA (1993b). Optic chiasm and infundibular decussation sites in the developing rat diencephalon are defined by glial raphes expressing p35 (lipocortin I, annexin I). *Dev. Dyn. 195:* 75-86.

McKanna JA, and Cohen S (1989). The EGF receptor kinase substrate p35 in the floor plate of the embryonic rat CNS. *Science 243:* 1477-1479.

McKeever WF, Sullivan KF, Ferguson SM, and Rayport M (1981). Typical cerebral hemisphere disconnection deficits following corpus callosum section despite sparing of the anterior commissure. *Neuropsychology 19:* 745-755.

McLaren A (1963). The distribution of eggs and embryos between sides in the mouse. *J. Endocrinol. 27:* 157-181.

McLaren A (1965). Genetic and environmental effects on foetal and placental growth in mice. *J. Reprod. Fertil. 9:* 79-98.

McLaren A, and Michie D (1960). Control of pre-natal growth in mammals. *Nature 187:* 363-365.

Mendez-Otero R, Schlosshauer B, Barnstable CJ, and Constantine-Paton M (1988). A developmentally regulated antigen associated with neural cell and process migration. *J. Neurosci. 8:* 564-579.

Miller MW, and Nowakowski RS (1988). Use of bromodeoxyuridine-immunohistochemistry to examine the proliferation, migration and time of origin of cells in the central nervous system. *Brain Res. 457:* 44-52.

Milner AD (1983). Neuropsychological studies of callosal agenesis. *Psychol. Med. 13:* 721-725.

Milner AD (1994). Visual integration in callosal agenesis. *In:* Callosal Agenesis - A Natural Split Brain? Lassonde M, and Jeeves MA (Eds.). New York: Plenum Press. pp.

171-184.

Milner AD, and Jeeves MA (1979). A review of behavioural studies of agenesis of the corpus callosum. *In:* Structure and Function of the Cerebral Commissures. Steele Russel I, Van Hof M, and Berlucchi G (Eds.). New York: MacMillan. pp: 428-448.

Milner AD, Jeeves MA, Silver PH, Lines CR, and Wilson J (1985). Reaction times to lateralized visual stimuli in callosal agenesis: Stimulus and response factors. *Neuropsychology 23:* 323-331.

Misson J-P, Austin CP, Takahashi T, Cepko CL, and Caviness VS Jr (1991). The alignment of migrating neural cells in relation to the murine neopallial radial glial fiber system. *Cereb. Cort. 1:* 221-229.

Misson J-P, Edwards MA, Yamamoto M, and Caviness VS Jr (1988). Identification of radial glial cells within the developing murine central nervous system: studies based upon a new immunohistochemical marker. *Dev. Brain Res. 44:* 95-108.

Mitchell DE, and Blakemore CB (1970). Binocular depth perception and the corpus callosum. *Vision Res. 10:* 49-54.

Monk M (1995). Epigenetic programming of differential gene expression in development and evolution. *Dev. Gen. 17:* 188-197.

Moss DJ, and White CA (1992). Solubility and posttranslational regulation of GP130/F11 - a neuronal GPI-linked cell adhesion molecule enriched in the neuronal membrane skeleton. *Eur. J. Cell Biol. 57:* 59-65.

Muente TF, and Heinze HJ (1991). Corpus-Callosum-Agenesie. Interhemiphaerische integration semantischer information [Corpus callosum agenesis. Interhemsipheric integration of semantic information (English translation provided by PM Schalomon)]. *Nervenarzt 62:* 629-636.

Müller U, Cristina N, Li Z-W, Wolfer DP, Lipp H-P, Rülicke T, Brandner S, Aguzzi A, and Weissmann C (1994). Behavioral and anatomical deficits in mice homozygous for a modified β-amyloid precursor protein gene. *Cell 79:* 755-765.

Neugebauer K, Tomaselli K, Lilien J, and Reichardt L (1988). N-cadherin, N-CAM and integrins promote retinal neurite outgrowth on astrocytes in vitro. *J. Cell. Biol. 107:* 1177-1187.

Nordlander R (1987). Axonal growth cones in the developing amphibian spinal cord. *J. Comp. Neurol. 263:* 485-498.

Norris CR, and Kalil K (1990). Morphology and cellular interactions of growth cones in the developing corpus callosum. *J. Comp. Neurol. 293:* 268-281.

Norris CR, and Kalil K (1991). Guidance of callosal axons by radial glia in the developing cerebral cortex. *J. Neurosci. 11:* 3481-3492.

Olavarria J, and van Sluyters RC (1985). Organization and postnatal development of callosal connections in the visual cortex of the rat. *J. Comp. Neurol. 239:* 1-26.

Olavarria J, Serra-Oller MM, Yee KT, and van Sluyters RC (1988). Topography of interhemispheric connections in neocortex of mice with congenital deficiencies of the callosal commissures. *J. Comp. Neurol. 270:* 575-590.

Olavarria J, Serra-Oller MM, Yee KT, and van Sluyters RC (1994). Pattern of interhemispheric connections in mice with congenital deficiencies of the corpus callosum. *In:* Callosal Agenesis - A Natural Split Brain? Lassonde M, and Jeeves MA (Eds.). New York: Plenum Press. pp. 135-146.

O'Leary DDM (1992). Development of connectional diversity and specificity in the mammalian brain by the pruning of collateral projections. *Curr. Opin. Neurobiol. 2:* 70-77.

Optiz JM (1993). Blastogenesis and the "primary field" in human development. *In:* Blastogenesis, Normal and Abnormal. Optiz JM (Ed.). New York: Wiley-Liss. pp. 3-37.

Optiz JM, and Gilbert EF (1982). Editorial comment: CNS anomalies and the midline as a "Developmental Field". *Am. J. Med. Gen. 12:* 443-455.

O'Shea KS, and Dixit VM (1988). Unique distribution of the extracellular matrix component thrombospondin in the developing mouse embryo. *J. Cell Biol. 107:* 2737-2748.

O'Shea KS, Rheinheimer JST, and Dixit VM (1990). Deposition and role of thrombospondin in the histogenesis of the cerebellar cortex. *J. Cell Biol. 110:* 1275-1283.

Ozaki HS, Murakami TH, Toyoshima T, and Shimada M (1984). Agenesis of the corpus callosum in ddN strain mouse associated with unusual facial appearance (flat-face). *Neurosci. Res. 1:* 81-87.

Ozaki HS, Murakami TH, Toyoshima T, and Shimada M (1987). The fibers which leave the Probst's longitudinal bundle seen in the brain of an acallosal mouse: A study with the horseradish peroxidase technique. *Brain Res. 400:* 239-246.

Ozaki HS, and Shimada M (1988). The fibers which course within the Probst's longitudinal bundle seen in the brain of a congenitally acallosal mouse: a study with the

horseradish peroxidase technique. *Brain Res. 441:* 5-14.

Ozaki HS, and Wahlsten D (1992). Prenatal formation of the normal mouse corpus callosum: A quantitative study with carbocyanine dyes. *J. Comp. Neurol. 323:* 81-90.

Ozaki HS, and Wahlsten D (1993). Cortical axon trajectories and growth cone morphologies in fetuses of acallosal mouse strains. *J. Comp. Neurol. 336:* 595-604.

Pandya DN, Hallett M, and Mukherjee SK (1969). Intra- and inter-hemispheric connections of the neo-cortical auditory system in the rhesus monkey. *Brain Res. 14:* 49-65.

Paterson JA (1983). Dividing and newly produced cells in the corpus callosum of adult mouse cerebrum as detected by light microscopic radioautography. *Anat. Anz. 153:* 149-168.

Paterson JA, Privat A, Ling EA, and Leblond CP (1973). Investigation of glial cells in semithin sections. III. Transformation of subependymal cells into glial cells, as shown by radio-autography after ^{3}H-thymidine injection in the lateral ventricle of the brain of young rats. *J. Comp. Neurol. 149:* 83-102.

Persson G (1970). Untersuchungen bei drei Fällen mit angeborenem Balkenmangel. *Psychiat. Neurol. Med. Psychol. 22:* 448-455.

Pikalow AS, Flynn ME, and Searls RL (1994). Development of cranial flexure and Rathke's pouch in the chick embryo. *Anat. Rec. 238:* 407-414.

Placzek M, Tessier-Lavigne M, Jessell T, and Dodd J (1990). Orientation of commissural axons *in vitro* in response to a floor plate-derived chemoattractant. *Development 110:* 19-30.

Pini A (1993). Chemorepulsion of axons in the developing mammalian central nervous system. *Science 261:* 95-98.

Pires-Neto MA, Lent R, and Hartmann ALC (1994). Topographic organization in the anterior commissure of developing hamsters. *Braz. J. Med. Biol. Res. 27:* 1369-1376.

Predy R, Singh D, Bhatnagar R, Singh R, and Malhotra SK (1987). A new protein (J1-31 antigen, 30kD) is expressed by astrocytes, Muller glia and ependyma. *Biosci. Rep. 7:* 491-502.

Preilowski B (1977). Phases of motor-skills acquisition: A neuropsychological approach. *J. Hum. Mvmt. Stud. 3:* 169-181.

Privat A, and Leblond CP (1972). The subependymal layer and neighboring region in the brain of the young rat. *J. Comp. Neurol. 146:* 277-302.

Probst M (1901). Über den bau des vollständigen balkenlosen grosshirns, sowie über mikrogyrie und heterotopie der grauen substanz. *Arch. Psychiatr. Nervenkr. 34:* 709-786.

Provinciali L, DelPesce M, Censori B, Quattrini A, Paggi A, Ortenzi A, Mancini S, Papo I, and Rychlicki F (1990). Evolution of neuropsychological changes after partial callosotomy in intractable epilepsy. *Epilepsy Res. 6:* 155-165.

Qui M-S, Anderson S, Meneses J, Pedersen R, and Rubenstein JLR (1995). *Emx-1* mutant mice exhibit abnormal cortical development. *Soc. Neurosci. Abstr. 21:* 793.

Raju T, Bignami A, and Dahl D (1981). *In vivo* and *in vitro* differentiation of neurons and astrocytes in the rat embryo. *Dev. Biol. 85:* 344-357.

Rakic P (1971). Guidance of neurons migrating to the fetal monkey neocortex. *Brain Res. 33:* 471-476.

Rakic P (1972). Mode of cell migration to the superficial layers of fetal monkey neocortex. *J. Comp. Neurol. 145:* 61-84.

Rakic P (1988). Specification of cerebral cortical areas. *Science 241:* 170-176.

Rakic P, and Yakovlev PI (1968). Development of the corpus callosum and cavum septi in man. *J. Comp. Neurol. 132:* 45-72.

Raper JA, and Kapfhammer JP (1990). The enrichment of a neuronal growth cone collapsing activity from embryonic chick brain. *Neuron 4:* 21-29.

Raper JA, Bastiani M, and Goodman CS (1983). Pathfinding by neuronal growth cones in grasshopper embryos. II. Selective fasciculation on specific axonal pathways. *J. Neurosci. 3:* 31-41.

Rauch RA, and Jinkins JR (1994). Magnetic resonance imaging of corpus callosum dysgenesis. *In:* Callosal Agenesis - A Natural Split Brain? Lassonde M, and Jeeves MA (Eds.). New York: Plenum Press. pp. 83-95.

Rauvala H, and Pihlaskari R (1987). Isolation and some characteristics of an adhesive factor of brain that enhances neurite outgrowth in central neurons. *J. Biol. Chem. 262:* 16625-16635.

Reeves AG (1991). Behavioral changes following corpus callosotomy. *Adv. Neurol.*

46: 437-443.

Risse GL, LeDoux J, Springer SP, Wilson DH, and Gazzaniga MS (1978). The anterior commissure in man: Functional variation in a multisensory system. *Neuropsychology 16:* 23-31.

Rogers SL, Letourneau PC, Peterson BA, Furcht LT, and McCarthy JB (1987). Selective interaction of peripheral and central nervous system cells with two distinct cell-binding domains of fibronectin. *J. Cell Biol. 105:* 1435-1442.

Ruegg MA, Stoeckli ET, Lanz RB, Streit P, and Sonderegger, P (1989). A homologue of the axonally secreted protein Axonin-1 is an integral membrane protein of nerve fiber tracts involved in neurite fasciculation. *J. Cell Biol. 109:* 2363-2378.

Rutishauser U, Acheson A, Hall AK, Mann DM, and Sunshine J (1988). The neural cell adhesion molecule (NCAM) as a regulator of cell-cell interactions. *Science 240:* 53-57.

Sandell JH, and Masland RH (1988). Photoconversion of some fluorescent markers to a diaminobenzidine product. *J. Histochem. Cytochem. 36:* 555-559.

Sass KJ, Novelly RA, Spencer DD, and Spencer SS (1988). Mnestic and attention impairments following corpus callosum section for epilepsy. *J. Epilepsy 1:* 61-66.

Sauer FC (1935a). Mitosis in the neural tube. *J. Comp. Neurol. 62:* 377-405.

Sauer FC (1935b). The cellular structure of the neural tube. *J. Comp. Neurol. 63:* 13-23.

Sauer FC (1936). The interkinetic migration of embryonic epithelial nuclei. *J. Morphol. 60:* 1-11.

Sauer FC (1937). Some factors in the morphogenesis of vertebrate embryonic epithelium. *J. Morphol. 61:* 563-579.

Sauerwein HC, Nolin P, and Lassonde M (1994). Cognitive functioning in callosal agenesis. *In:* Callosal Agenesis - A Natural Split Brain? Lassonde M, and Jeeves MA (Eds.). New York: Plenum Press. pp. 221-234.

Schiffer D, Giordana MT, Cavalla P, Vigliani MC, and Attanasio A (1993). Immunohistochemistry of glial reaction after injury in the rat: double stainings and markers of cell proliferation. *Int. J. Dev. Neurosci. 11:* 269-280.

Schmidt SL, and Lent R (1987). Effects of prenatal irradiation on the development

of cerebral cortex and corpus callosum of the mouse. *J. Comp. Neurol. 264:* 193-204.

Schmidt S, Manhaes A, and DeMoraes V (1991). The effects of total and partial callosal agenesis on the development of paw preference performance in the BALB/cCF mouse. *Brain Res. 545:* 123-130.

Schmued LC (1990). A rapid, sensitive histochemical stain for myelin in frozen brain sections. *J. Histochem. Cytochem. 38:* 717-720.

Schnitzer J, Franke WW, and Schachner M (1981). Immunocytochemical demonstration of vimentin in astrocytes and ependymal cells of developing and adult mouse nervous system. *J. Cell Biol. 90:* 435-447.

Segraves MA, and Rosenquist AC (1982a). The distribution of the cells of origin of callosal projections in cat visual cortex. *J. Neurosci. 2:* 1079-1089.

Segraves MA, and Rosenquist AC (1982b). The afferent and efferent callosal connections of retinotopically defined areas in cat cortex. *J. Neurosci. 2:* 1090-1107.

Senft SL (1990). Prenatal central vibrissal pathways labeled with DiI and DiA. *Soc. Neurosci. Abstr. 16:* 1215.

Serafini T, Kennedy TE, Galko MJ, Mirzayan C, Jessell TM, and Tessier-Lavigne M (1994). The netrins define a family of axon outgrowth-promoting proteins homologous to C. elegans UNC-6. *Cell 78:* 409-425.

Sergent J (1986). Subcortical coordination of hemisphere activity in commissurotomized patients. *Brain 109:* 357-369.

Sergent J (1990). Furtive incursions into bicameral minds: Integrative and coordinating role of subcortical structures. *Brain 109:* 537-568.

Seymour RM, and Berry M (1975). Scanning and transmission electron microscopy studies of interkinetic nuclear migration in the cerebral vesicles of the rat. *J. Comp. Neurol. 160:* 105-126.

Shipley MT (1975). The topographical and laminar organization of the presubiculum's projection to the ipsi- and contralateral entorhinal cortex in the guinea pig. *J. Comp. Neurol. 160:* 127-146.

Shirasaki R, Tamada A, Katsumata R, and Murakami F (1995). Guidance of cerebellofugal axons in the rat embryo: Directed growth toward the floor plate and subsequent elongation along the longitudinal axis. *Neuron 14:* 961-972.

Shoukimas GM, and Hinds JW (1978). The development of the cerebral cortex in the embryonic mouse: An electron microscopic serial section analysis. *J. Comp. Neurol. 179:* 795-830.

Sidman RL, Miale IL, and Feder N (1959). Cell proliferation and migration in the primitive ependymal zone: an autoradiographic study of histogenesis in the nervous system. *Exp. Neurol. 1:* 322-333.

Sidman RL, Angevine JB Jr, and Taber Pierce E (1971). *Atlas of the Mouse Brain and Spinal Cord.* London: Oxford University Press.

Silver J (1993). Glia-neuron interactions at the midline of the developing mammalian brain and spinal cord. *Perspect. Dev. Neurobiol. 1:* 227-236.

Silver J, and Ogawa MY (1983). Postnatally induced formation of the corpus callosum in acallosal mice on glia-coated cellulose bridges. *Science 220:* 1067-1069.

Silver J, Edwards MA, and Levitt P (1993). Immunocytochemical demonstration of early appearing astroglial structures that form boundaries and pathways along axon tracts in the fetal brain. *J. Comp. Neurol. 328:* 415-436.

Silver J, Lorenz SE, Wahlsten D, and Coughlin J (1982). Axonal guidance during development of the great cerebral commissures: Descriptive and experimental studies, in vivo, on the role of preformed glial pathways. *J. Comp. Neurol. 210:* 10-29.

Silver J, Smith GM, Miller RH, and Levitt PR (1985). The immature astrocyte: Its role during normal CNS axon tract development and its ability to reduce scar formation and promote axonal regeneration when transplanted in the brains of adults. *Soc. Neurosci. Abstr. 11:* 334.

Simon DK, and O'Leary DDM (1992). Development of topographic order in the mammalian retinocollicular projection. *J. Neurosci. 12:* 1212-1232.

Smart IHM (1973). Proliferative characteristics of the ependymal layer during the early development of the mouse neocortex: a pilot study based on recording the number, location and plane of cleavage of mitotic figures. *J. Anat. 116:* 67-91.

Smart IHM (1976). A pilot study of cell production by the ganglionic eminences of the developing mouse brain. *J. Anat. 121:* 71-84.

Smart IHM (1984). Histogenesis of the mesocortical area of the mouse telencephalon. *J. Anat. 138:* 537-552.

Smart IHM (1985). A localised growth zone in the wall of the developing mouse telencephalon. *J. Anat. 140:* 397-402.

Smiley JF, and Goldman-Rakic PS (1993). Heterogeneous targets of dopamine synapses in monkey pre-frontal cortex demonstrated by serial section electron microscopy: a laminar analysis using the silver-enhanced diaminobenzidine sulfide (SEDS) immunolabeling technique. *Cereb. Cort. 3:* 223-238.

Smith G, Rutishauer U, Silver J, and Miller R (1990). Maturation of astrocytes in vitro alters the extent and molecular basis of neurite outgrowth. *Dev. Biol. 138:* 377-390.

Snow DM, Lemmon V, Carrino D, Kaplin H, and Silver J (1990). Sulfated proteoglycans present in astroglial barriers inhibit neurite outgrowth in vitro. *Exp. Neurol. 109:* 111-130.

Snow DM, Steinler D, and Silver J (1990). Molecular and cellular characterization of the glial roof plate of the spinal cord and optic tectum: a possible role for a proteoglycan in development of an axon barrier. *Dev. Biol. 138:* 359-376.

Snow DM, Watanabe M, Letourneau PC, and Silver J (1991). A chondroitin sulfate proteoglycan may influence the direction of retinal ganglion cell outgrowth. *Development 113:* 1473-1485.

Sorra KE, and Harris KM (1993). Occurrence and three-dimensional structure of multiple synapses between individual radiatum axons and their target pyramidal cells in hippocampal area CA1. *J. Neurosci. 13:* 3736-3748.

Sperry RW (1968). Hemisphere disconnection and unity in conscious awareness. *Am. Psychol. 27:* 723-733.

Sperry RW, Gazzaniga MS, and Bogen JE (1969). Interhemispheric relationships: The neocortical commissures; syndromes of hemisphere disconnection. *In:* Handbook of Clinical Neurology, vol.4: Disorders of Speech Perception and Symbolic Behavior. Vinken PJ, and Bruyn GW (Eds.). New York: Elsevier. pp. 273-290.

Spudich JL, and Koshland DE Jr (1976). Non-genetic individuality: chance in the single cell. *Nature 262:* 467-471.

Sretavan DW, Puré E, Siegel MW, and Reichardt LF (1995). Disruption of retinal axon ingrowth by ablation of embryonic mouse optic chiasm neurons. *Science 269:* 98-101.

Stahl B, Mueller B, von Boxberg Y, Cox EC, and Bonhoeffer F (1990). Biochemical characterization of a putative axonal guidance molecule of the chick visual system. *Neuron*

5: 733-743.

Stefanko SZ, and Schenk VWD (1979). Anatomical aspects of the agenesis of the corpus callosum in man. *In:* Structure and Function of the Cerebral Commissures. Steele Russel I, Van Hof M, and Berlucchi G (Eds.). New York: MacMillan. pp. 479-482.

Steward O (1984). Lesion-induced neuroplasticity and the sparing or recovery of function following early brain damage. *In:* Early Brain Damage, vol. 1. Almli CR, and Finger S (Eds.). Orlando: Academic Press. pp. 59-77.

Stumpo DJ, Bock CB, Tuttle JS, and Blackshear PJ (1995). MARCKS deficiency in mice leads to abnormal brain development and perinatal death. *Proc. Nat. Acad. Sci. USA 92:* 944-948.

Sturrock RR (1976). Development of the mouse anterior commissure. I. A comparison of myelination in the anterior and posterior limbs of the anterior commissure of the mouse brain. *Anat. Histol. Embryol. 5:* 54-67.

Sturrock RR (1979). A quantitative lifespan study of changes in cell number, cell division and cell death in various regions of the mouse forebrain. *Neuropathol. Appl. Neurobiol. 5:* 433-456.

Sturrock RR (1980). Myelination of the mouse corpus callosum. *Neuropathol. Appl. Neurobiol. 6:* 415-420.

Sturrock RR, and Smart IMH (1980). A morphological study of the mouse subependymal layer from embryonic life to old age. *J. Anat. 130:* 391-415.

Sullivan MV, and Hamilton CR (1973). Interocular transfer of reversed and non reversed discriminations via the anterior commissure in monkeys. *Physiol. Behav. 10:* 355-359.

Swanson LW, and Cowan WM (1977). An autoradiographic study of the organization of the efferent connections of the hippocampal formation in the rat. *J. Comp. Neurol. 172:* 49-84.

Swanson LW, and Cowan WM (1979). The connections of the septal region in the rat. *J. Comp. Neurol. 186:* 621-656.

Swanson LW, Wyss JM, and Cowan WM (1978). An autoradiographic study of the organization of intrahippocampal association pathways in the rat. *J. Comp. Neurol. 181:* 681-716.

Swanson LW, Köhler C, and Björklund A (1987). The limbic region. I. The septohippocampal system. *In:* Handbook of Chemical Neuroanatomy. Vol. 5: Integrated Systems of the CNS, Part I. Björklund A, Hökfelt T, and Swanson LW (Eds.). Amsterdam: Elsevier, pp. 125-277.

Tan S-S, and Breen S (1993). Radial mosaicism and tangential cell dispersion both contribute to mouse neocortical development. *Nature 362:* 638-640.

Tessier-Lavigne M (1992). Axon guidance by molecular gradients. *Curr. Opin. Neurobiol. 2:* 60-65.

Tessier-Lavigne M (1994). Axon guidance by diffusible repellants and attractants. *Curr. Opin. Gen. Dev. 4:* 596-601.

Tessier-Lavigne M, Placzek M, Lumsden AGS, Dodd J, and Jessell TM (1988). Chemotropic guidance of developing axons in the mammalian central nervous system. *Nature 336:* 775-778.

Tessier-Lavigne M, and Placzek M (1991). Target attraction: are developing axons guided by chemotropism? *Trends Neurosci. 14:* 303-310.

Timpl R, Rohde H, Gehron Robey P, Rennard SI, Foidart J-M, and Martin GR (1979). Laminin - a glycoprotein from basement membranes. *J. Biol. Chem. 254:* 9933-9937.

Tomasch J (1954). Size, distribution, and number of fibres in the human corpus callosum. *Anat. Rec. 119:* 119-135.

Tomasch J, and MacMillan A (1957). The number of fibers in the corpus callosum of the white mouse. *J. Comp. Neurol. 107:* 165-168.

Tuckett F, and Morriss-Kay GM (1985). The kinetic behavior of the cranial neural epithelium during neurulation in the rat. *J. Embryol. Exp. Morphol. 85:* 111-119.

Turner DL, and Cepko CL (1987). A common progenitor for neurons and glia persists in the rat retina in development. *Nature 328:* 131-136.

Valentino KL, and Jones EG (1982). The early formation of the corpus callosum: a light and electron microscopic study in foetal and neonatal rats. *J. Neurocytol. 11:* 583-609.

Valentino KL, Jones EG, and Kane SA (1983). Expression of GFAP immunoreactivity during development of long fiber tracts in the rat CNS. *Dev. Brain Res.*

9: 317-336.

van Groen T, and Wyss JM (1988). Species differences in hippocampal commissural connections: Studies in rat, guinea pig, rabbit, and cat. *J. Comp. Neurol. 267:* 322-334.

van Overbeeke JJ, Hillen B, and Vermeij-Keers C (1994). The arterial pattern at the base of arhinencephalic and holoprosencephalic brains. *J. Anat. 185:* 51-63.

von Bartheld CS, Cunningham DE, and Rubel EW (1990). Neuronal tracing with DiI: Decalcification, cryosectioning, and photoconversion for light and electron microscopic analysis. *J. Histochem. Cytochem. 38:* 725-733.

Voneida TJ, Vardaris RM, Fish SE, and Reiheld CT (1981). The origin of the hippocampal commissure in the rat. *Anat. Rec. 201:* 91-103.

Wahlsten D (1974a). Heritable aspects of anomalous myelinated fibre tracts of the forebrain of the laboratory mouse. *Brain Res. 68:* 1-18.

Wahlsten D (1974b). A developmental time scale for postnatal changes in brain and behavior of B6D2F_2 mice. *Brain Res. 72:* 251-264.

Wahlsten D (1975). Genetic variation in the development of mouse brain and behavior: Evidence from the middle postnatal period. *Dev. Psychobiol. 8:* 371-380.

Wahlsten D (1981). Prenatal schedule of appearance of mouse brain commissures. *Dev. Brain Res. 1:* 461-473.

Wahlsten D (1982a). Deficiency of corpus callosum varies with strain and supplier of the mice. *Brain Res. 239:* 329-347.

Wahlsten D (1982b). Genes with incomplete penetrance and the analysis of brain development. *In:* Genetics of the Brain. Lieblich I (Ed.). Amsterdam: Elsevier Biomedical, pp. 367-391.

Wahlsten D (1982c). Mice in utero while their mother is lactating suffer higher frequency of deficient corpus callosum. *Dev. Brain Res. 5:* 354-357.

Wahlsten D (1982d). Mode of inheritance of deficient corpus callosum in mice. *J. Hered. 73:* 281-285.

Wahlsten D (1983). Maternal effects on mouse brain weight. *Dev. Brain Res. 9:* 215-221.

Wahlsten D (1984). Growth of the mouse corpus callosum. *Dev. Brain Res. 15:* 59-67.

Wahlsten D (1987a). Defects of the fetal forebrain in mice with hereditary agenesis of the corpus callosum. *J. Comp. Neurol. 262:* 227-241.

Wahlsten D (1987b). Three sources of individual differences. *Can. Psychol. 28(2a)* Abstr 640.

Wahlsten D (1989a). Deficiency of the corpus callosum: Incomplete penetrance and substrain differentiation in BALB/c mice. *J. Neurogenet. 5:* 61-76.

Wahlsten D (1989b). Genetic and developmental defects of the mouse corpus callosum. *Experientia 45:* 828-838.

Wahlsten D, and Bulman-Fleming B (1987). The magnitudes of litter size and sex effects on brain growth of BALB/c mice. *Growth 51:* 240-248.

Wahlsten D, and Bulman-Fleming B (1994). Retarded growth of the medial septum: a major gene effect in acallosal mice. *Dev. Brain Res. 77:* 203-214.

Wahlsten D, and Jones G (1983). Structural changes in brains of mice with agenesis of the corpus callosum. *Soc. Neurosci. Abstr. 9:* 494.

Wahlsten D, and Schalomon PM (1994). A new hybrid mouse model for agenesis of the corpus callosum. *Behav. Brain Res. 64:* 111-117.

Wahlsten D, and Smith G (1989). Inheritance of retarded forebrain commissure development in fetal mice: Results from classical crosses and recombinant inbred strains. *J. Hered. 80:* 11-16.

Wahlsten D, and Sparks V (1995). New recombinant inbred strains expressing 100% total absence of the corpus callosum. *Soc. Neurosci. Abstr. 21:* 796.

Wahlsten D, and Wainwright P (1977). Application of a morphological time scale to hereditary differences in prenatal mouse development. *J. Embryol. Exp. Morph. 42:* 79-92.

Wahlsten D, Blom K, Stefanescu R, Conover K, and Cake H (1987). Lasting effects on mouse brain growth of 24 hr postpartum deprivation. *Int. J. Dev. Neurosci. 5:* 71-75.

Wahlsten D, Sparks V, and Bishop KM (1996). Rapid emergence of absent corpus callosum in recombinant inbred lines derived from the 129 and BALB/c mouse strains:

support for a two-locus model. *Submitted.*

Wainwright P (1980). Relative effects of maternal and pup heredity on postnatal mouse development. *Dev. Psychobiol. 13:* 493-498.

Wainwright P, and Gagnon M (1984). Effects of fasting during gestation on brain development in BALB/c mice. *Exp. Neurol. 85:* 223-228.

Wainwright P, and Stefanescu R (1983). Prenatal protein deprivation increases defects of the corpus callosum in BALB/c laboratory mice. *Exp. Neurol. 81:* 694-702.

Wainwright P, Pelkman C, and Wahlsten D (1989). The quantitative relationship between nutritional effects on preweaning growth and behavioral development in mice. *Dev. Psychobiol. 22:* 183-195.

Walsh C, and Cepko CL (1988). Clonally related cortical cells show several migration patterns. *Science 241:* 1342-1345.

Wang L-C, Baird DH, Hatten ME, and Mason CA (1994). Astroglial differentiation is required for support of neurite outgrowth. *J. Neurosci. 14:* 3195-3207.

Ward R, Tremblay L, and Lassonde M (1987). The relationship between callosal variation and lateralization in mice is genotype-dependent. *Brain Res. 424:* 84-88.

Wetts R, and Fraser SE (1988). Multipotent precursors can give rise to major cell types of frog retina. *Science 239:* 1142-1145.

Wiebold JL, and Becker WC (1987). Inequality in function of the right and left ovaries and uterine horns of the mouse. *J. Reprod. Fertil. 79:* 125-134.

Williams RW, Bastiani MJ, Lia B, and Chalupa LM (1986). Growth cones, dying axons and developmental fluctuations in the fiber population of the cat's optic nerve. *J. Comp. Neurol. 246:* 32-69.

Wilson CL, Isokawa M, Babb TL, and Crandall PH (1990). Functional connections in the human temporal lobe. I. Analysis of limbic system pathways using neuronal responses evoked by electrical stimulation. *Exp. Brain Res. 82:* 279-292.

Wilson CL, Isokawa M, Babb TL, Crandall PH, Levesque MF, and Engel J (1991). Functional connections in the human temporal lobe. II. Evidence for a loss of functional linkage between contralateral limbic structures. *Exp. Brain Res. 85:* 174-187.

Wisniewski KE, and Jeret JS (1994). Callosal agenesis: Review of clinical,

pathological, and cytogenetic features. *In:* Callosal Agenesis - A Natural Split Brain? Lassonde M, and Jeeves MA (Eds.). New York: Plenum Press. pp. 1-6.

Witter MP, Griffioen AW, Jorritsma-Byham B, and Krijnen JLM (1988). Entorhinal projections to the hippocampal CA1 region in the rat: an underestimated pathway. *Neurosci. Lett. 85:* 193-198.

Wolff JR, and Zaborszky L (1979). On the normal arrangement of fibres and terminals and limits of plasticity in the callosal system of the rat. *In:* Structure and Function of the Cerebral Commissures. Steele Russel I, Van Hof M, and Berlucchi G (Eds.). New York: MacMillan. pp. 147-154.

Wyss JM, Swanson LW, and Cowan WM (1980). The organization of the fimbria, dorsal fornix and ventral hippocampal commissure in the rat. *Anat. Embryol. 158:* 303-316.

Wyss JM (1981). An autoradiographic study of the efferent connections of the entorhinal cortex in the rat. *J. Comp. Neurol. 199:* 495-512.

Yaginuma H, Homma S, Kunzi R, and Oppenheim RW (1991). Pathfinding by growth cones of commissural interneurons in the chick embryo spinal cord: a light and electron microscopic study. *J. Comp. Neurol. 304:* 78-102.

Yen SH, and Fields KL (1981). Antibodies to neurofilament, glial filament, and fibroblast intermediate filament proteins bind to different cell types of the nervous system. *J. Cell. Biol. 88:* 115-126.

Zaki W (1985). Le processus dégénératif au cours du développement du corps calleux [The degenerative process during the development of the corpus callosum (English translation provided by JM Lassalle)]. *Archiv. Anat. Micr. Morphol. Expér. 74:* 133-149.

Zamenhof S (1987). Quantitative studies of mitoses in fetal rat brain: orientations of the spindles. *Dev. Brain Res. 31:* 143-146.

Zeki SM (1973). Comparison of the cortical degeneration in the visual regions of the temporal lobe of the monkey following section of the anterior commissure and the splenium. *J. Comp. Neurol. 148:* 167-176.

Zheng JQ, Felder M, Connor JA, and Poo MM (1994). Turning of nerve growth cones induced by neurotransmitters. *Nature 368:* 140-144.

Zhukareva V, and Levitt P (1995). The limbic system-associated membrane protein (LAMP) selectively mediates interactions with specific central neuron populations. *Development 121:* 1161-1172.

APPENDIX A

An accurate quantification of the developing mouse corpus callosum has not yet been reported. Similar studies in the rat (Gravel *et al*, 1990), cat (Berbel and Innocenti, 1988), and rhesus monkey (LaMantia and Rakic, 1990b) have demonstrated changes in midsagittal CC area, axon number, axon diameter, and myelin content during callosal development. Such data for the mouse would be extremely valuable in comparing CC functional sparing between the acallosal strains and normal strains. A pilot study was performed to indicate the viability of such a study within the mouse.

A 19.1g, 42 day old, female $B6D2F_2$ mouse was anaesthetized with sodium pentobarbital (240mg/kg body weight) and perfused intracardially with 10mL 0.01M PBS, followed by 25mL of 1% paraformaldehyde and 1% glutaraldehyde in 0.1M phosphate buffer (pH 7.4), followed by 200mL of 4.3% glutaraldehyde in 0.1M phosphate buffer (pH 7.4). After perfusion the skin and skull top were removed to facilitate perfusate entry into the brain and the head was post-fixed in the second fixative overnight. The brain was then extracted, trimmed (removing olfactory lobes, meninges, optic nerve, and all non-cerebral structures past the posterior border of the cortices) and sagittally sectioned at 200μm using a vibratome and steel blade. Three serial sections on either side of midline were kept and stored overnight in the first fixative. Sections were washed (3x10min) in sucrose-phosphate buffer (pH 7.2), post-fixed in 2% OsO_4 in sucrose-phosphate buffer (pH 7.2) for 2 hours, then rinsed (5x10min) in a sucrose-acetate buffer (pH 5.0), stained *en bloc* using 2% uranyl

acetate in acetate buffer (pH 5.2) for 1 hour, and then rinsed again (3x10min) in sucrose-acetate buffer (pH 5.0). Sections were then dehydrated through an ethanol series (1x10min 30%; 1x10min 50%; 1x10min 70%; 1x10min 90%; 1x10min 95%; 2x15min 100%), and then rinsed in propylene oxide (2x15min). They were then rinsed (1x15min) in a 1:1 mixture of propylene oxide and Epon 812 followed by incubation in fresh Epon 812 for 48 hours at room temperature and then a further 48 hours at 60°C for polymerization.

The resulting tissue blocks were cut into three pieces containing the genu, truncus and splenium (estimated) of the CC each of which were then sectioned individually. Several 1μm sections were cut using 6mm tungsten-coated glass knives on a Reichert-Jung Ultracut E ultramicrotome, heat mounted to glass slides and stained with toluidine blue for 5 minutes. The CC area was traced using a Leitz Laborlux microscope with an attached drawing tube and measured using a Numonics graphics tablet connected to a PC and the morphometry analyzed by SigmaScan (Jandel Scientific). Care was taken to limit tracing to the CC proper, thus excluding the dorsal columns of the fornix, the superior fornix, and the longitudinal striae.

Thin sections (70-100nm) were then cut and collected onto 300 mesh CuPd grids, stained for 1 hour with uranyl acetate (aq) and then 1-2 minutes in lead citrate (aq). Sections were observed using a Philips 400 TEM at 100kV. Low power was used to select a grid pore from the middle of the section. Consecutive photographs were taken of this area at a magnification of 6700x and a montage of these photographs was created using 8x10 prints. Three areas measuring 900cm^2 (representing an actual area of 27.69μm^2 within the CC) were selected and within this area, measurements were made of axon numbers, axon diameters,

and myelin content (measured as number of lamellae). Data from within these three areas were averaged and extrapolated to the area of the callosal section being measured, and then to the entire CC.

Total area of the CC was 0.726mm^2. The total number of axons was found to be 7.1 million. Of these, 847,000 (13.5%) were myelinated. Mean diameter of the myelinated axons was 0.74μm (±0.18) with an average of 6.3 (±1.9) lamellae (accounting for approximately 20% of the diameter). Mean diameter of unmyelinated axons was 0.11μm (±0.04). Throughout the CC, total non-axonal tissue accounted for 37.2% of the total area.

These results were only meant to provide a very quick estimate of axon numbers within normal mice. The small sample size and limited sampling areas within the CC will of course greatly confound both the reliability and validity of these findings, however they may be useful if considered simply as a rough estimate. The number is a reasonable estimate, based on the numbers reported for other animals.